IFAC

INTERNATIONAL FEDERATION
OF AUTOMATIC CONTROL

WARSZAWA 1969

Chemical and Allied

Mass Exchange Processes, Distillation

Fourth Congress of the International Federation of Automatic Control
Warszawa 16–21 June 1969

TECHNICAL SESSION
53

Organized by
Naczelna Organizacja Techniczna w Polsce

INTERNATIONAL FEDERATION OF AUTOMATIC CONTROL

Chemical and Allied

Mass Exchange Processes, Distillation

TECHNICAL SESSION No 53

FOURTH CONGRESS OF THE INTERNATIONAL
FEDERATION OF AUTOMATIC CONTROL
WARSZAWA 16 – 21 JUNE 1969

Organized by
Naczelna Organizacja Techniczna w Polsce

Contents

Wydawnictwa Czasopism Technicznych NOT - Polska

Zakład Poligraficzny WCT NOT. Zam. 117/69.

ЗАДАЧИ СТАТИСТИЧЕСКОГО СИНТЕЗА СИСТЕМ АВТОМАТИЧЕСКОЙ ОПТИМИЗАЦИИ МАССООБМЕННЫХ УСТАНОВОК.

В.И. ИВАНЕНКО, Д.В. КАРАЧЕНЕЦ,
ИНСТИТУТ КИБЕРНЕТИКИ,
КИЕВ, С С С Р .

I. В ряде отраслей промышленной технологии для получения чистых продуктов широкое распространение получили массообменные (ректификационные, абсорбционные и др.) установки[1-3].

Значительные энергозатраты, связанные с проведением массообменного процесса[4], и высокие требования, предъявляемые к чистоте получаемых продуктов, делают весьма актуальной задачу оптимизации массообменных установок. Сложность этой задачи обусловлена нелинейностью характеристик объекта и его многомерностью, наличием возмущающих воздействий, приводящих к дрейфу экстремума, и существенным уровнем помех.

Ощутимые трудности связаны здесь с проблемой получения информации, необходимой для целей управления. Так, применяемым на практике методам определения состава исходных и конечных продуктов разделения присущи, как правило, значительные случайные ошибки измерения, а в ряде случаев анализ состава некоторых продуктов не производится вообще.

Эти особенности объекта управления требуют, естественно, привлечения статистических методов для синтеза системы автоматической оптимизации (САО).

Детерминированный подход[5] к решению задачи оптимизации массообменного процесса допустим, с учетом сказанного выше, лишь в частных случаях.

В литературе до настоящего времени нет примеров решения задачи статистического синтеза САО применительно к рассматриваемым процессам. Отсутствует также достаточно четкая постановка задачи. Такое положение, по нашему мнению, сдерживает в значительной степени разработку и промышленное внедрение САО в данной области.

В настоящем докладе исследуется задача оптимизации стационарных режимов процесса.

В качестве примера рассматриваются две типичных массообменных установки: ректификационная колонна обезбензоливания

(рис. Iа) в производстве этилбензола[6] и выпарная колонна (рис. Iб) в производстве этилового спирта[7] x).

Выходными переменными в ректификационной колонне являются величины x_{wl} и x_{dh} xx), которые представляют собой концентрации нежелательных примесей в конечных продуктах разделения.

При некоторых допущениях можно считать, что входными переменными процесса являются параметры питательной смеси F, $\bar{x}_F$ (основные возмущения) и потоки пара V_w и флегмы L_ϕ, подаваемых в колонну.

Эффективность процесса в колонне оценивается стоимостью процесса в единицу времени[6]:

$$W = a_L L_\phi + a_d x_{dh} \qquad (I)$$

при условии

$$x_{wl} \leq x^*_{wl} \quad (x^*_{wl} = const). \qquad (2)$$

Учитывая действие случайных факторов в системе, эффективность данного процесса, как показано в работе[6], целесообразно вместо (I) и (2) оценивать стоимостью процесса в виде:

$$W = a_L L_\phi + a_d x_{dh} + G(x_{wl}). \qquad (3)$$

В качестве $G(x_{wl})$ рассмотрим ступенчатую

$$G(x_{wl}) = \begin{cases} 0, & \text{при } x_{wl} \leq x^*_{wl} \\ G_0, & \text{при } x_{wl} > x^*_{wl} \end{cases} \qquad (4)$$

и гладкие функции "штрафа"

$$G(x_{wl}) = a_w \cdot x^p_{wl}. \qquad (5)$$

Выходной переменной в выпарной колонне является концентрация x_w. Входные переменные - параметры F, x_F питательной смеси (основные возмущения) и паровой поток V_w.

---

x) Основные сведения о данных установках приведены в Приложении.

xx) Все обозначения, применяемые в тексте, даны в конце доклада.

Эффективность процесса в выпарной колонне также можно оценивать стоимостью процесса в единицу времени[7]:

$$W = a_v V_w + a_w x_w. \qquad (6)$$

2. В ректификационной колонне отсутствуют датчики величин x_{wl} и x_{dh}. Наличие ряда неконтролируемых возмущений, накладываемых на потоки V_w и L_φ, и высокая чувствительность составов конечных продуктов к этим потокам, требуют стабилизации температуры на "контрольных" тарелках t_y и $t_н$, соответственно в укрепляющей и исчерпывающей секции колонны.

Задаваемые значения этих температур могут рассматриваться в качестве управляющих воздействий при решении задачи статической оптимизации процесса.

При этом зависимость от управлений и основных возмущений переменной x_{dh}, например, может быть представлена в общем случае, как:

$$x_{dh} = x_{dh}(t_y, t_н, F, \bar{x}_F). \qquad (7)$$

Аналогичные зависимости могут быть записаны также для величин L_φ и x_{wl}, входящих в (3).

Проведенные исследования стационарных режимов процесса обезбензоливания[6] позволили получить простую и пригодную для целей синтеза САО модель статики процесса в виде:

$$\begin{aligned} L_\varphi &= a_0 + a_1 U_1 + a_2 U_2, \\ x_{wl} &= A_1 \cdot \exp(-B_1 \mu - C_1 U_1), \\ x_{dh} &= A_2 \cdot \exp(B_2 \mu + C_2 U_2), \end{aligned} \qquad (8)$$

где

$$\mu = x_{Fl} - x^*_{Fl}, \quad U_1 = t_н - t^*_н, \quad U_2 = t_y - t^*_y. \qquad (9)$$

В (8) $a_0, a_1, a_2, A_1, A_2, B_1, B_2, C_1, C_2$ - коэффициенты, зависящие от расхода питания F. Величины x^*_{Fl}, $t^*_н$ и t^*_y в (9) - константы.

Структурная схема системы управления процессом обезбензоливания с учетом возможности измерения F и μ должна иметь вид, представленный на рис. 2а.

Система является комбинированной. Регулирование по откло-

нению используется для стабилизации косвенных показателей процесса (температур $t_н$, $t_у$) и позволяет нейтрализовать влияние возмущений $Z_{L,V}$, приводящих к изменению потоков L и V в колонне. Компенсация основных возмущений F, μ по расходу и составу питания производится автоматическим оптимизатором АО на основе математической модели процесса (8), (9) таким образом, чтобы величины L_φ, x_{wl}, x_{dh} соответствовали оптимальному значению некоторого показателя качества.

В выпарной колонне управляющим воздействием является расход пара V_w.

Статические характеристики выпарной колонны[7] показывают, что при постоянном расходе питания F выходная переменная x_w может быть, с хорошим приближением, представлена в виде:

$$x_w = A \cdot \exp(B\mu + cU), \qquad (10)$$

где

$$\mu = x_F - x_F^*, \quad U = V_w^* - V_w. \qquad (11)$$

В (10) и (11) A, B, C, V_w^* - коэффициенты, зависящие от расхода питания F, а x_F^* - константа.

Величины F, μ и x_w могут быть измерены и соответствующая этому случаю структурная схема САО показана на рис. 2б. Здесь обратная связь замыкается по величине x_w, которая измеряется в дискретные моменты времени $s = \frac{\tau}{\Delta\tau}$, где τ - время и $\Delta\tau$ - интервал квантования, датчиком H с погрешностью h. Причем

$$(y_w)_s = (x_w)_s + h_s. \qquad (12)$$

Будем считать, что возмущение F по расходу питания измеряется точно. Его компенсация при этом не представляет особых затруднений и далее не рассматривается.

Существующие методы определения состава питания связаны, в обоих случаях, со значительными ошибками измерения e и в s-й момент времени в АО вводится значение

$$\omega_s = \mu_s + e_s. \qquad (13)$$

Возмущения μ являются случайными функциями времени, которые с хорошим приближением могут быть описаны стационарным марковским процессом[6,7]. При этом, для значений μ в соседние дискретные моменты времени плотность вероятностей перехода имеет вид:

$$P(\mu_{s+1}/\mu_s) = \frac{1}{\sigma_\Delta \cdot \sqrt{2\pi}} \cdot \exp\left\{-\frac{(\mu_{s+1} - \bar{\lambda}\mu_s)^2}{2\sigma_\Delta^2}\right\}, \qquad (14)$$

где $0 < \bar{\lambda} < 1$.

Погрешности измерений h_s и e_s представляют собой последовательности независимых случайных величин, распределенных по нормальным законам с нулевыми математическими ожиданиями и дисперсиями σ_h^2 и σ_e^2, соответственно.

В дальнейшем будем обозначать через W_s стоимость процесса за промежуток времени от момента s до момента $s+1$.

3. Перейдем непосредственно к задаче статистического синтеза автоматических оптимизаторов АО, показанных на рис.2.

Будем считать оптимальной систему, в которой достигается минимум функционала

$$\rho = \lim_{n\to\infty} \frac{1}{n} \sum_{s=1}^{n} R_s, \qquad (15)$$

где удельный риск $R_s = M\{W_s\}$, M - символ математического ожидания, ρ представляет собой среднюю стоимость процесса за один такт.

А. Рассмотрим синтез АО для компенсации возмущения μ по составу питания ректификационной колонны.

Здесь возмущение μ_s остается постоянным на промежутке времени от s до $s+1$ [x]. Измеренное значение ω_s величины μ_s вводится в АО в момент s. АО выбирает управления U_{1s} и U_{2s} на основе имеющейся в момент s информации о возмущении μ_s. Можно показать, что эта информация в данном случае при больших s определяется достаточными

---

x) Постоянство μ_s на одном интервале объясняется наличием промежуточных емкостей питательной смеси.

транзитивными статистиками m_s и σ_s и

$$P(\mu_s) = \frac{1}{\sigma_s\sqrt{2\pi}} \exp\left\{-\frac{(\mu_s - m_s)^2}{2\sigma_s^2}\right\} \qquad (16)$$

С помощью основного уравнения марковских процессов и формулы Байеса апостериорные значения m_{s+1} и σ_{s+1} после наблюдения ω_{s+1} определяются в виде:

$$m_{s+1} = \frac{m^0_{s+1}\sigma_e^2 + \omega_{s+1}\cdot(\sigma^0_{s+1})^2}{(\sigma^0_{s+1})^2 + \sigma_e^2}, \qquad (17)$$

$$\sigma^2_{s+1} = \frac{(\sigma^0_{s+1})^2\cdot\sigma_e^2}{(\sigma^0_{s+1})^2 + \sigma_e^2},$$

где m^0_{s+1} и $(\sigma^0_{s+1})^2$ – априорные к $(s+1)$-му шагу значения математического ожидания и дисперсии величины μ_{s+1}, причем

$$m^0_{s+1} = \bar{\lambda}\cdot m_s,$$
$$(\sigma^0_{s+1})^2 = \bar{\lambda}^2\cdot\sigma_s^2 + \sigma_\Delta^2. \qquad (18)$$

Рассмотрим условный удельный риск r_s:

$$r_s = M\left\{W_s / m_s, \sigma_s, u_{1s}, u_{2s}\right\} = \qquad (19)$$

$$= \int_{(\mu_s)} W_s(\mu_s, u_{1s}, u_{2s})\cdot P(\mu_s / m_s, \sigma_s)\cdot d\mu_s.$$

Риск r_s с учетом (3), (8), (16) равен:

$$r_s = \lambda_L\cdot(a_0 + a_1 u_{1s} + a_2 u_{2s}) + \lambda_d\cdot\exp\left(c_2 u_{2s} + b_2 m_s + \frac{b_2^2\cdot\sigma_s^2}{2}\right) + J, \qquad (20)$$

где J при ступенчатой (4) функции "штрафа" (случай I) имеет вид:

$$J = G_0\cdot\Delta\tau\cdot\Phi^*\left[\frac{1}{\sigma_s}\left(\frac{1}{b_1}\ln\frac{x^*_{wl}}{A_1} - c_1 u_{1s}\right) - \frac{m_s}{\sigma_s}\right], \qquad (21)$$

и при гладкой (5) функции "штрафа" (случай 2):

$$J = \lambda_w\cdot\exp\left[-\rho c_1 u_{1s} - \rho b_1 m_s + \frac{(\rho b_1)^2\sigma_s^2}{2}\right]. \qquad (22)$$

в (20), (21), (22):

$$\alpha_L = a_L \cdot \Delta\tau, \quad \alpha_d = A_2\, a_d \cdot \Delta\tau, \quad \alpha_w = A_1\, a_w \cdot \Delta\tau$$

и $\Phi^*[\cdot]$ – нормальная функция распределения.

Рассматриваемая задача является байесовой и оптимальная стратегия, минимизирующая R_s, является детерминированной.[8] Нетрудно показать, что минимум τ_s достигается на той же стратегии, что и минимум R_s.

Оптимальные управления в s-ый момент времени в обоих случаях равны:

$$U_{1s}^* = (g_{0,1})_s - g_{1,1} \cdot m_s, \tag{23}$$

$$U_{2s}^* = (g_{0,2})_s - g_{1,2} \cdot m_s, \tag{24}$$

где

$$g_{1,1} = \frac{B_1}{C_1}, \quad g_{1,2} = \frac{B_2}{C_2},$$
$$(g_{0,2})_s = \frac{1}{C_2}\left(\ln\frac{-a_2 \cdot \alpha_u}{C_2 \cdot \alpha_d} - \frac{B_2^2 \cdot \sigma_s^2}{2}\right). \tag{25}$$

Коэффициент $(g_{0,1})_s$ в (23) зависит подобно $(g_{0,2})_s$ от статистики σ_s. Для случая ступенчатой и гладкой функции "штрафа" эта зависимость имеет разный вид.

Управлениям (23), (24) соответствуют оптимальные условные риски, равные

$$\tau_s^* = C_0^*(\sigma_s) + C_1^* \cdot m_s. \tag{26}$$

Коэффициент C_1^* постоянен, а C_0^* зависит от σ_s. Здесь также вид зависимости различен для случаев I и 2.

Минимальное значение удельного риска R_s^* равно:

$$R_s^* = \int_{(m_s)} \tau_s^*(m_s, \sigma_s) \cdot P(m_s) \cdot dm_s. \tag{27}$$

Т.к. m_{s+1} и σ_{s+1} (17) не зависят от управлений (23), (24), то последние являются оптимальными и в смысле минимизации функционала ρ (15).

Этот факт, как известно[9], всегда имеет место в системах

автоматической компенсации.

При $s \to \infty$ риск R_s^* имеет предел, равный

$$\lim R_s^* = R^* = \rho^*, \qquad (28)$$

где ρ^* - минимальная средняя стоимость процесса за один такт.

Доказательство (28) кратко сводится к следующему.

Нетрудно убедиться, что последовательность σ_s, определяемая выражениями (I7), (I8), сходится к пределу, который обозначим через σ_∞.

Кроме того, можно показать, что последовательность величин m_s образует регулярный марковский процесс, имеющий предельное нормальное распределение с математическим ожиданием, равным нулю.

При этом

$$R^* = \rho^* = C_0^*(\sigma_\infty). \qquad (29)$$

Когда σ_s становится достаточно близким к σ_∞, режим слежения за возмущением μ будем называть стационарным, а стратегию, соответствующую этому режиму, - стационарной стратегией[10].

Так как время работы системы значительно превышает время переходного процесса $\sigma_s \to \sigma_\infty$, то АО целесообразно рассчитывать только на стационарный режим слежения. Соответствующая этому случаю структурная схема АО представлена на рис. 3.

На рис. 4 показан переходный процесс, связанный с изменением σ_s в начале работы САО. В качестве априорной информации о величине μ в момент $s = 0$ принят абсолютный закон распределения μ, который, с учетом (I4), является нормальным с нулевым математическим ожиданием и дисперсией σ_μ^2, равной

$$\sigma_\mu^2 = \frac{\sigma_\Delta^2}{1 - \bar{L}^2}. \qquad (30)$$

Переходный процесс практически заканчивается за несколько шагов.

Полученные результаты дают также возможность оценить эффект, достигаемый от применения АО.

Б. Рассмотрим синтез АО в системе оптимизации выпарной колонны (рис. 2б). Здесь особый интерес представляют процессы протекающие в замкнутой схеме. Для их изучения предположим, что цепь компенсации μ отсутствует и помеха $g = 0$.

Будем считать возмущение μ_s также постоянным на промежутке времени от s до $s+1$ [x]. Измеренное значение $(y_w)_s = y_s$ величины $(x_w)_s = x_s$ вводится в АО в момент $s+1$, т.е. в АО имеется запаздывание на один такт.

Покажем, что как и в предыдущем случае, информацию в АО о возмущении μ в s -ый момент времени можно определять с приемлемой точностью достаточными статистиками.

Пусть в момент s выбора управления U_s в АО известно, что на интервале от s до $s+1$ возможные значения величины μ_s распределены по нормальному закону (I6), который будем называть априорным в s -м такте.

К моменту $s+1$ в АО поступает измерение y_s, равное

$$y_s = A \cdot \exp(B\mu_s + C U_s) + h_s. \qquad (3I)$$

Линеаризуя выражение (3I) в точке m_s, σ_s [II] и применяя формулу Байеса, можно показать, что апостериорное распределение μ_s (после измерения y_s) также подчинено нормальному закону с параметрами

$$\tilde{m}_s = \frac{m_s \cdot (\tilde{\sigma}_h)_s^2 + \tilde{y}_s \cdot \sigma_s^2}{\sigma_s^2 + (\tilde{\sigma}_h)_s^2}, \qquad (32)$$

$$\tilde{\sigma}_s^2 = \frac{\sigma_s^2 \cdot (\tilde{\sigma}_h)_s^2}{\sigma_s^2 + (\tilde{\sigma}_h)_s^2},$$

где

$$\tilde{y}_s = \beta_s \cdot y_s + m_s - \frac{1}{B}, \qquad (33)$$

$$(\tilde{\sigma}_h)_s^2 = \beta_s^2 \cdot \sigma_h^2 \qquad (34)$$

и

$$\beta_s = \frac{1}{A \cdot B \cdot \exp(B m_s + C U_s)}. \qquad (35)$$

---

x) Это ограничение в рассматриваемой задаче не является принципиальным.

С помощью основного уравнения марковских процессов определяем, далее, априорный закон распределения величины μ_{s+1} который, очевидно, является нормальным с параметрами

$$m_{s+1} = \bar{a} \cdot \tilde{m}_s, \qquad (36)$$
$$\sigma^2_{s+1} = \bar{a}^2 \cdot \tilde{\sigma}^2_s + \sigma^2_a.$$

Таким образом, информация в АО о возмущении μ_s в момент s выбора управления U_s может быть определена достаточными транзитивными статистиками m_s и σ_s. Естественно, что этот вывод справедлив при больших s.

Так как m_{s+1} и σ_{s+1} зависят от управления на предыдущем шаге, то управление U_s, минимизирующее удельный риск R_s, не является теперь оптимальным в смысле минимизации функционала ρ (I5).

Это обстоятельство является проявлением возможности активного накопления информации в АО о возмущающем воздействии в замкнутых системах[9].

Отыскание в таких системах оптимальной стратегии, доставляющей минимум функционалу ρ, оказывается весьма трудной задачей.

Один из возможных подходов к решению этой задачи в случае марковских объектов и функционала (I5) может быть развит на основе идеи, изложенной в работе[I2].

Предположим, что процесс оканчивается в момент времени $s = S$. Введем отсчет времени от момента S в обратном направлении, так что $\kappa = S - s$.

Обозначим через

$$U_\kappa = U(m_\kappa, \sigma_\kappa) \qquad (37)$$

стратегию АО, а через $v_\kappa(m_\kappa, \sigma_\kappa, U)$:

$$v_\kappa(m_\kappa, \sigma_\kappa, U) = M\left\{\sum_{i=1}^{\kappa} (W_i / m_\kappa, \sigma_\kappa, U)\right\} - \qquad (38)$$

математическое ожидание полной стоимости процесса за κ шагов при фиксированной некоторым образом стратегии (37) и при условии, что к моменту κ система находилась в состоянии $(m_\kappa, \sigma_\kappa)$. В этом случае для величины $v_\kappa(m_\kappa, \sigma_\kappa, U)$ имеет место следующее рекуррентное соотношение:

$$v_k(m_k, б_k, u) = \alpha_w \exp(c u_k + в m_k + \frac{в^2 \cdot б_k^2}{2}) + \alpha_v \cdot V_w^* - \tag{39}$$

$$- \alpha_v \cdot u_k + \int_{(m_{k-1})} v_{k-1}(m_{k-1}, б_{k-1}, u) \cdot N(M_{k-1}, D_{k-1}) \cdot dm_{k-1},$$

где $N(M_{k-1}, D_{k-1})$ - нормальный закон распределения плотности вероятности величины m_{k-1} с математическим ожиданием M_{k-1} и дисперсией D_{k-1},

$$\alpha_w = A \cdot a_w \cdot \Delta\tau, \quad \alpha_v = a_v \cdot \Delta\tau$$

(a_w и a_v - коэффициенты в (6)).

Асимптотическое поведение величины $v_k(m_k, б_k, u)$ при стратегии (44) и $k \to \infty$ может быть представлено в виде:

$$v_k(m_k, б_k, u) = k \cdot \rho(u) + T(m_k, б_k, u), \tag{40}$$

где $T(m_k, б_k, u)$ - "весовая" функция состояния $m_k, б_k$ при стратегии (37).

На основе выражений (39) и (40) может быть сконструирована процедура последовательных приближений в пространстве стратегий [13], обеспечивающая сходимость к оптимальной стратегии $u^* = u^*(m, б)$, которая сообщает минимальное значение ρ^* величине ρ.

Однако и при данном подходе определение оптимальной стратегии связано с большим объемом вычислений.

В некоторых случаях достаточно хорошее приближение к оптимальной стратегии может быть получено, если управления выбирать в виде[14]:

$$u_s = u_s'(m_s, б_s) + u_s''(m_s, б_s, \bar{\theta}), \tag{41}$$

где $u_s'(m_s, б_s)$ - составляющая управления u_s, выбираемая из условия минимизации удельного риска R_s, $u_s''(m_s, б_s, \bar{\theta})$ - составляющая u_s, обеспечивающая активное накопление информации в АО о возмущении.

При фиксированном виде функции $u_s''(m_s, б_s, \bar{\theta})$ значение вектора параметров $\bar{\theta}$, оптимальное в смысле минимизации функционала ρ, может быть иногда легко определено.

Например, при

$$U_s''(m_s, \sigma_s, \bar{\theta}) = \text{const} = \theta, \qquad (42)$$

можно показать, что в рассматриваемой замкнутой схеме при управлении (4I), (42)

$$\lim_{s\to\infty} R_s = \rho(\theta) = \frac{\alpha_v}{c}\cdot \exp(c\theta) + \\ + \alpha_v \cdot V_w^* - \alpha_v \cdot \left(\frac{1}{c}\ln\frac{\alpha_v}{c\cdot\alpha_w} + \theta - \frac{\beta^2\cdot\sigma_\infty^2(\theta)}{2c}\right), \qquad (43)$$

где $\sigma_\infty(\theta)$ - предел достаточной статистики σ_s при $s\to\infty$.

Оптимальная величина „изучающей добавки" θ определяется путем минимизации $\rho(\theta)$.

Некоторые результаты выполненных расчетов приведены на рисунках. На рис. 5 и 6 показаны, соответственно, зависимость стоимости процесса и выходной величины объекта от управления U при разных значениях μ. Расчеты оптимальных значений θ^* "изучающей добавки" θ производились для разных значений дисперсий σ_h^2 и σ_Δ^2 (рис. 7). На рис. 8 показана относительная величина снижения стоимости процесса, выраженная в процентах.

Введение в алгоритм управления специальной "изучающей добавки" позволяет иногда существенно снизить среднюю стоимость процесса.

При синтезе АО мы пренебрегали влиянием помехи g (рис.2б) Учет этой помехи при известном законе ее распределения не представляет здесь принципиальных трудностей.

Выше мы также опустили из рассмотрения цепь компенсации μ. Дополнительная информация, поступающая в АО по этой цепи, на основе результатов, которые получены в п. 3А, может быть учтена с помощью приемов, описанных в работе [14].

4. Изложенный в докладе подход к синтезу САО массообменных установок базируется на методах теории статистических решений. Он требует тщательного предварительного изучения объекта управления: выбора функции цели и построения математических моделей, которые включают также вероятностные характеристики неизмеряемых величин и погрешностей измерения.

При этом подходе мы получаем возможность не только синтезировать оптимальный алгоритм АО, но и оценить экономичес-

кий эффект, достигаемый при применении АО. Развитие этого подхода позволит на этапе проектирования производить оценку экономической целесообразности того или другого варианта системы управления массообменным процессом путем сравнения его с оптимальной САО.

Необходимые дальнейшие исследования в области статистического синтеза систем управления массообменными установками связаны с учетом динамики процесса, построением достаточно простых и общих для целого класса установок статических и динамических моделей и изучением ряда других вопросов.

Результаты решения задачи синтеза САО, изложенные в п.3А, были использованы при разработке и внедрении в производство системы автоматического управления ректификационной колонны обезбензоливания в цехе этилбензола Днепродзержинского химкомбината.

П Р И Л О Ж Е Н И Е .

I. Ректификационная установка обезбензоливания в производстве этилбензола предназначена для выделения бензола из многокомпонентной смеси, содержащей также этилбензол, изопропилбензол, диэтилбензол и полиалкилбензолы. Питательная смесь поступает в установку с одной из трех емкостей, подключаемых последовательно на ректификацию. Средний состав смеси (в мол. долях) следующий: бензол - 0,6, этилбензол - 0,25, изопропилбензол - 0,06, диэтилбензол - 0,07, полиалкилбензолы - 0,02. Установка содержит ректификационную колонну, испарители, теплообменник для подогрева питательной смеси кубовым остатком, конденсаторы (предварительный и основной) и флегмовую емкость. Колонна(диаметром I600 мм) имеет 59 колпачковых тарелок. Питание подается на 25 тарелку. Испарители обогреваются глухим водяным паром.

2. Выпарная (бражная) колонна предназначена для перегонки спиртовых бражек. Общая характеристика колонны: диаметр - 2000 мм, число ситчатых тарелок - 22. Колонна обогревается открытым паром, подаваемым под нижнюю тарелку. Питание (бражка) поступает на верхнюю тарелку. Бражка может рассматриваться как бинарная смесь этилового спирта и воды. Среднее содержание этанола в бражке 8,5% объемных.

Обозначения: F - расход питательной смеси, L - поток орошения (L_φ - поток флегмы), V - паровой поток (V_w - поток пара, поступающего под нижнюю тарелку), x - концентрация ($\bar{x}$ - вектор концентраций), t - температура, a_L, a_d, a_w, a_v - удельные коэффициенты стоимости, G_0 - стоимость в единицу времени повторной переработки кубового остатка.

Индексы относятся: F - к питательной смеси, w - к кубовому остатку, d - к дистилляту, l - к бензолу, h - к этилбензолу.

ЛИТЕРАТУРА.

I. А.Н.Плановский, П.И.Николаев. Процессы и аппараты химической технологии. М., Гостоптехиздат, I960.

2. В.В.Кафаров. Основы массопередачи. М., Госиздат, "Высшая школа", I962.

3. В.Н.Стабников, Е.Е.Харин. Теоретические основы перегонки и ректификации спирта. М., Пищепромиздат, I95I.

4. В.М.Платонов, Б.Г.Берго. Разделение многокомпонентных смесей. М., изд. "Химия", I965.

5. И.В.Анисимов, А.Е.Власов, В.Б.Покровский. Оптимизация процесса ректификации в тарельчатых колоннах. Автоматика и телемеханика, № 6, I966.

6. Д.В.Караченец. Синтез системы автоматической оптимизации режимов ректификационной установки обезбензоливания. Диссертация, I966.

7. М.Л.Мандельштейн. Исследование брагоректификационного аппарата как объекта управления. Диссертация, I968.

8. Д.Блекуэлл, М.А.Гиршик. Теория игр и статистических решений. М., ИИЛ, I958.

9. А.А.Фельдбаум. Основы теории оптимальных автоматических систем. М., изд. "Наука", I966.

IO. В.И.Иваненко. К синтезу замкнутых адаптивных систем управления стационарными объектами. Кибернетика, № 4, I968.

II. В.С.Пугачев. Теория случайных функций. М., Физматгиз, I962.

I2. Р.А.Ховард. Динамическое программирование и марковские процессы. М., изд. "Советское радио", I964.

I3. Р.Беллман. Процессы регулирования с адаптацией. М., изд. "Наука", I964.

I4. В.П.Живоглядов. Автоматические системы с накоплением информации. Фрунзе, изд. "ИЛИМ", I966.

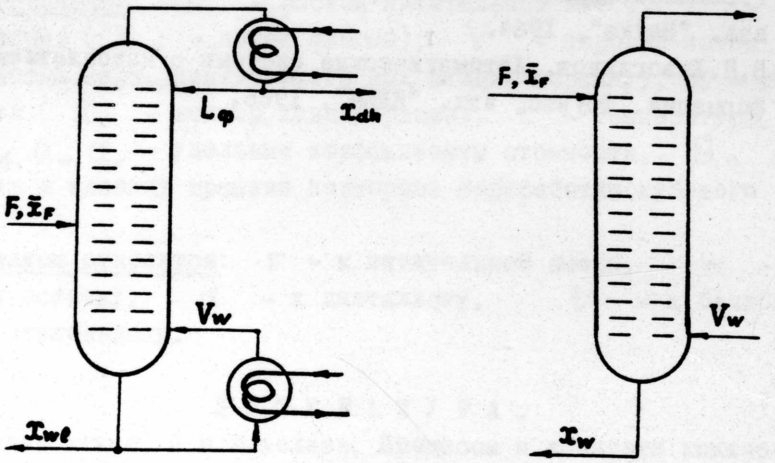
L_φ
x_{dh}
F, $\bar{x}_F$
V_w
$x_{wℓ}$
а)
F, $\bar{x}_F$
V_w
x_w
б)

Рис. 1

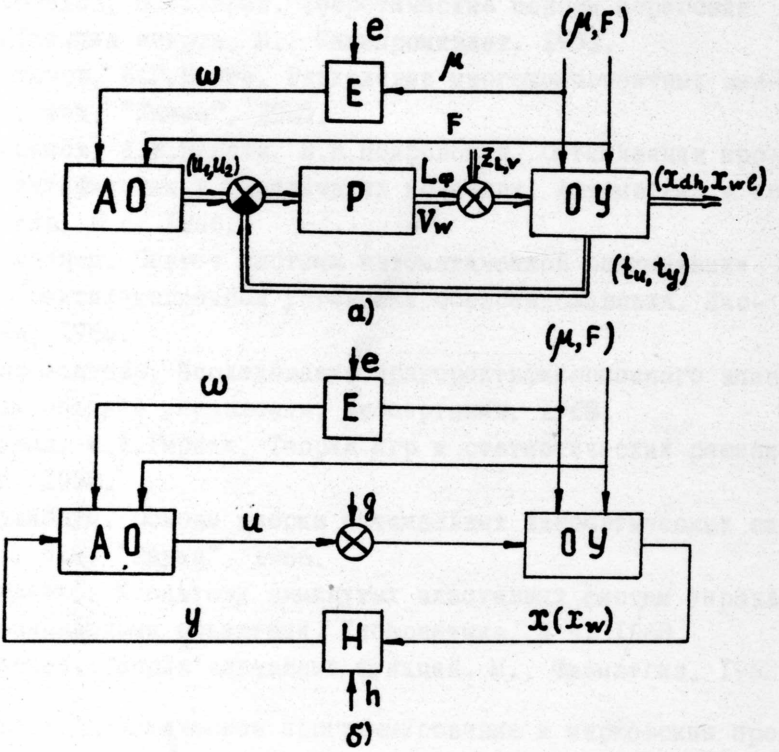
e
(μ,F)
ω
E
μ
F
АО
(u_1,u_2)
Р
L_φ
$\bar{z}_{L,V}$
V_w
ОУ
$(x_{dh},x_{wℓ})$
(t_u,t_y)
а)
e
(μ,F)
ω
E
АО
u
g
ОУ
y
H
x(x_w)
h
б)

Рис. 2

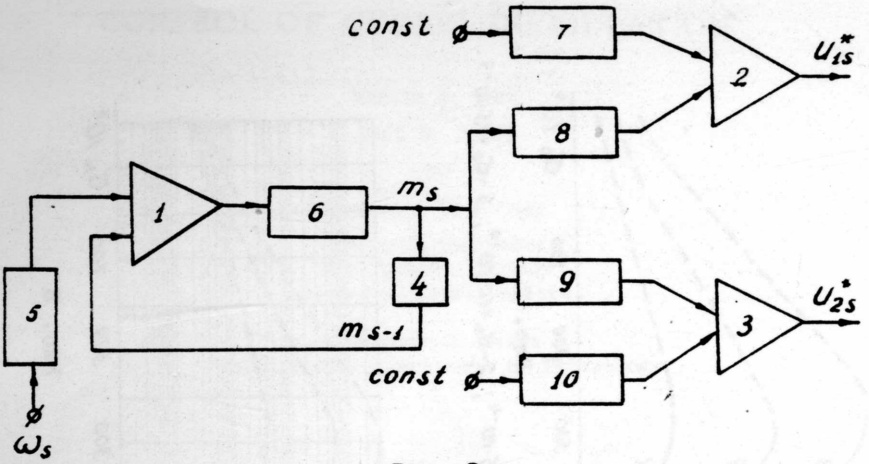

Рис. 3

1,2,3 - суммирующие блоки

4 - звено задержки на один такт

5 - 10 - постоянные коэффициенты

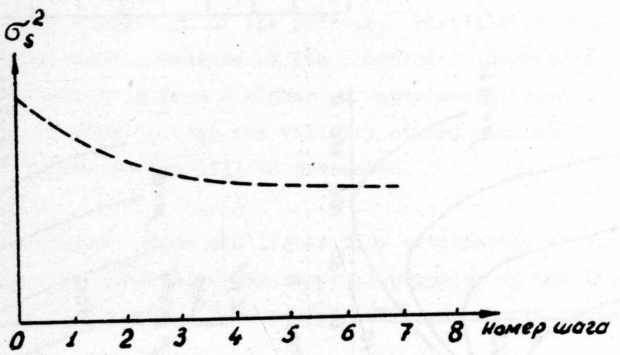

Рис. 4

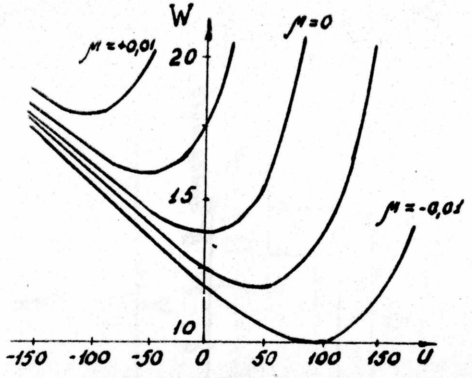

Рис. 5

Параметры задачи	
A	$40 \cdot 10^{-6}$
B	220
C	0,022
α_v	0,04
α_w	1,818
V_w^*	14
$\bar{\alpha}$	0,995

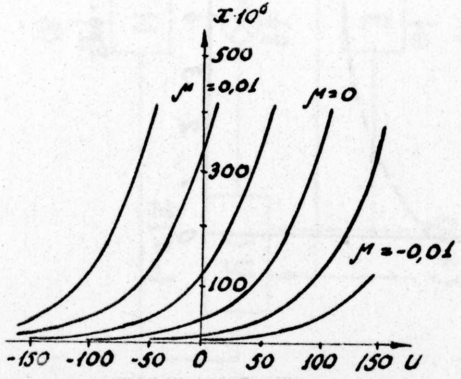

Рис. 6

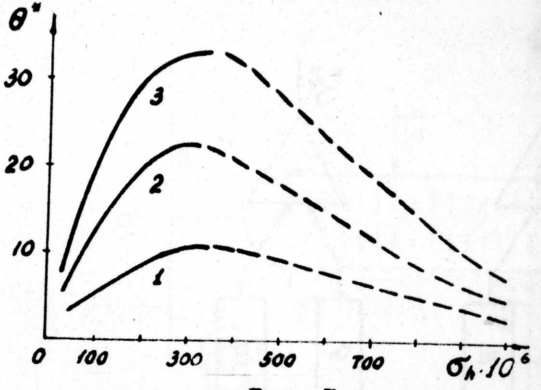

Рис. 7

1 - $\sigma_\Delta = 5 \cdot 10^{-4}$; 2 - $\sigma_\Delta = 10 \cdot 10^{-4}$; 3 - $\sigma_\Delta = 15 \cdot 10^{-4}$

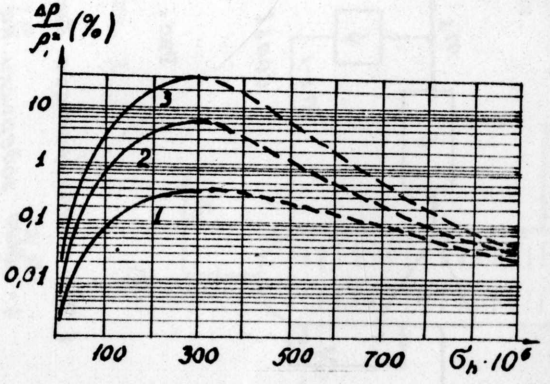

Рис. 8

CONTROL OF CYCLIC DISTILLATION

Harold L. Wade
Carl H. Jones
and
Terrence B. Rooney
Research Engineers
The Foxboro Company
Foxboro, Massachusetts

Lawrence B. Evans
Massachusetts Institute of Technology

Introduction

Increased process efficiency and equipment capacity are among the benefits which result from controlled cycling of many of the operations which are traditionally maintained in the steady state. Considerable evidence supports this idea which was introduced by Cannon.[2]

The successful design and operation of a cyclic process demands a good understanding of the dynamics of the process and its control system. To gain an insight into the problems associated with industrial-scale cyclic processes, a study was made of cyclic distillation based upon a digital computer simulation of the process. Distillation was selected as a specific example because of its commercial importance and because results were available from a number of experimental studies[7, 13, 14, 19] which could be used to test the validity of the simulation. The results of this investigation will be presented.

Cyclic Distillation

In cyclic distillation, vapor and liquid flow alternately through the column for short-time intervals. No vapor is supplied in the liquid flow period (LFP) and in the vapor flow period (VFP), no liquid is supplied.

Studies of cyclic distillation have been carried out by a number of investigators. Theoretical analyses have been presented by Horn[10], Robinson and Engel[18], Sommerfeld[20], and Chien[4]. Experimental work has been recorded by McWhirter and Cannon[13], Gaska and Cannon[7], McWhirter and Lloyd[14], Schrodt[19], and Gerster and Scull[8].

Three major criteria govern the operating efficiency of a cyclic distillation column. The contents of a tray should exactly replace those on the tray below in the LFP without the presence of liquid mixing effects. This is called the liquid plug flow condition. Flow periods should be exactly defined with no liquid leakage in the VFP or vice versa. Axial mixing and liquid entrainment in the vapor phase should be minimized. The control objective is to maintain the column as close as economically possible to peak efficiency and maximum capacity.

Figure 1 shows the equipment which may be used in cyclic distillation. The section titled Simulation Results describes and discusses various strategies which may be adopted in manipulation of the isolating valves.

Schrodt[19] employed perforated trays without downcomers in a 15-tray, 12-inch diameter cyclic distillation column. Despite unimpeded mixing of liquid acceptable tray efficiencies were observed. This cyclic unit proved superior in flexibility and throughput characteristics to the same unit operated in a continuous manner. However, Schrodt observed that the operation was hydrodynamically unstable with the lower trays draining in the LFP before those higher in the column. Analyses of cyclic distillation behavior which give an intimation of such instabilities are not available.

Gerster and Scull[8] have described operating problems which are different from those encountered by Schrodt. Studying the absorption of ammonia into water from a carrier air stream, they observed excessive liquid accumulations on the lower trays.

Mathematical Model of Cyclic Distillation

The dynamic model of the cyclic column used in this study to simulate single-cycle detailed behavior, consists of three parts:

1. Differential equations, based on the conservation laws, describe for each stage the rate of change of certain state variables. For the nth stage and the ith component, the following equations apply with the nomenclature listed at the end of this paper:

$$\frac{dN_n}{dt} = V_{n-1} - V_n + L_{n+1} - L_n \qquad (1)$$

$$\frac{dC_{in}}{dt} = V_{n-1}\, y_{i(n-1)} - V_n\, y_{in} + L_{n+1}\, x_{i(n+1)} - L_n\, x_{in} \qquad (2)$$

$$\frac{dE_n}{dt} = V_{n-1}\, H_{n-1} - V_n\, H_n + L_{n+1}\, h_{n+1} - L_n\, h_n \qquad (3)$$

2. Physical property relations comprise a set of algebraic equations which relate the intensive variables (temperature composition, pressure, etc.) for each stage at a given instant to the state variables at that instant. For the nth stage, the following equations apply:

Composition $$x_{in} = C_{in}/N_n \quad (4)$$

Specific enthalpy of liquid $$h_n = E_n/N_n \quad (5)$$

Temperature $$\theta_n = \theta_{ref} + h_n / \Sigma \ (x_{in} C_{pLi}) \quad (6)$$

Vapor pressure $$P_{in} = F_i \exp\left(-\lambda_i/R\theta_n\right) \quad (7)$$

Vapor phase composition $$y_{in} = (P_i/\pi_n)\ x_{in} \quad (8)$$

Specific enthalpy of vapor $$H_n = \Sigma\ y_{in}\left[C_{pVi}\ (\theta_n - \theta_{ref}) + \lambda_i\right] \quad (9)$$

Molal density of liquid $$\rho_{Ln} = \left[\Sigma\ x_{in}/\rho_i\right]^{-1} \quad (10)$$

Molal density of vapor $$\rho_{Vn} = \pi_n/R\theta_n \quad (11)$$

Molecular weight of liquid $$M_{Ln} = \Sigma\ x_{in} M_i \quad (12)$$

Molecular weight of vapor $$M_{Vn} = \Sigma\ y_{in} M_i \quad (13)$$

Head of liquid on tray $$d_{Ln} = N_n/\rho_{Ln} A_T \quad (14)$$

Assumptions in the physical property equations include ideal thermodynamic behavior of the fluids and constant specific and latent heats.

3. Tray performance equations relate vapor and liquid flow rates leaving each stage to the instantaneous liquid head on and the pressure difference across each stage.

Two tray performance models were considered: a simple heuristic model (Model A) and a more detailed model based upon analysis of the hydrodynamics of the tray (Model B). Each model will be described in the following section with some comments as to its relative merit.

Tray Performance Equations Employed in Simulation

Tray Model A

Let $$P_d = \pi_{n+1} - \pi_n - d_{Ln}\ \rho_{Ln} \quad (15)$$

Then the flow through the holes in a tray is given by:

$$v = J_V \phi A_T \rho_V \sqrt{2 g_c P_d/\rho_V} \quad \text{when } P_d > 0 \qquad (16)$$

$$v = 0 \quad \text{when } P_d \leq 0$$

and

$$l = J_L \phi A_T \rho_L \sqrt{2 g_c (B-P_d) / \rho_L} \quad \text{when } P_d < B \qquad (17)$$

$$l = 0 \quad \text{when } P_d \geq B$$

It is known that the simultaneous flow of vapor and liquid through a tray can occur. The bias B is introduced to equation 17 to force this to be the case in the model with no other physical justification. When B is equal to zero, simultaneous vapor and liquid flow cannot occur.

In Model A, the bias becomes the determining factor for liquid flow in the liquid flow period. No physical intuition can be employed in selection of a value for the bias, and a more realistic model is desired. However, subsequent studies indicated that cyclic distillation can reasonably be simulated employing equations as simple as those of Model A.

Tray Model B

A more detailed model was developed from ideas proposed by Prince and Chan[3,15]. Four modes of behavior are possible for a particular perforation in the tray:

a) Bubbling - passing only vapor in an upward direction.

b) Draining - passing only liquid in a downward direction.

c) Bridging - passing neither vapor nor liquid.

d) Simultaneously passing vapor and liquid.

It is assumed that only the first two modes are present and that any hole may intermittently switch from bubbling to draining or vice versa.

Schematically, the plate is illustrated in Figure 2 where the proportion of total holes which are bubbling vapor is β. Assume that all holes which are draining carry liquid head d_2 and holes which pass vapor experience liquid head d_1. Orifice equations applied to each zone of the tray surface give:

$$v = J_V \phi A_T \beta \rho_V \sqrt{2 g_c (\Delta\pi - d_1 \rho_L)/\rho_V} \qquad (18)$$

$$l = J_L \phi A_T (1-\beta) \rho_L \sqrt{2 g_c (d_2 - \Delta\pi/\rho_L)} \qquad (19)$$

Let these equations be contracted to

$$\underline{v} = \beta \sqrt{\Delta\pi - d_1\rho_L} \qquad (20)$$

$$\underline{l} = (1-\beta) \sqrt{d_2 \rho_L - \Delta\pi} \qquad (21)$$

where $\underline{v} = v/J_V \phi A_T \sqrt{2 g_c \rho_V}$

and $\underline{l} = l/J_L \phi A_T \sqrt{2 g_c \rho_L}$

Then it follows that

$$d_2 - d_1 = (1/\rho_L)\ (\underline{l}^2/(1-\beta)^2 + \underline{v}^2/\beta^2) \qquad (22)$$

Employ the assumption that minimizes (d_2-d_1) as suggested by Prince and Chan[3,15]. Then it can be shown that:

$$\beta \min = \frac{\underline{v}^{0.667}}{\underline{l}^{0.667} + \underline{v}^{0.667}} \qquad (23)$$

The nominal head on the tray is

$$d_L = \beta d_1 + (1-\beta)\ d_2 \qquad (24)$$

Another relation is needed to determine the rate of liquid weepage. In the absence of experimental correlation, it is postulated that the fluid mechanics of a perforated plate can be described by a behavior law of the type:

$$l \times v = K\ (d_2-d_1) \qquad (25)$$

Equation 25 assumes that a high flow of one phase corresponds to a low flow of the other. The last equation also introduces a measure of self regulation into the description of tray performance.

It is assumed that the time required to establish vapor-liquid equilibrium is short compared with the time required for the occurrence of significant changes in liquid composition and energy. So the pressure above a tray is the vapor pressure of the liquid on that tray at its current temperature and composition. Entrainment of liquid in the ascending vapor is assumed to be negligible and liquids are assumed to mix instantaneously.

Method of Simulation

The method of applying Equations (1-25) in the digital simulation to advance the calculation one time-step from time t_1 to $t_2 = t_1 + \Delta t$ involves:

(a) Based upon previously computed or initially assumed values of the holdup, temperature and composition profiles at time t_1, use the physical property relations to compute the pressure above each tray of the column.

(b) Solve the tray performance equations for the vapor and liquid flows leaving each stage in the column. These flows are assumed to be constant during the interval between t_1 and t_2.

(c) Numerically integrate the differential equations describing the conservation laws to determine the temperature, holdup and composition at time t_2. This integration can be simply carried out using Euler's method.

After performance of the last step, the computation is set for the next pass and begins again with the first step. The simulation program used in this work was written in Fortran IV; all computations were performed using an IBM System 360/40.

In order to achieve numerical stability in the integration of the differential equations, it was necessary to use relatively small time-steps (0.05 seconds).

Simulation Results

Tray Models A and B were used initially to study the following five control configurations, employing the isolating facilities shown in Figure 1 as they are required:

1. No isolation of either the condenser or the reboiler from the column in the LFP. Steam is supplied to reboiler and cooling water to condenser only during the VFP. Figure 3 summarizes flow profiles over a single cycle, which are typical of those from tray Models A and B with reboiler and condenser dynamics neglected.
2. Reboiler isolated in the LFP. Otherwise similar to Configuration 1. Figure 4 shows flow profiles from Configuration 2.
3. Condenser isolated in the LFP. Otherwise similar to Configuration 1. Figure 5 shows flow profiles from Configuration 3.
4. Isolation of condenser and reboiler in LFP. Otherwise similar to Configuration 1. Results are plotted in Figure 6.
5. Configuration 1 with instantaneous pressure equalization in the LFP. The manifold line on Figure 2 is assumed connected through suitable valves to the space between each pair of trays.

Configurations 2 and 4 assumed that liquid falling from the bottom tray is removed from the column and there is no vapor pressure difference across this tray. Therefore, liquid flow through the bottom tray depended only on the liquid head effect. This assumption had no effect on the other trays in the column.

Schrodt[19] observed that the bottom plates tended to drain completely before the upper plates started to drain. The simulation of Configuration 2, which is similar to Schrodt's experiment, does predict that dead time exists between commencement of liquid flow from adjacent trays. Thus, liquid flow from the lower trays commenced before flow from the higher trays during the LFP.

Dead time before the start of liquid flow from a particular tray was observed during the switch from VFP to LFP in Configuration 1. Higher trays in the column showed greater delay. Resumption of vapor flow was slightly delayed when the column was switched back from LFP to VFP.

In Configuration 2, reboiler pressure during the LFP remained constant and liquid flow from above caused a cooling of liquid on the bottom tray. Consequently, the beginning of the vapor flow period showed a sharp spike in the vapor flow to the first tray, which reduced the previously mentioned delay in vapor flow resumption.

Configuration 3 showed a pressure buildup at the top of the column, which tended to favor liquid flow. Liquid flow at the bottom followed a behavior pattern similar to that in Configuration 1, and progressed up to the middle of the column. As a result, in Configuration 3 liquid flow occurs last in the middle of the column.

The simulation of Configuration 4 produced a combination of the effects noted by the simulations of Configurations 2 and 3. At the start of the LFP, liquid flow activity began at both ends of the column and progressed to the middle after a slight delay. At the start of the VFP, a pressure difference existed at both ends of the column, which accelerated resumption of vapor flow.

Condenser isolation, as shown in Configurations 3 and 4, helps eliminate early drainage of the bottom trays. The two configurations are nearly alike, but if heat exchanger dynamic effects were included, Configuration 4 would have proved best.

Configuration 5, as used by Robinson[17], indicated that removal of the vapor pressure gradient allows liquid to flow under its own influence and stabilizes operation. All pressure manifold valves were open throughout the LFP. The manifold valves were closed in the VFP to permit normal operation. In this simulation, no account was taken of pressure equalization dynamics within the manifold, which would have a delaying effect on pressure profile destruction. However, the result was indicative of the beneficial effect of such a manifold, if it can be satisfactorily operated.

The long-term operation which shows the progress of composition disturbances over many cycles and which simulates the in-tray mixing phenomena, was not considered in this work.

Conclusions Regarding Cyclic Distillation

Experimentation with the simulation showed that it was apparently not possible to establish a constant liquid flow from each tray without

the deliberate destruction of the vapor pressure profile, as in Configuration 5. It appeared that cyclic distillation naturally maintained an approximately constant vapor pressure profile throughout the LFP when no manifolding facilities were employed. This lead to an unbalanced operation.

Furthermore, it appeared that tray free area adjustment could do little to stabilize all the liquid flows at a constant value throughout the column. Thus, it has been tentatively concluded that a physical method of maintaining tray level is required in place of the natural regulation hitherto presumed to exist.

Over short, one-cycle time intervals, Models A and B can be employed to simulate cyclic column behavior. The presented models are convenient tools which may be used for study purposes in parallel with the development of cyclic process technology. It is clearly established that close attention to both control and process design considerations is needed to insure that a cyclic distillation unit operates in a stable manner.

Concluding Remarks

Liquid-liquid extraction is another process which promises to benefit from the introduction of controlled cycling. Belter and Speaker[1] described the advantage of introducing controlled cycling to the multiple stage extraction column. Stevens and Brutvan[21] have studied the controlled cycling of centrifugal liquid-liquid extraction equipment and demonstrated significant capacity and efficiency improvements.

Other studies have been published about periodic chemical reactor operation[5], dynamic batch processing[6], chromatographic reactors[9], pulsed distillation[11], crystal purification[12] and size separation[16].

It becomes apparent in reviewing this field that the most suitable cyclic processing equipment may be quite different from that used generally for steady state processing. For instance, the contact condenser, where a spray of cool product into the overhead vapor stream causes condensation, is well suited for cyclic distillation. Such a condenser is readily switched "on" and "off" and the condenser cold zone is greatly reduced in extent. Also, large scale fluidic devices may find extensive application in replacing the on-off valves generally used at the present time. There are numerous novel and practical approaches to controlled cycling processing available for consideration.

Before the introduction of controlled cycling, a control objective was to eliminate dynamic phenomena. The concept of controlled cycling proposes to use dynamic phenomena advantageously. The idea is well

supported practically and theoretically and presents a rewarding and challenging area for joint process technology and process control development.

Nomenclature

A_T	area of tray
B	"bias" differential pressure, psi
C_{pL}	specific heat of liquid phase (molal basis)
C_{pV}	specific heat of vapor phase (molal basis)
C	total molal quantity of component on tray n
d_L	liquid depth on tray
E	total internal energy of liquid phase
F	constant in vapor pressure equation
g_c	gravitational constant
h, H	specific enthalpy of liquid and vapor phases
$J_V J_L$	dimensionless flow factors for vapor and liquid flow rates
K	constant
l	mass liquid flow rate
$\underline{l}$	normalized liquid flow rate (Tray Flow Model B)
L	molal liquid flow rate
M	molecular weight of pure components
M_L, M_V	molecular weights of liquid and vapor phase mixture respectively
N	total molal holdup of material on tray
P_d	pressure difference across holes in tray (see Equation 15)
P	vapor pressure of pure components
R	gas constant
v	mass vapor flow rate
$\underline{v}$	normalized vapor flow rate (Tray Flow Model B)
V	molal vapor flow rate
x,y	liquid and vapor mole fraction respectively
β	fractional part of free tray area passing vapor
ϕ	fractional free area on tray
π	total pressure
$\Delta\pi$	vapor pressure difference causing vapor flow
λ	heat of vaporization

ρ_L, ρ_V	molal density of liquid and vapor mixture respectively
ρ	pure component molal density
θ	temperature

Suffixes

i	pure component i
n	tray number in column
L	liquid
V	vapor
ref	reference condition
min	minimum value

Tray numbering convention

Suffix n+1	tray above tray n in column
Suffix n-1	tray below tray n in column

References

1. Belter, P. A. and S. M. Speaker
   Ind. Eng. Chem., Process Design & Dev., 6, 36, 1967
2. Cannon, M. R., Oil Gas J., 51, 1952
3. Chan, B. K. C. and R. G. H. Prince, AIChE J., 12, 232, 1966
4. Chien, H. H., J. T. Sommerfeld, V. N. Schrodt, and P. E. Parisot
   Separation Science 2, 281-317, 1966
5. Douglas, J. M.
   Ind. Eng. Chem., Process Design & Dev., 6, 43, 1967
6. Evangelista, J. J. and S Katz
   Ind. Eng. Chem., 60, 25, 1968
7. Gaska, R. A. and M. R. Cannon
   Ind. Eng. Chem., 53, 631, 1961
8. Gerster, J. A. and H. Scull
   "Performance of Tray Columns Operated in the Cycling Mode"
   Referenced facts are as orally presented at 60th Annual Meeting of AIChE, Nov. 26-30, 1967
9. Gore, F. E.
   Ind. Eng. Chem., Process Design & Dev., 6, 10, 1967
10. Horn, F. J. M.
    Ind. Eng. Chem., Process Design & Dev., 6, 30, 1967
11. McGurl, G. V. and R. N. Maddox
    Ind. Eng. Chem., Process Design & Dev., 6, 6, 1967
12. McKay, D. L. and H. W. Goard
    Ind. Eng. Chem., Process Design & Dev., 6, 16, 1966

13. McWhirter, J. R. and M. R. Cannon
Ind. Eng. Chem., 53, 633, 1961

14. McWhirter, J. R. and W. A. Lloyd
Chem. Eng. Prog., 59, 58, 1963

15. Prince, R. G. H. and B. K. C. Chan
Trans, Inst. Chem. Engrs. (UK), 43, 1965

16. Robertson, D. C. and A. J. Engel
Ind. Eng. Chem., Process Design & Dev., 6, 2, 1967

17. Robinson, R. G.
"A Theoretical Analysis of Controlled Cycling Mass Transfer Operations and an Investigation of Oxygen Absorption in Controlled Cycling Apparatus", PhD Thesis, Penn State University, Dec. 1964

18. Robinson, R. G. and A. J. Engel
Ind. Eng. Chem., 59, 25, 1967

19. Schrodt, V. N., J. T. Sommerfeld, O. R. Martin, P. E. Parisot, and H. H. Chien, "Plant - Scale Study of Controlled Cyclic Distillation". Chemical Engineering Sciene 22 (5). 759-767. 1967

20. Sommerfeld, J. T., V. M. Schrodt, P. E. Parisot, and H. H. Chien
Separation Science 1, 245-279, 1966

21. Stevens, J. E. and D. R. Brutvan
Paper 51C, 60th Annual Meeting AIChE

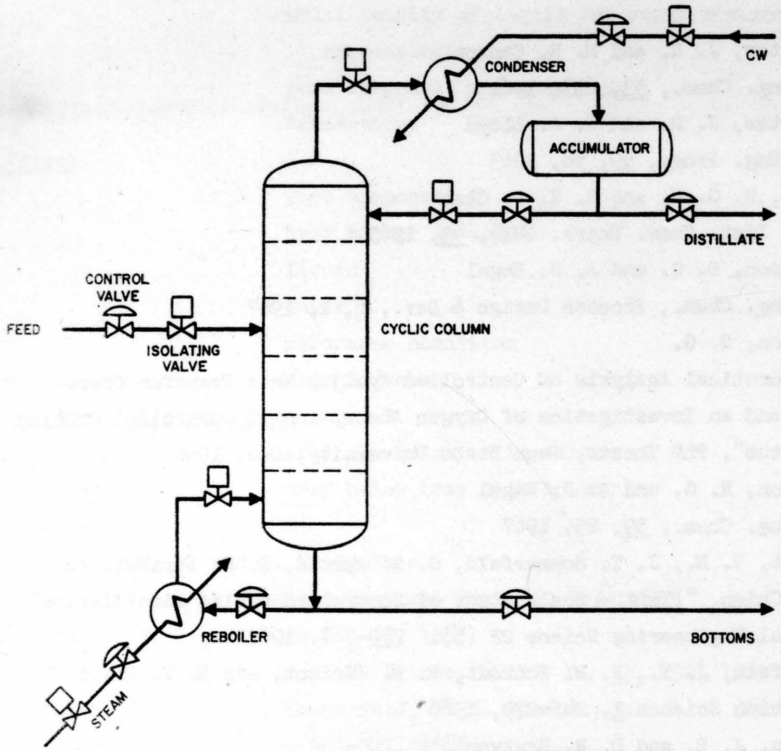

Figure 1 - General equipment configuration for cyclic distillation.

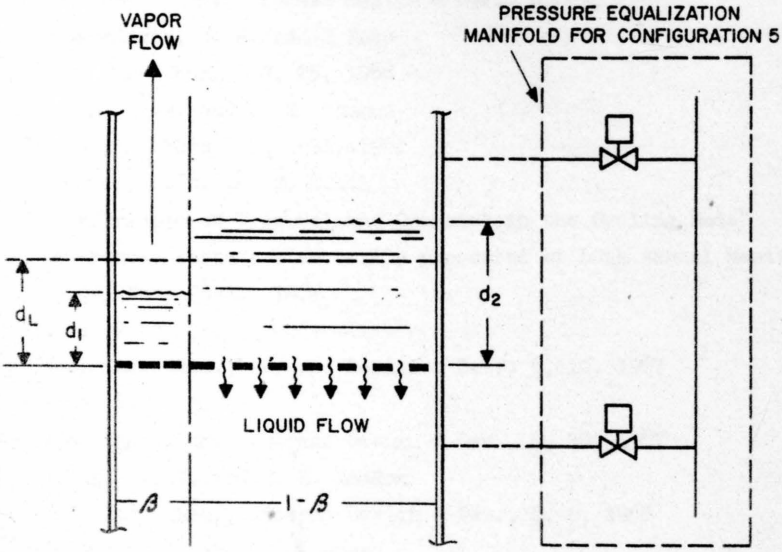

Figure 2 - Tray assumed for flow model B.

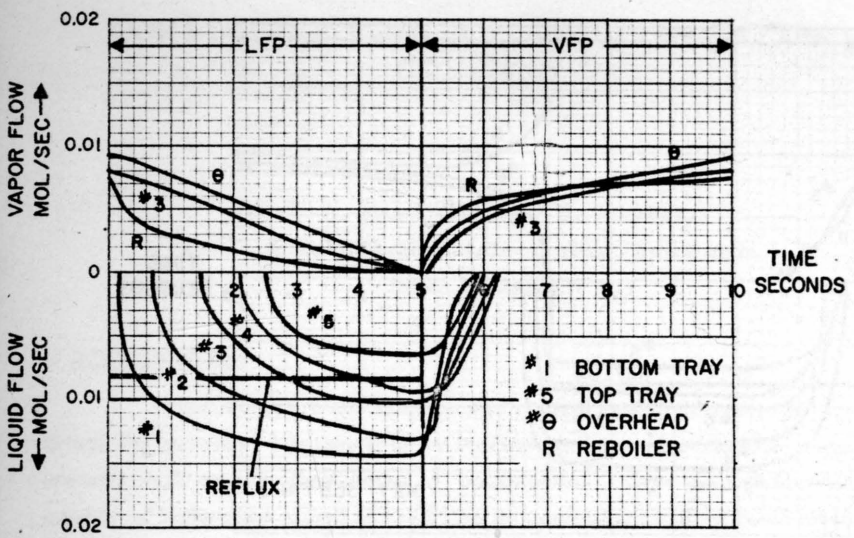

Figure 3 - Configuration No. 1 - No reboiler or condenser isolation.

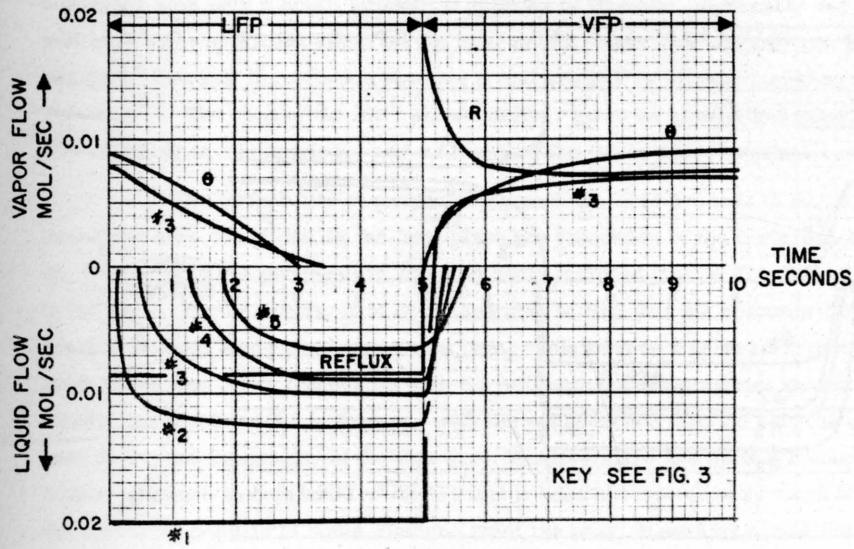

Figure 4 - Configuration No. 2 - Reboiler only isolated.

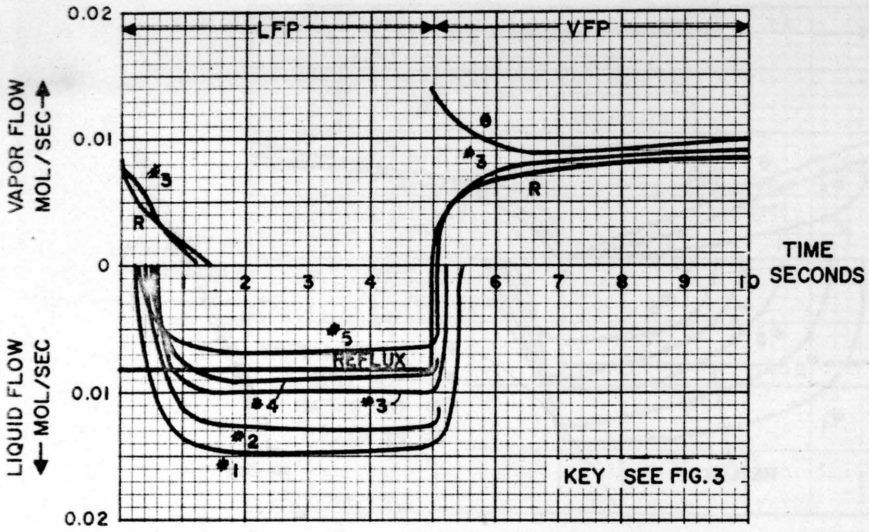

Figure 5 - Configuration No. 3 - Condenser only isolated.

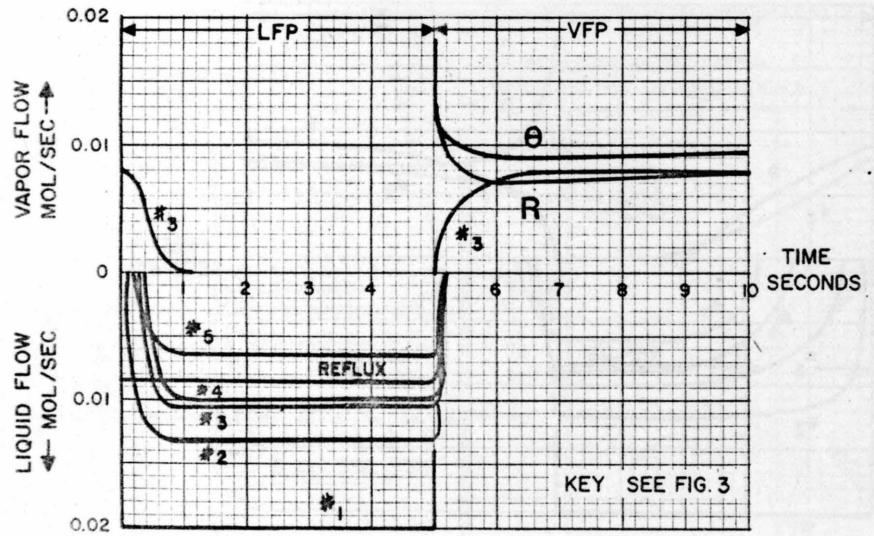

Figure 6 - Configuration No. 4 - Reboiler and condenser isolated.

CONSTRAINT CONTROL ON DISTILLATION COLUMNS

by

A. Maarleveld and J.E. Rijnsdorp
Koninklijke/Shell-Laboratorium, Amsterdam
(Shell Research N.V.)

I. INTRODUCTION

The modern trend in automatic control is to increase profit in the most direct way possible, whether it be by increasing the production rate, reducing the specific costs or any other means of "optimization". Over the last few decades a number of techniques aimed at achieving this optimization have been developed. They range from simple off-line manual calculations to complicated on-line computer calculations. So far, however, most of the applications in industry have been of the static type; and it is only recently that the results of studies on dynamic optimization seem to have come within the reach of the process control engineer.

The beau idéal of a control engineer considering optimizing control is a process with only a small number of degrees of freedom (preferably one) that will have any significant effect on the total profit. When there is only one such degree of freedom the relation between it and profit P is often depicted as in Figure 1[(a)]. The "top of the hill" should neither move so slowly that automatic hill-climbing is meaningless, nor so fast that the top is never reached.

The probability of encountering such an ideal process is small. We ourselves have found that in the first place the frequency of the disturbances and the dynamics of the process are often so badly matched that on-line hill-climbing is too slow. Furthermore, it is not uncommon to find that the optimum cannot be reached without some plant constraint being violated (see Figure 1(b)). For instance, when heavy fuel oil is combusted with the optimum (stoichiometric) amount of air, usually too much smoke is formed, with the consequence that the critical constraint here is the smoke density in the flue gas. Finally, there are quite a number of instances where the optima are so flat that it does not matter very much whether the operating point is at some distance from the peak or even on one of the neighbouring constraints (see Figure 1[(c)]).

A similar reasoning also applies to cases with more than one degree of freedom. If the relationships $P = P(V_1, \ldots V_n)$ and $C_i = C_i(V_1, \ldots V_n)$ are not too non-linear, the point of most economic operation will usually be found at the intersection of as many constraints as there are degrees of freedom (see Figure 2 for n = 2).

If the constraints for the most economic operation are always the same, automatic control is very simple: one uses as many control loops as there are constraints, each control loop being associated with a particular constraint. If there is severe interaction some form of non-interacting control can be applied. It may incidentally be noted that for not too large disturbances such a control scheme is optimal in the dynamic sense also[1]. More interesting are cases where the point of most economic operation lies on different constraints for different operating conditions (different throughput, feed composition, etc.). Then control has to be switched automatically from one set of constraints to another. It is this type of automatic control which we mean in talking of "constraint control", and which we shall seek to illustrate in this paper, taking a simple distillation process as our example.

II. DEGREES OF FREEDOM IN A SIMPLE DISTILLATION PROCESS

The distillation process considered here is the one shown in Figure 3. Feed flow rate and composition will be considered to be independent variables. There are seven control valves in all. Five of these are not available for optimization purposes:

H_W, the amount of feed bypassed around the first feed preheater. Since, in the example chosen, waste heat is recovered, closing the bypass is the optimum solution, and the control valve can be omitted.

D, usually, as in the example, used for accumulator level control,

B, usually used for bottom level control,

R and H_B, used for top and bottom quality control. One is always used for keeping the most valuable product at its quality constraint; the other can be used in the same way for the other product, or, which is more often the case, is used to set an optimum reflux or reboil ratio. (This is an example of the flat optimum shown in Figure 1(c).)

The remaining degrees of freedom for optimization are:

H_F, valve in the heating medium line to the second feed preheater,

C, valve in the cooling water line to the condenser. It could equally well be any other valve influencing condenser cooling. This valve can be used for pressure

control, in which case the column pressure P (set point of the pressure controller) is the actual degree of freedom.

What now are the effects of H_F and P on the economy of operation? Regarding H_F, or better the distribution of heat over feed preheater and reboiler, it could be said that heat introduced via the reboiler is used more efficiently in that it increases the vapour flow, and so improves the separation, on all the trays, whereas heat transferred via the feed preheater increases the vapour flow in the rectifying section only. However, one must consider the total cost of heating, and not simply the heat requirement expressed in thermal units. It could well be that the specific cost of feed preheating is lower than that of reboiling, and it will depend on the ratio of these specific costs as well as on the location of the feed inlet (the lower the feed inlet, the more efficient the feed preheating) whether it is in fact more profitable to make as much or as little use of feed preheating as possible.

As for the column pressure P it is generally true to say that separation is easier (requires less vapour flow) at lower pressures because the relative volatilities of the components are higher*. On the other hand, decreasing the pressure generally increases the heat of vaporization, which means that more heat is needed to generate the same vapour flow rate. For columns operating at low reflux ratios, this second effect can be more significant than the first, because the (fixed) top product flow rate constitutes the major part of the vapour flow rate. However, in the case of columns operating at not too low reflux rates it has been found that the first effect is the more significant, thus making it profitable to aim for the lowest possible column pressure.

One way in which operation at a lower pressure than the design pressure can be accomplished arises out of the fact that in the design of a distillation column less favourable conditions are assumed than in fact prevail on average during actual operation. The condenser, in particular, is made so large that the design throughput will still be guaranteed if the cooling water gets heated and when there is dirt and scale inside the tubes, even though for most of the time, in actual operation, conditions will be less severe and the condenser will have a surplus capacity. It is by utilizing this surplus capacity that the column can be operated at a lower pressure. A similar situation can exist with respect to the other degrees of freedom.

---

* This might not be true where chemically unrelated components have to be separated, but the same concept of constraint control can still be applied, albeit in the opposite direction (increasing pressure).

III. COST AND CONSTRAINT DIAGRAM

The effect of the two degrees of freedom on the economy of operation can be determined quantitatively and plotted in a diagram as shown in Figure 4. In drawing up this diagram the following assumptions have been made:

(a) Both products have to be kept just at the specification limits. For a given feed, this virtually fixes the amounts of top and bottom product.

(b) Cooling and pumping costs are negligible. Hence, economy of operation is completely determined by the total heating costs in feed preheater and reboiler together.

(c) The specific costs of feed preheating (in the second preheater) and reboiler heating are known, or at least their ratio. They are not significantly affected by changes in the operation of the column.

(d) The pumping capacity is always ample.

It should be noted that these particular assumptions are not essential to the method of approach described here.

The dotted lines in Figure 4 are lines for equal total heating cost (expressed in arbitrary units). Feed vaporization is expressed as the increase in column vapour flow passing through the feed tray per unit of feed. It appears that, in the example given, the specific cost of feed preheating is not very low and the feed inlet is not close to the bottom, otherwise the slope of the cost lines would be infinite or even positive.

It follows from the figure that the optimum operating point is somewhere in the lower left-hand corner of the diagram: as little (expensive) feed preheating as possible and column pressure as low as possible. However, there is generally only a limited area of the diagram within which operation is feasible. The limits are formed by the maximum capacity of the reboiler and of the condenser, the maximum and minimum capacity of the second feed preheater, and the maximum loading of the trays in the stripping and rectifying sections of the column. These form constraints, which can be depicted in the same diagram as the cost lines (see Figures 5 and 6). These constraints are derived as follows:

$H_{B\,max}$: The heat flow in the reboiler is dependent on the temperature difference between column bottom and heating medium. The column temperatures increase with column pressure, with the consequence that the heating medium valve has to be opened further to introduce the same amount of heat. But there will come a point, at a certain column pressure, when the heating medium valve cannot be opened any further, i.e. the constraint will have been reached. The constraint line has a positive slope, because more feed preheat involves less reboiler heat,

and thus a higher column pressure can be tolerated. If the feed flow increases, then the column vapour flow has to be increased accordingly. But this will be possible only if the temperature difference in the reboiler is increased, and hence the column pressure is decreased. This thus means that on an increase in throughput the constraint line will shift to the left.

C_{max}: The heat flow in the condenser is dependent on the temperature difference between column top and cooling water. In this case, therefore, the constraint is reached when the top temperature, and hence the column pressure, is low. If the feed preheating is increased, however, the column vapour flow will increase due to less economical use of the total heat (see Figure 4), and the condenser constraint will be reached at a somewhat higher column pressure. On an increase in throughput the constraint line will shift to the right. The location of the line is, of course, also dependent on the cooling water temperature. In winter the minimum column pressure is lower than it is under summer conditions.

$H_{F\,min}$ and $H_{F\,max}$: There are two constraint lines related to the second feed preheater. Firstly, if the heating medium valve to the preheater is closed, then the feed temperature (and feed vaporization) will depend on the usage of (cheap) waste heat. Let us now assume that under these conditions the feed enters the column below bubble point, so that feed vaporization is negative. Clearly, the higher the column pressure, the more the feed will be subcooled. Consequently, the $H_{F\,min}$-line will have a negative slope. Secondly, when the heating medium valve is fully open, the feed may be assumed to be above bubble point. If now the column pressure and hence the column temperatures increase, the difference between feed and column temperature will become smaller, so that feed vaporization will tend to zero.

R_{max} and S_{max}: When the column pressure is changed, there are two effects on the loading of the trays, working in opposite directions:

(a) If the pressure is decreased, the relative volatility will be increased, and hence the internal column flows can be decreased, as shown in Figure 7. This has an unloading effect on the trays. Consequently, upon an increase in pressure the internal liquid and vapour flow rates in the column have to be increased to keep the products on specification. In the neighbourhood of the convergence pressure of the mixture this increase in the column flows, and hence in the tray load, will be very marked.

(b) With a decrease in pressure the vapour density ρ_v decreases. To maintain the same (mass or molal) vapour flow therefore the velocity U_v has to be increased in the same ratio, which means that, being mainly determined by the kinetic energy of the vapour, $\rho_v . U_v^2$, the tray load is increased.

This means that tray constraints are found both when the pressure is increased and when it is reduced. Furthermore, if the feed preheating is increased the vapour flow in the rectifying section will be larger, and hence the range of column pressures allowing feasible operation will be smaller. When the rate of feed vaporization is increased still more the trays in the rectifying section will be overloaded irrespective of the pressure. A similar reasoning holds for the trays in the stripping section and for a subcooled feed. The tray constraint lines are given in Figure 6. If the column throughput increases, the feasible area shrinks. For a column operating at point A, the maximum throughput increases with increasing pressure; for point B it increases with decreasing pressure.

IV. CONSTRAINT CONTROL SCHEME

The cost lines of Figure 4 and the constraint lines of Figures 5 and 6 can be combined in one diagram. The result, for different column throughputs, is given in Figure 8.

The point of optimum operation is denoted by Q. With a low throughput the trays are not loaded to capacity, and Q lies on the intersection of C_{max} and $H_{F\,min}$ (Fig. 8(a)). This means the valve in the cooling water line to the condenser is completely open and the valve in the (relatively expensive) heating medium to the feed preheater is closed.

If the throughput increases, all the constraint lines will shift towards the centre of the diagram, but the tray constraints will move faster than the others. At throughput F_2 (Fig. 8(b)) the optimum operating point is found when the top cooling is still maximum but the feed preheater valve has had to be partly opened to unload the stripping section trays. If the throughput increases even further, the condenser valve will have to be partly closed and operation will be at its optimum point when all trays are just loaded to capacity (Fig. 8(c)).

In the control scheme shown in Figure 9 the switching from one set of constraints to another is performed automatically. The loading of the trays is ascertained by measuring the pressure difference over the two sections. Since the tray load control is critical, the differential pressure controllers must manipulate a control valve which has a rapid and strong effect on the vapour flow. Their out-

puts pass to the high-pressure selectors H_1 and H_2, which allow the higher of the two signals to pass on. When the actual pressure difference is smaller than the maximum difference tolerated, the dPC outputs are both minimum, in which case 3 psig. is passed to the cooling water valve, just sufficient to keep it wide open. Further, the balancing controller BC is forced to keep the valve H_F closed. This is the situation illustrated in Figure 8(a).

If the column throughput increases, dP_S will increase and the output of dP_SC will start to rise as soon as $dP_{S\,max}$ is reached. The cooling water valve will then be partly closed, and since the two inputs to BC will not now be equal, the H_F valve will be partly opened. This has the effect of unloading the stripping section trays, until a new equilibrium is reached. Then the two signals to BC will be equal to 3 psig., so that the output of H_2 will be minimum again and the cooling water valve will be fully open. This is the situation illustrated in Figure 8(b). It is also important to note in this connexion that initially the tray load is controlled by valve C, which ensures fast and powerful action, but that this function is later taken over by H_F, which has a slower and weaker effect on tray load.

If the throughput increases further, the trays in the rectifying section also might become overloaded. Then the output signal of dP_RC will increase. The ultimate result will be that BC will eventually adjust valve H_F in such a way that the outputs of the two dPC's are equal again (both sections just loaded to capacity) and that valve C will be partly closed. This corresponds to the situation shown in Figure 8(c).

Summarizing, we see that always the relevant set of constraints is selected, and that the transition from one set to another is smooth and safe (initial action with a fast valve, final adjustment with a slow valve).

The scheme can easily be extended if the process involves more constraints than are mentioned here, such as a minimum and/or maximum column pressure, or maximum reflux pump capacity[4]. It can also be simplified if, within the range of throughputs considered, certain constraints are never reached.

V. EXPERIMENTAL RESULTS

Figure 10 gives the results for an actual refinery column: a deisopentanizer at the Shell Nederland Refinery, Pernis. The numbers by the (dotted) cost lines represent the cost per unit time expressed in arbitrary units. Two constraint lines are given for the condenser, one for average winter conditions and one for average summer conditions. For throughputs below 2000 tons/day the tray

constraints do not play any role. Here, in fact, the "constraint control scheme". is simply a matter of keeping the cooling water valve fully open and the feed pre-heater valve closed. With throughputs above 2000 t/d, however, the trays in the stripping section might become overloaded. Then a control scheme like the one shown in Figure 9 is applicable. If there is no danger of the trays in the rectifying section becoming overloaded dP_RC and H_2 can be omitted.

The omission of any form of pressure control was not found to have a detrimental effect on the operation of the column. However, good automatic quality control[2,3] proved to be essential in order to reap the full benefits of constraint control.

VI. CONCLUSION

For many processes optimal operation means operation on or close to a number of constraints. If the relationships are not too non-linear the optimum operating point is at the intersection of as many constraints as there are degrees of freedom left for optimization. This simplifies the optimization procedure considerably, with the result that in place of a hill-climbing technique, a number of conventional feedback controllers can be used. However, when the constraints are liable to shift significantly during operation, a slightly more elaborate control scheme is required.

ACKNOWLEDGEMENT

The authors would like to acknowledge the contributions to this work from M. Veldkamp, who was responsible for most of the numerical and part of the experimental work, and from J. Werkema and H. Bollen, who also participated in the experimental work.

REFERENCES

1. J.E. Rijnsdorp, Chem. Eng. Progr., July 1967, pp. 97-116, Appendix II.
2. J.A. van Kampen, Conv. Adv. Aut. Control, Inst. Mech. Engrs., Nottingham (England), Proc. Inst. Mech. Engrs. (London), 179(1964-65), part 3H. "Automatic control by chromatographs of the product quality of a distillation column".
3. J.E. Rijnsdorp, J.A. van Kampen and H. Bollen, 3rd IFAC Congress, London, June 1966 "Automatic feedback control of two product qualities of a distillation column".
4. British Patents nos. 1,005,336; 1,018,884; 1,020,477; 1,023,294; 1,024,316 and 1,026,356.

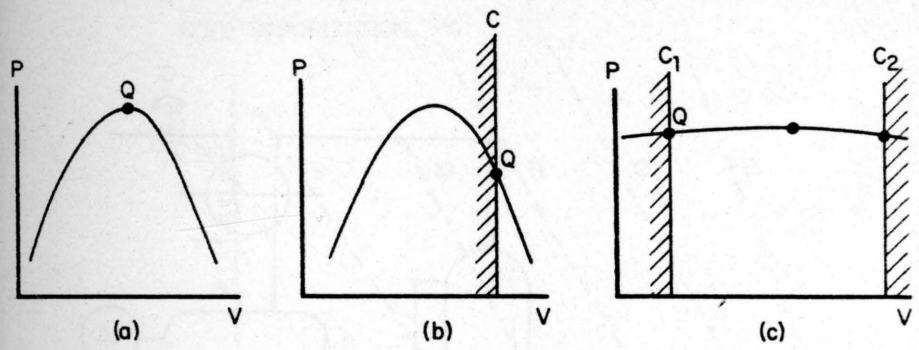

Fig. 1. Optimal operation with and without constraints

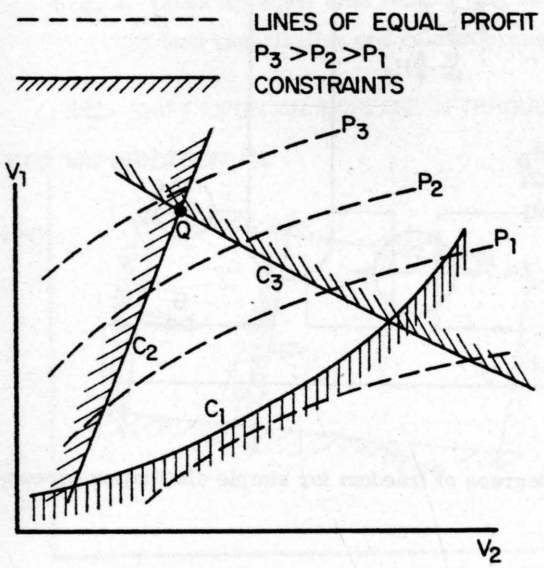

Fig. 2. Optimal operation at intersection of two constraints when there are two degrees of freedom

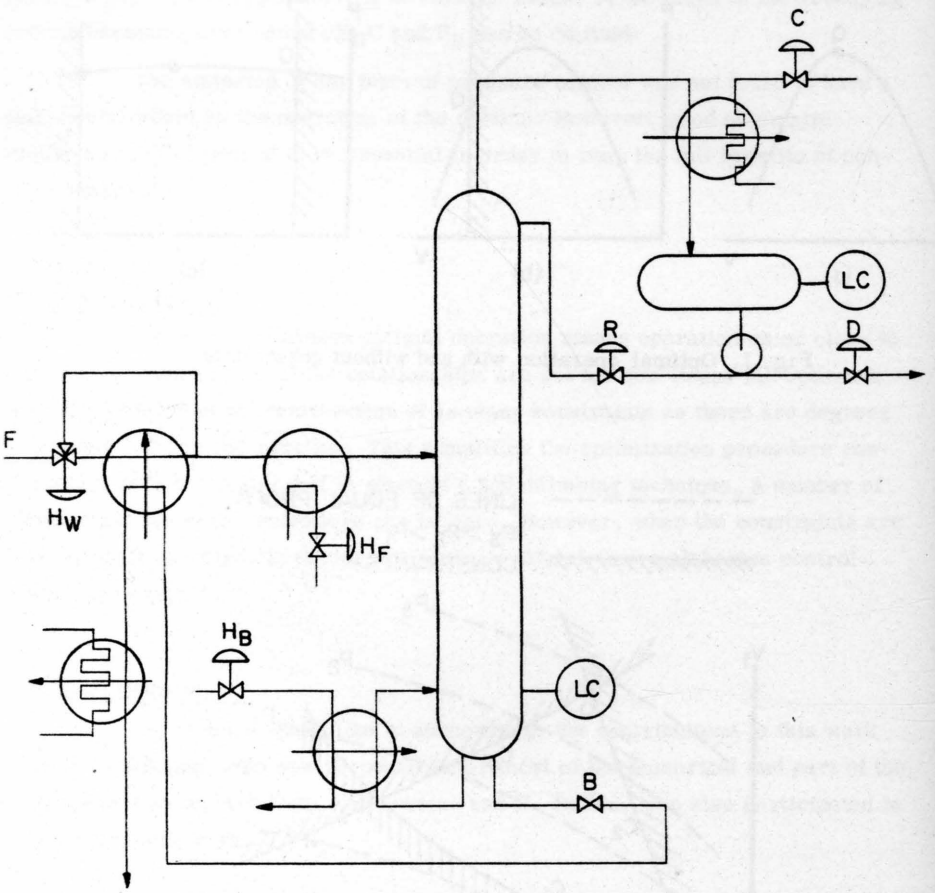

Fig. 3. Degrees of freedom for simple distillation process

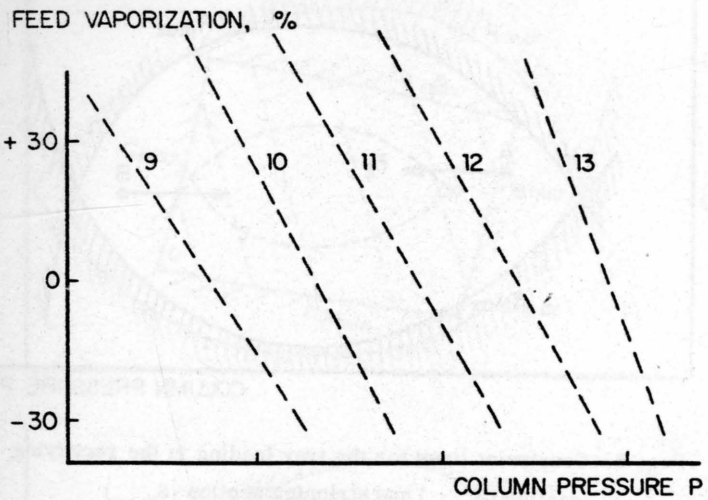

Fig. 4. Lines for equal total heating cost as a function of feed vaporization and column pressure

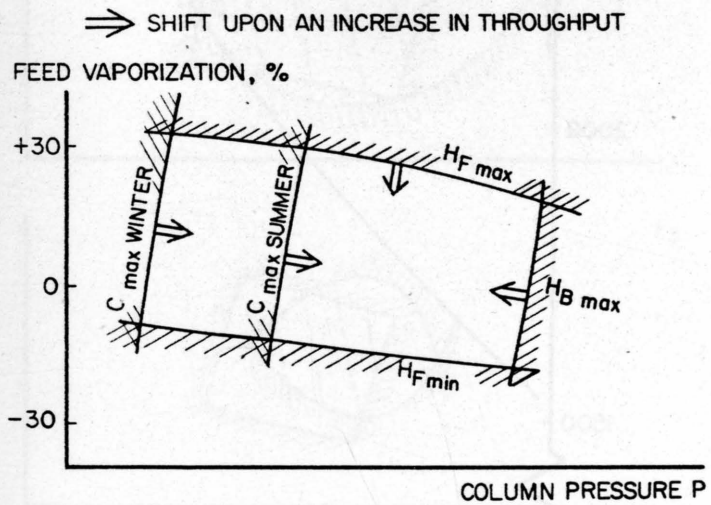

Fig. 5. Constraint lines for reboiler, condenser and feed preheater

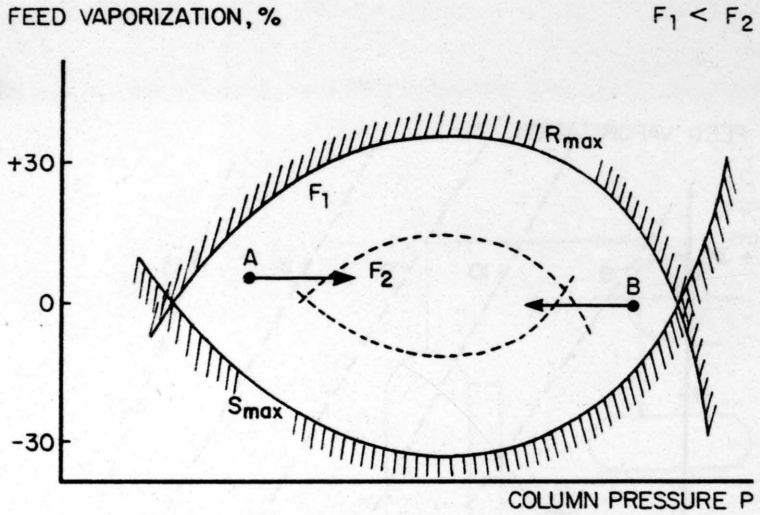

Fig. 6. Constraint lines for the tray loading in the rectifying section (R_{max}) and stripping section (S_{max})

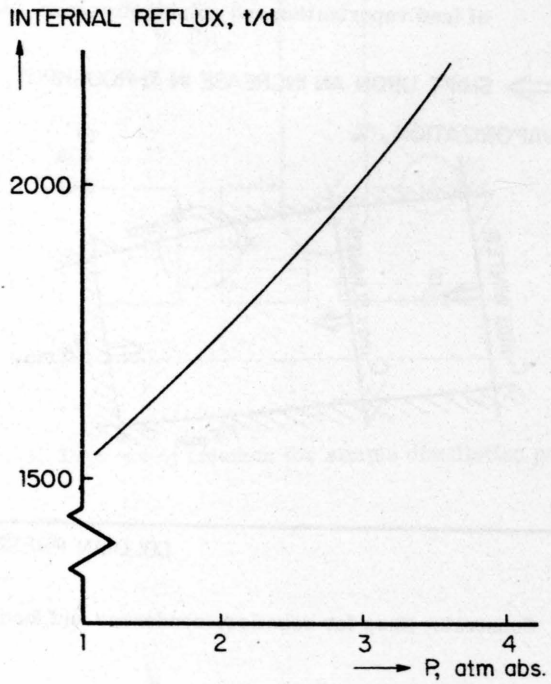

Fig. 7. Relation between required reflux and column pressure for a deisopentanizer (feed: 1500 t/d)

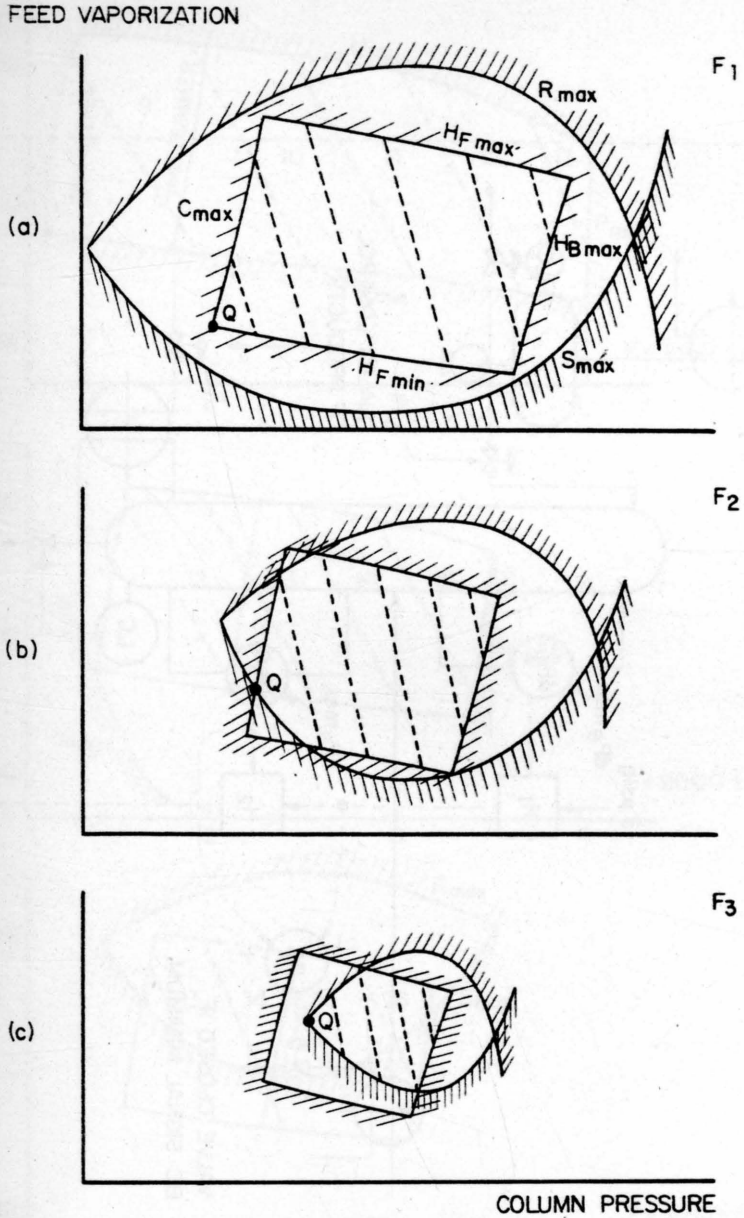

Fig. 8. Constraint diagrams for different throughputs F ($F_1 < F_2 < F_3$)

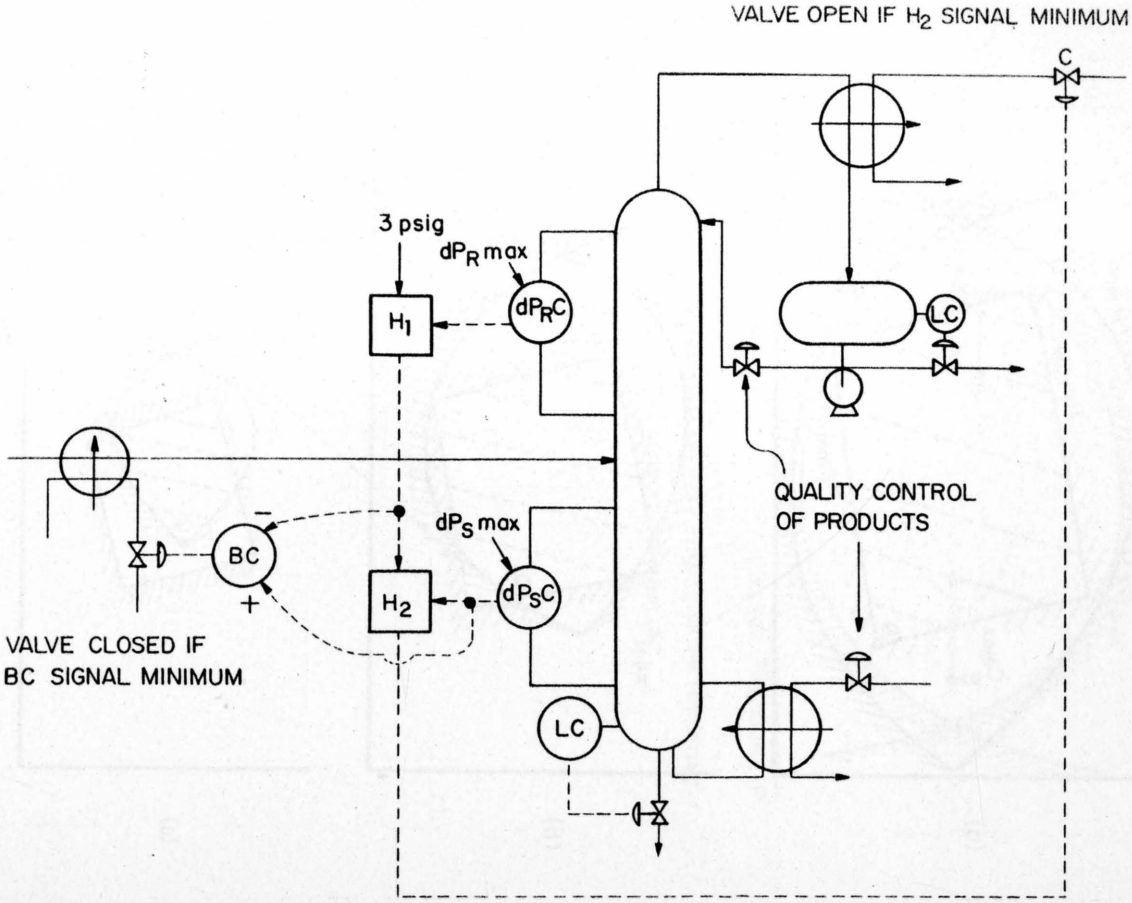

Fig. 9. Constraint control scheme for a simple distillation column

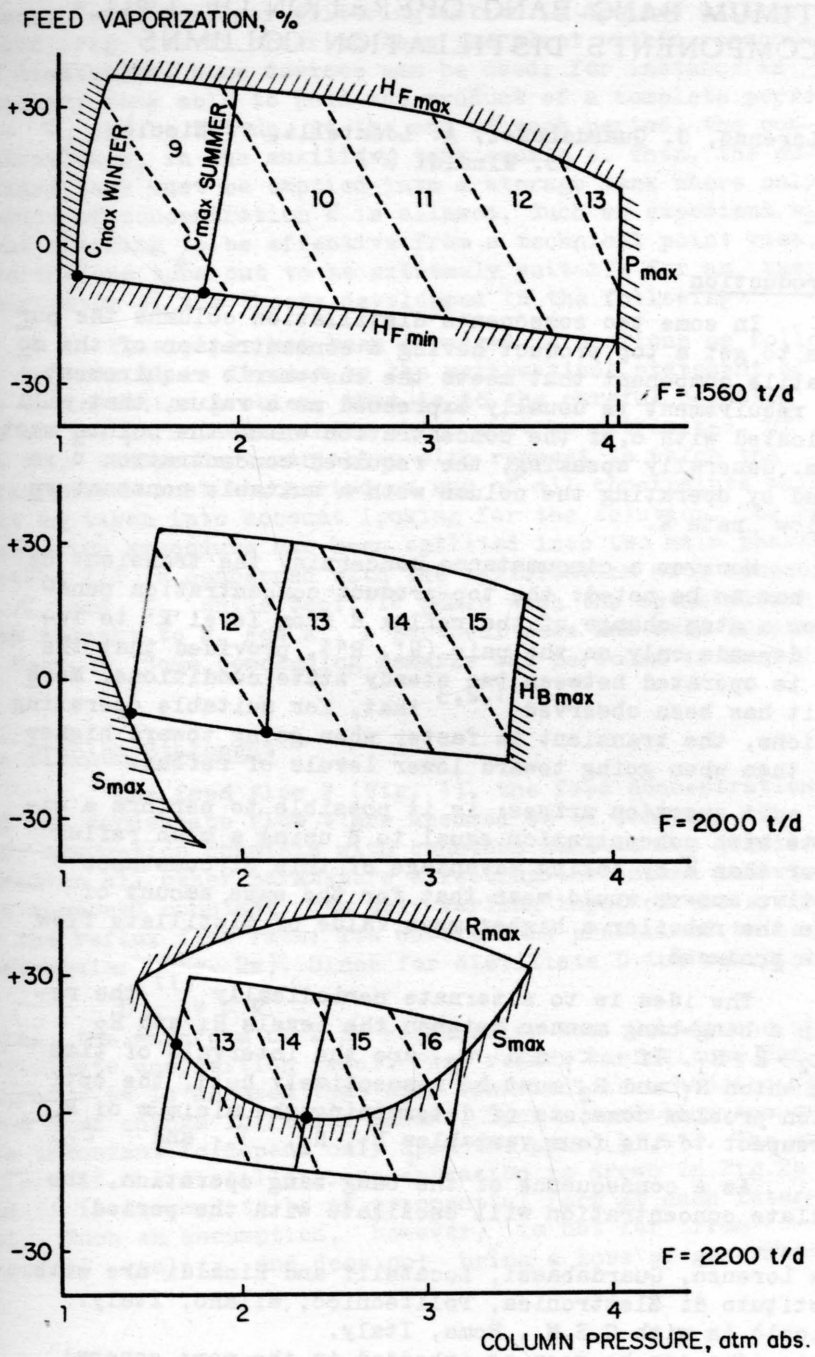

Fig. 10. Constraint diagrams for a deisopentanizer

OPTIMUM BANG-BANG OPERATION OF TWO COMPONENTS DISTILLATION COLUMNS

F. De Lorenzo, G. Guardabassi, A. Locatelli, V. Nicolò, S. Rinaldi (°)

I. Introduction

In some two components distillation columns the purpose is to get a top product having a concentration of the more volatile component that meets the customer's requirement. Such a requirement is usually expressed as a value, that will be indicated with $\bar{c}$, of the concentration which the column must perform. Generally speaking, the required concentration $\bar{c}$ is obtained by operating the column with a suitable constant reflux flow rate $\bar{R}$.

However a circumstance concerning the transient behavior has to be noted: the top-product concentration behavior for a step change of the reflux R from level R' to level R" depends only on the pair (R', R"), provided that the column is operated between two steady state conditions. Moreover, it has been observed [1,2,3] that, for suitable operating conditions, the transient is faster when going toward higher levels than when going toward lower levels of reflux.

A question arises: is it possible to perform a distillate with concentration equal to $\bar{c}$ using a mean reflux R_m lower than $\bar{R}$ by taking advantage of this circumstance ? A positive answer would mean that for the same amount of heat to the reboiler a higher mean value of distillate flow rate is produced.

The idea is to alternate periodically [(1)] the reflux in a bang-bang manner between the levels R_1 and R_2 with $R_2 > \bar{R} > R_1$. If τ_1 and τ_2 are the intervals of time during which R_1 and R_2 must be respectively held, the optimization problem consists of determining the minimum of R_m with respect to the four variables R_1, R_2, τ_1 and τ_2.

As a consequence of the bang-bang operation, the distillate concentration will oscillate with the period

---

(°) De Lorenzo, Guardabassi, Locatelli and Rinaldi are with Istituto di Elettronica, Politecnico, Milano, Italy. Nicolò is with C.S.M., Roma, Italy.

1) This idea can be seen as imbedded in the more general philisophy of optimal periodical operation introduced by Horn and Lin [4].

$\tau_1 + \tau_2$, so that to smooth fluctuations a tank of greater capacity when stronger filtering action is desired will be needed (Fig. 1). In order to keep the plant within reasonable dimensions, some devices can be used: for instance an auxiliary tank able to hold the product of a complete period $\tau_1 + \tau_2$ can be set up. At the end of each period, the concentration c_T in the auxiliary tank equals $\bar{c}$. Then, the auxiliary tank must be emptied into a storage tank where only product of concentration $\bar{c}$ is allowed. Such an expedient without claiming to be effective from a technical point view, nevertheless turns out to be extremely suitable for an easy description of the theory developped in the following.

This paper has been arranged in sections as follows. Section II is devoted to the mathematical statement of the optimization problem, that is to the careful pointing out of the performance index which must be extremized, of the four indipendent variables with respect to which the optimization must be carried on and of all constraints which must be taken into account looking for the solution. The optimization procedure has been splitted into two main phases. Section III is concerned with the optimization with respect to τ_1 and τ_2, while Sect. IV deals with the optimization with respect to R_1 and R_2. A particul case has been treated in Sect. V. Some concluding remarks can be found in Sect.VI.

II. Problem Statement

The feed flow F (Fig. 1), the feed concentration and the condensate flow V are assumed to be constant. The last assumption consists with constant heat to the reboiler. Moreover all other parameters affecting the column behavior are supposed constant. The only variing input of the system is the reflux flow rate: its waveform is prescribed to be rectangular (Fig. 2a). Since for distillate D the equation:

$$D = V - R$$

holds, the waveform of D is rectangular too. Variations of distillate composition result from reflux variations; furthermore it is assumed that each transient is exhausted before next change in reflux occurs. Such a condition ensures the transient to depend only upon the pair (R',R"). The waveform of the distillate concentration is drown in Fig.2b and it is assumed to be of exponential form at each interval. Such an assumption, however, is not far from physical reality and does not bring a loss of genera-

lity of results [2].

In Fig. 2b, c_1 and c_2 are the steady state concentrations corresponding to R_1 and R_2 which can be determined from the steady state characteristic:

$$c = c(R) . \tag{1}$$

Besides, owing to the fact that the transient depends only on the pair (R', R"), i. e. on the pair (R', ΔR), $\Delta R = R" - R'$, the time constant T is still function of R' and ΔR:

$$T = T(R', \Delta R). \tag{2}$$

Therefore, the two time constants T_1 and T_2 indicated in Fig. 2b are given by:

$$\begin{aligned} T_1 &= T(R_1, R_2 - R_1) \\ T_2 &= T(R_2, R_1 - R_2). \end{aligned} \tag{3}$$

For the above assumptions about the nature of the transients of the distillate concentration, the time intervals τ_1 and τ_2 have to be chosen sufficiently large. Therefore the constraints:

$$\begin{aligned} \tau_1 &\geqslant k\, T_1 \\ \tau_2 &\geqslant k\, T_2 \end{aligned} \tag{4}$$

must be fulfilled.

In eqs. (4) k is a suitable constant which has to be big enough in order that the transient could be practically considered exhausted. On the other hand a great value of k implies certainly a large period $\tau_1 + \tau_2$ of operation: therefore the dimensions of the auxiliary tank increase. As a conclusion, small values of k consistent with the above assumptions are to be preferred. In practice, values of k ranging between 4 and 5 seem to be appropriate.

---

(2) If such an assumption is not met, an equivalent exponential transient between the same levels will be considered: the equivalence is here taken in the sense that the areas subtended by both the real and equivalent transient are equal.

The value c_T of the concentration of the distillate in the auxiliary tank at the end of a period $\tau_1 + \tau_2$ must equal the desired value $\bar{c}$:

$$c_T = \frac{\int_0^{\tau_1} (V-R_2)\, c(t)dt + \int_{\tau_1}^{\tau_1+\tau_2} (V-R_1)\, c(t)\, dt}{(V-R_1)\,\tau_2 + (V-R_2)\,\tau_1} = \bar{c} \qquad (5)$$

Eq. (5) implies that

$$R_1 \leqslant \bar{R}$$
$$R_2 \geqslant \bar{R} \qquad (6)$$

Since

$$V - F \leqslant R \leqslant V$$

it follows from eq. (6)

$$V - F \leqslant R_1 \leqslant R$$
$$\bar{R} \leqslant R_2 \leqslant V .$$

These inequalities determine in the plane (R_1, R_2) a closed region Ω_M. Nevertheless other circumstances might impose different types of constraints, so that the region Ω where it is possible to choose the values R_1 and R_2 turns out to be generally smaller than the region Ω_M.

The minimum of the mean value R_m of the reflux is searched: this means that the ratio of distillate flow rate to heat flow to the reboiler is maximum.

The mean value R_m of the reflux is given by:

$$R_m = \frac{R_2\,\tau_1 + R_1\,\tau_2}{\tau_1 + \tau_2} \qquad (7)$$

Therefore, the following minimization problem will be investigated:

$$R_m^o = \min_{\substack{R_1,R_2 \\ \tau_1,\tau_2}} \{R_m\} = \min_{\substack{R_1,R_2 \\ \tau_1,\tau_2}} \left\{ \frac{R_2\,\tau_1 + R_1\,\tau_2}{\tau_1 + \tau_2} \right\} \qquad (8)$$

where R_1 and R_2 belong to Ω, τ_1 and τ_2 satisfy eq. (4) and (5) is taken into account (3). This optimization problem can be conveniently solved in two steps, as it is shown in Fig. 3 where the specific symbolism of Structural Programming has been adopted. Then the minimization procedure will follow the sequence of sections S_1 and S_2 drawn in Fig. 3 where the condition $c_T = \bar{c}$ is entailed by the fact that both S_1 and S_2 cut the arrow representing c_T.

According to Fig. 3, the first step of problem solution consists of finding the minimum of R_m with respect to τ_1 and τ_2, regarding R_1, R_2 and c_T as prescribed, i.e.:

$$R_{m\tau} = \min_{\substack{\tau_1 \geq k\,T_1 \\ \tau_2 \geq k\,T_2}} \{R_m\} = \min_{\substack{\tau_1 \geq k\,T_1 \\ \tau_2 \geq k\,T_2}} \left\{ \frac{R_2\,\tau_1 + R_1\,\tau_2}{\tau_1 + \tau_2} \right\} \qquad (9)$$

The values of τ_1 and τ_2 which are the solutions of eq.(9) will result, of course, to be functions of R_1 and R_2:

$$\begin{aligned} \hat{\tau}_1 &= \hat{\tau}_1 \ (R_1, R_2) \\ \hat{\tau}_2 &= \hat{\tau}_2 \ (R_1, R_2) \end{aligned} \qquad (10)$$

Next step (section S_2 of Fig. 3) is the minimization of R_m with respect to R_1 and R_2:

$$R_m^o = \min_{(R_1,R_2)\in\Omega} \{R_{m\tau}\} = \min_{(R_1,R_2)\in\Omega} \left\{ \frac{R_2\hat{\tau}_1 + R_1\hat{\tau}_2}{\hat{\tau}_1 + \hat{\tau}_2} \right\} \qquad (11)$$

Therefore, the values R_1^o and R_2^o which solve eq.(11) and

---

(3) It is to be noted that even a small decrease of reflux mean value might correspond to a high increase of the ratio of distillate mean flow rate D_m to the distillate flow rate $\bar{D}$ of the constant reflux operation. In fact it turns out that $D_m/\bar{D} = 1+(1-R_m/\bar{R})\bar{R}/D$) hence for columns with high values of the reflux ratio it is possible to get, by means of the bang-bang operation, considerable increases of distillate mean flow rate at the desired concentration $\bar{c}$, even if the value of R_m is not very different from $\bar{R}$.

the corresponding values τ_1° and τ_2° derived from eqs.(10) are the solution of the optimization problem described by eq.(8).

III. Optimization vs. Time Intervals

The first step of the optimization problem is presented in this section. Therefore, eqs.(10) must be found, regarding the values of R_1, R_2 and c_T as prescribed.

According with the above assumptions about the waveform of c(t) and the values of τ_1 and τ_2, the following approximation can be done:

$$\int_0^{\tau_1} (V-R_2)\, c(t)dt \cong \int_0^{\infty} (V-R_2)\left[c_2-(c_2-c_1)e^{-t/T_1}\right]dt .$$

The same approximation is valid also for the same integral appearing in eq.(5) which therefore becomes:

$$\frac{(V-R_2)\left[c_2\,\tau_1-(c_2-c_1)T_1\right]+(V-R_1)\left[c_1\,\tau_2\,(c_1-c_2)T_2\right]}{(V-R_1)\,\tau_2+(V-R_2)\,\tau_1}=\bar{c} \qquad (12)$$

From eq.(12) it follows:

$$\tau_2 = \alpha\ \tau_1 + \beta \qquad (13)$$

where

$$\alpha = \frac{(V-R_2)\ (c_2-\bar{c})}{(V-R_1)\ (\bar{c}-c_1)}$$

$$\beta = \frac{\left[T_2(V-R_1)-T_1(V-R_2)\right]\ (c_2-c_1)}{(V-R_1)\ (\bar{c}-c_1)} \qquad (14)$$

Substituting eq.(13) into eq. (7) one obtains:

$$R_m = R_1 + (R_2 - R_1)\ \frac{1}{\tau_1(1+\alpha)+\beta} \qquad (15)$$

Then the minimization can be carried out with respect to τ_1 only, provided that τ_1 and τ_2 satisfy the constraints given by eqs.(4) which, in sight of eq.(13), become:

$$\tau_1 \geq k\ T_1$$
$$\tau_1 \geq \frac{k\ T_2 - \beta}{\alpha} \qquad (16)$$

Moreover, since at this stage R_1 and R_2 must be regarded as prescribed, the value of τ_1 minimizing the following expression:

$$f(\tau_1) = \frac{\tau_1}{\tau_1(1+\alpha) + \beta} \qquad (17)$$

yields also the minimum for eq.(15). Hence, from what stated above, the optimization problem becomes:

$$\min_{\tau_1} \left\{ \frac{\tau_1}{\tau_1(1+\alpha) + \beta} \right\}$$

where τ_1 is constrained by eqs. (16).

Since $f(\tau_1)$, as given by eq.(17), is a monotonic increasing function of τ_1, it turns out that the optimal value of τ_1 is:

$$\hat{\tau}_1 = \max \left\{ k\ T_1,\ \frac{k\ T_2 - \beta}{\alpha} \right\} \qquad (18')$$

and, consequently,

$$\hat{\tau}_2 = \max \left\{ k\alpha T_1 + \beta\ ,\ k\ T_2 \right\} \quad . \qquad (18")$$

In order to obtain eqs.(10) it is necessary to substitute in eqs. (18') and (18") the expression of T_1, T_2, α and β as functions of the reflux levels R_1 and R_2.

In conclusion, once R_1 and R_2 have been fixed, eqs. (18') and (18"), with eqs. (14) and (3) taken into account, determine the values of τ_1 and τ_2 corresponding to the optimal bang-bang operation of the column giving the prescribed value $\bar{c}$ of the concentration c_T.

The results given by eqs. (18') and (18") can also be presented in a different way. With this aim in the operation adopting

$$\tau_1 = k\ T_1$$
$$\tau_2 = k\ T_2 \qquad (19)$$

is now considered. Moreover let c_T^* be the concentration in the auxiliary tank at the end of a period, resulting from the operation defined by eqs. (19). Depending upon the values R_1 and R_2, one of the following situations might occur:

a) $c_T^* < \bar{c}$: then, in order to satisfy eq.(5), the first time interval τ_1 must be increased. The optimal choice is

$$\hat{\tau}_1 = \frac{k\,T_2 - \beta}{\alpha}$$
$$\hat{\tau}_2 = k\,T_2 \qquad (20)$$

b) $c_T^* > \bar{c}$: then τ_2 must be increased, i.e.:

$$\hat{\tau}_1 = k\,T_1$$
$$\hat{\tau}_2 = k\,\alpha\,T_1 + \beta \qquad (21)$$

c) $c_T^* = \bar{c}$: in this particular case eq.(5) results already satisfied. Hence the equality:

$$k\,T_2 = k\,\alpha\,T_1 + \beta \qquad (22)$$

holds.

The locus Γ of points satisfying eq.(22) constitutes the boundary between the regions A and B where situations a) and b) respectively occur (Fig. 4). In the following the subsets of Ω belonging to A and B will be called Ω_A and Ω_B i.e.:

$$\Omega_A = \Omega \cap A$$
$$\Omega_B = \Omega \cap B \ .$$

It can be easily seen that the point $(\bar{R},\bar{R})$, representative of a steady operation, belongs to Γ .

From a physical point of view the optimal solution admits some comments.

It is interesting to point out that at least one of the two time intervals τ_1, τ_2 must be the shortest

possible with regard to the constraints expressed by eqs.(4).

Taking into account the linear relation between τ_1 and τ_2 given by eq .(13), it follows that, among all possible bang-bang operations between two levels of reflux which give the required concentration, the optimal one has the minimum period $\tau_1 + \tau_2$.

The circumstance that at least one of the two time intervals τ_1 and τ_2 has to be minimal, implies that R_m is a monotonic increasing function of k. Hence, also for such a reason, smaller values of k are to be preferred, provided that the assumption previously stated be satisfied.

IV. Optimization vs. Reflux Levels

The results of the preceding section are completely general. Infact, no assumptions have been done about the nature of the functions given by eqs. (1) and (2). For further investigations such assumptions can not be omitted. Substituting eqs. (18') and (18") into eq.(7) with eqs.(14), (1) and (3) taken into account, the optimality criterion R_m turns out to be a function of R_1 and R_2 only. Because of the complexity of functions (1) and (2) the optimization problem stated by eq. (11) can not be solved in an analytical way.

On the other hand, it is alwys possible to solve it numerically through a suitable seeking method. The here presented procedure comes out to be really effective if eqs.(1) and (2) are known. Usually, the greatest difficulties are met in getting the function $T(R', \Delta R)$ so that sometimes it is better to approach the whole problem from a different point of view. For instance, a direct simulation of column behavior can be employed: then the unknown values of the four variables R_1, R_2, τ_1 and τ_2 can be reached by means of an appropriate seeking method.

If this is the case, in order to reduce the computational complexity, it is obviously suitable to use dynamical models of the distillation column with a low number of state variables.

Since only some what particular operating conditions (step changes of the reflux) must be simulated, even extremely simple models can fit the reality in a satisfactory way.

V. Particular Case

With the aim of showing how the optimal pulsed operation can be more advantageous than the constant reflux ope

ration, it is now presented and extremely simple particular case.

The eqs.(1) and (2) are specified under the assumption that eq.(1) is linear and that the time constants T_1 and T_2 (see Fig. 2b) depend only upon the sign of reflux variation. These two assumptions do not seem to be very close to the reality; however, they can be thought valid in some cases as first rough approximation. Moreover, as it is shown in the sequel, they entail extremely simple and meaningful results which can be utilized, for instance, as starting point for a more sophisticated search of the true optimum.

In what follows the parameter which plays an essential role is:

$$\rho = \frac{T_2}{T_1} \quad . \tag{23}$$

It can be easily proved [6] that, in the particular case now considered, for all point of the region A the following relation holds:

$$\frac{\partial R_{m\tau}}{\partial R_1} < 0 \tag{24}$$

while, for all points of the region B, the relation:

$$\frac{\partial R_{m\tau}}{\partial R_2} > 0 \tag{25}$$

is valid.

Such properties imply that the optimal working point in Ω belongs to the set Φ consisting of the "right boundary" Φ_A^r of the region Ω and of the "inferior boundary" Φ_B^i of the region $A\Omega_B$, obtained from the region Ω as Fig. 4 shows, where a very strange region Ω has been chosen for the sake of better clarifying the determination of Φ .

The problem of the determination of the optimal point Q on the line Φ_Γ defined (see Fig. 4 where $\Phi_\Gamma = \gamma_{45}$) by:

$$\Phi_\Gamma = \Phi \cap \Gamma$$

is now approached.

With this aim the line Γ is first considered. As far as marking the values of $R_{m\tau}$ along the line Γ is concerned, the following property holds [6]. In any point of Γ the mean reflux $R_{m\tau}$ increases with the distance from the origin of the plane (R_1,R_2) of the straight line with slope equal to $-\rho$ passing through such a point.

According to the above assumptions about eqs.(1) and (2) and substituting eqs. (14) and (23) into eq.(22), the following equation for Γ is obtained:

$$(k-1)\,\rho\,R_1^2 + (1+\rho)\,R_1R_2 + (k-1)R_2^2 - \left\{V\left[1+(k-1)\rho\right] + k\rho\bar{R}\right\}R_1 -$$

$$- \left\{V\left[(k-1)+\rho\right] + k\bar{R}\right\}R_2 + kV(1+\rho)\bar{R} = 0 \,.$$

Therefore, the line Γ is a conic [6] which in the point $(\bar{R},\bar{R})$ has tangent with slope given by:

$$\left.\frac{d\,R_2}{d\,R_1}\right|_{\bar{R},\bar{R}}^{\Gamma} = -\frac{1+\rho(k-1)}{\rho+k-1} \,.$$

Since, for $\rho > 1$, this function assumes values larger than $-\rho$, then, in view of the previously mentioned property, the optimal point P in Ω_M, which, in view of eqs.(24) and (25), is surely on Γ, is the point T in which the tangent of Γ has slope equal to $-\rho$ provided that such a point [4] belongs to Ω_M (Fig. 5a); otherwise, P is the intersection of Γ with the upper or left boundary of Ω_M (Fig. 5b). Since the line Γ is a conic and the value of $R_{m\tau}$ for any point of Γ is an increasing function of the distance from the origin of the straight line with slope equal to $-\rho$ passing through such a point, it turns out that $R_{m\tau}$ is a convex function on Γ in Ω_M attaining its minimum value in P. For this reason, going back to the problem of finding the optimal point Q in Φ_Γ it is possible to conclude that if $P \in \Phi_\Gamma$ then $Q \equiv P$, while if $P \notin \Phi_\Gamma$ then Q is one of the intersection points of Γ with Ω.

---

(4) The line Γ has two points where the tangent has slope equal to $-\rho$. Nevertheless one of these points is always the point (V,V) which does not belong [6] to Ω_M. Therefore here and in what follows only the other point is considered.

Once the optimal point Q in ϕ_Γ has been determined, before going on in the search of the optimal point S in $\phi - \phi_\Gamma$, it is possible, taking into account eqs.(24) and (25), to eliminate some subsets of $\phi - \phi_\Gamma$. As an example, consider Fig. 6 where $\phi = \gamma_{12} \cup \gamma_{23} \cup \gamma_{24}$ and $\phi_\Gamma = \gamma_{23}$. Let the point 3 be the optimal one in ϕ_Γ. Therefore, moving on Γ from $(\bar{R},\bar{R})$ to the point 3, the mean reflux $R_{m\tau}$ decreases. Hence the operations corresponding to each point of γ_{12} and γ_{24} are not to be examined. If on the contrary, the optimal point on ϕ_Γ is the point 2, the search of the optimum must be extended also to γ_{12} and γ_{24}.

In conclusion, the procedure for the determination of the optimal point in Ω may be summarized in the symbolic flow chart of Fig. 7.

As far as the determination of the point Q is concerned, it is useful to remind that the mean reflux $R_{m\tau}$ is a convex function on Γ in Ω_M with a minimum in P. Furthermore it is worth noting that in order to determine the set $\phi - \phi_\Gamma$, once the points Q_i and Q are known, it is not necessary (Fig.8a) to plot the line Γ, provided that a trial carried on by means of eqs. (18'), (18"), (20) and (21) has estabilished which ones of the subregions of Ω not intersected by Γ belong to the region A or B. Finally, taking into account the property stated in eqs.(24) and (25) is then possible to reduce further on the set $\phi - \phi_\Gamma$ (Fig.8b). Once the optimal point in Ω has been found, it is necessary, in order to implement eventually the bang-bang operation represented by such a point, to compare it with the constant reflux operation: with this aim, it is worth to consider, inside Ω_M, the region $\Omega_{\bar{R}}$ where any optimal bang-bang operation has mean reflux $R_{m\tau}$ lower than $\bar{R}$. In order to determine such a region it is sufficient to plot in the regions A and B the contour line with $R_{m\tau} = \bar{R}$. In the particular case here esamined, such a line turns out to be composed by the two straight lines defined [6] by:

$$R_2 = -\rho(k-1)R_1 + \rho(k\bar{R} - V) + V$$

$$R_1 = -\frac{1}{\rho}(k-1)R_2 + \frac{1}{\rho}(k\bar{R} - V) + V \quad .$$

Hence, since the optimal bang-bang operation has to be determined among the ones which have mean reflux lo-

wer than $\bar{R}$, the subbegions of Ω not belonging to $\Omega_{\bar{R}}$ must be eliminated; in the above outlined procedure (see also the flow chart of Fig. 7) the region Ω is then substituted by the region Ω^* defined by:

$$\Omega^* = \Omega \cap \Omega_{\bar{R}} \quad .$$

This last consideration holds also for the general case where the region $\Omega_{\bar{R}}$ is not determinable in such a simple way.

VI. Concluding Remarks

This paper has been devoted to the determination of the optimal pulsed operation of a two component distillation column. The mean value of reflux (distillate) flow rate has been chosen as performance index to be minimized (maximized) provided that the distillate has the prescribed concentration. In this work it has been done the assumption that the only input to the system were the reflux, chosen varying in a bang-bang manner between two levels R_1 and R_2. Furthermore, the transient behavior of top product concentration for a reflux switching has been considered of exponential type and exhausted before the next change have occurred. Under these restrictions, the problem of finding the optimal values of the reflux levels R_1 and R_2 and of the time intervals τ_1 and τ_2 has been reduced to the much simpler problem of the determination of only the two reflux levels R_1 and R_2 in the region Ω of their admissible values.

In a particular case it has been possible to solve the problem completely, or, at least, to reduce the region Ω, inside which the optimum operation point has to be searched, to a set of lines.

Having discussed the possibility of producing a distillate with the prescribed concentration, operating the column in a not classical way, is, afterall, the essence of this work. The idea is to run the distillation column in a periodical manner instead of in a stationary one.

The determination of the optimal periodical operation [4] would have required an accurate dynamical model of the distillation column and the solution of a variational problem. For the particular class of periodical operations here considered (bang-bang operation between two levels of reflux) it has been instead possible, solving a much simpler problem of extremizing a function, to determine the

optimal periodical running without the knowledge of the complete dynamical model of the distillation column: only the behavior for steps in reflux has been infact considered known.

The particular case examined in Sect. V has however pointed out that often the optimal periodical operation, among the ones considered, has to be preferred to the classical one. It should therefore be desiderable to pursue the investigation in order to ascertain the eventual further advantages connected to other kinds of periodical operations.

Acknowledgment

This research has been supported by SNAM Progetti-ENI under contract n. 480.

The authors are deeply indebted with prof.V. Gervasio of SNAM Progetti for having suggested the problem and to prof. E. Biondi of Politecnico di Milano for stimulating discussions.

References

[1] J.S. MOCZEK, R.E. OTTO, T.J. WILLIAMS "Approximation Models for the Dynamic Response of Large Distillation Columns" Proceedings of the 2nd IFAC Congress, Basle, Switzerland, 1963.

[2] P. CASALE"On the Control of a Distillation Column by Means of an On-line Digital Computer". Int. Rep. n. 2721 of SNAM Lab., S.Donato Milanese, June 1965, (in Italian).

[3] Y.KATO "Dynamic Characteristics of Binary System Distillation Column" Trans. Soc. Instrum. Control Engrs., vol. 3, n. 2, pp. 83-94, June 1967, (in Japanese).

[4] F.J.M. HORN, R.C. LIN "Periodic Process: a Variational Approach" I & EC Process Design and Development, vol.6, n. 1, Jan. 1967.

[5] F. BRIOSCHI, A.LOCATELLI "Extremization of a Constra-

ined Multivariable Function: Structural Programming" IEEE Trans. SSC, vol. 3, n. 2, pp. 105-111, Nov.1967.

[6] F. DE LORENZO, G.GUARDABASSI, A.LOCATELLI, V. NICOLO', S. RINALDI "Optimum Bang-Bang Operation of a Two Components Distillation Column" Internal Report of Istituto di Elettrotecnica ed Elettronica del Politecnico di Milano - SNAM Progetti n. 68-4, July 1968 (in Italian).

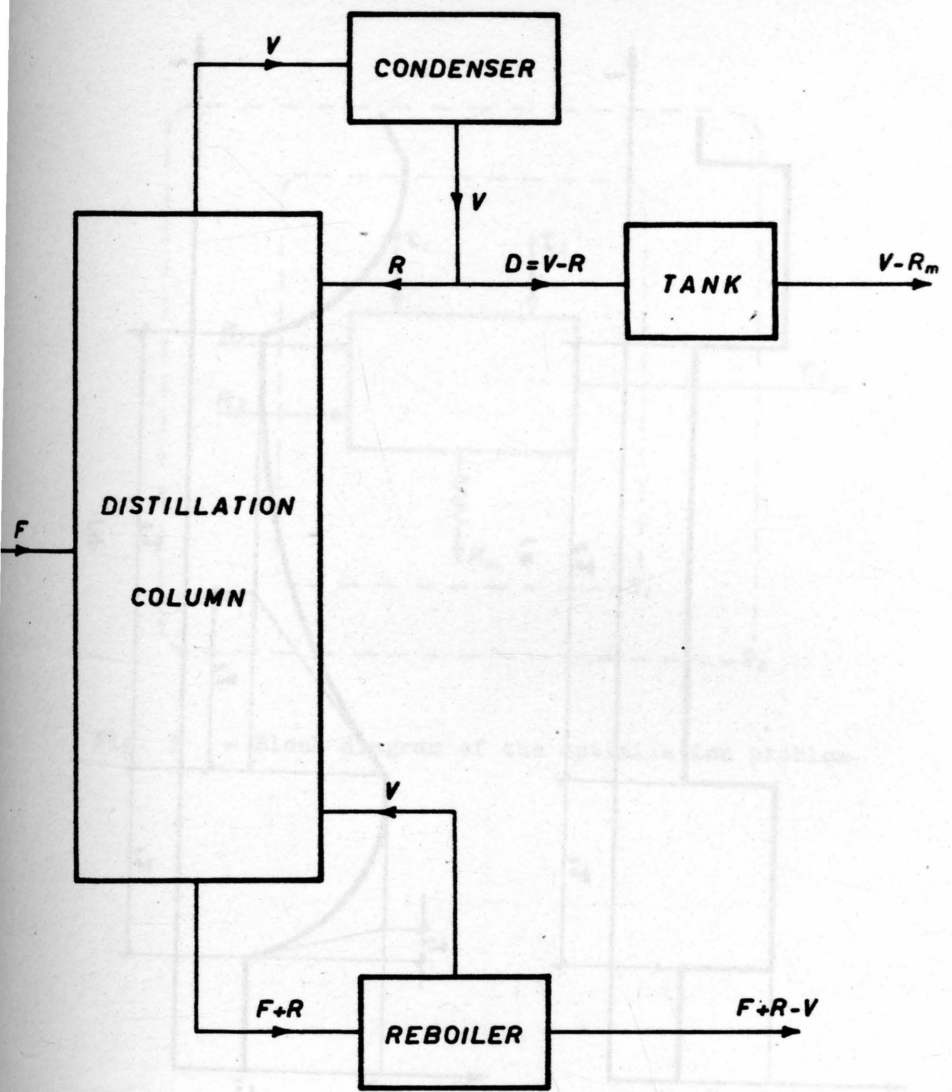

Fig. 1 - Flow rate scheme of the distillation system.

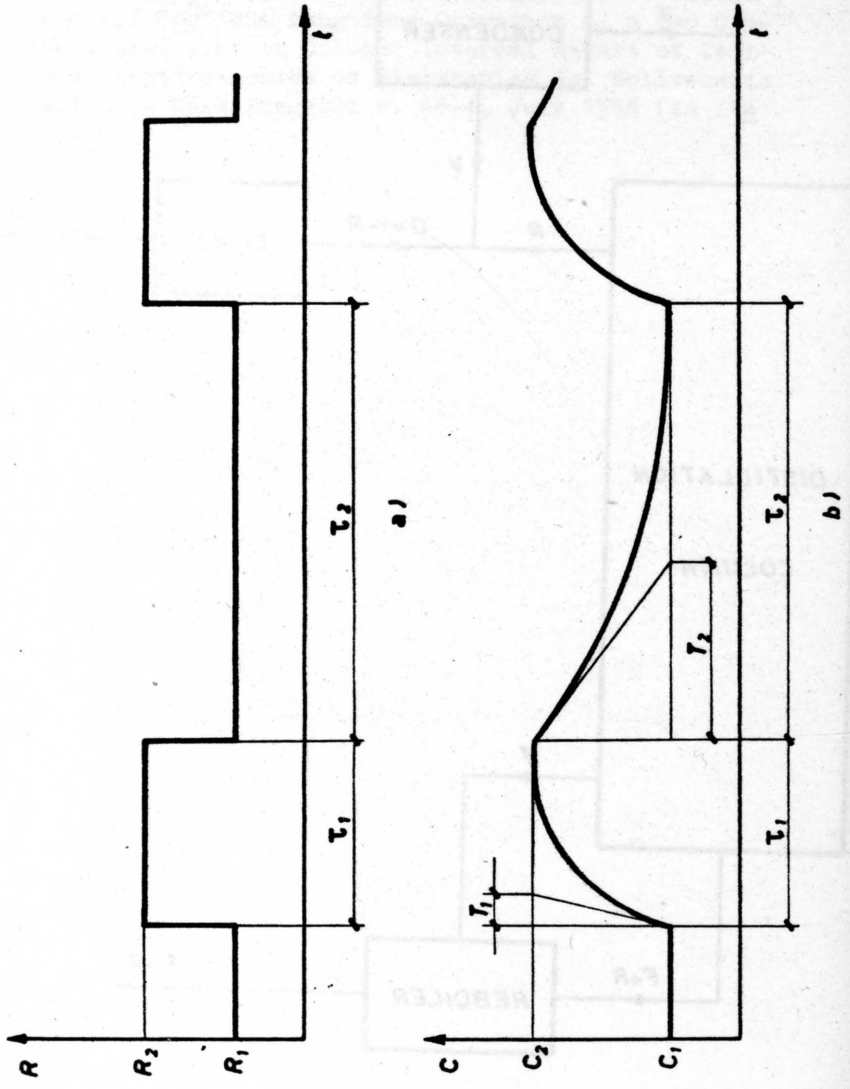

Fig. 2 - Waveforms of ‹a› reflux flow rate, ‹b› distillate concentration.

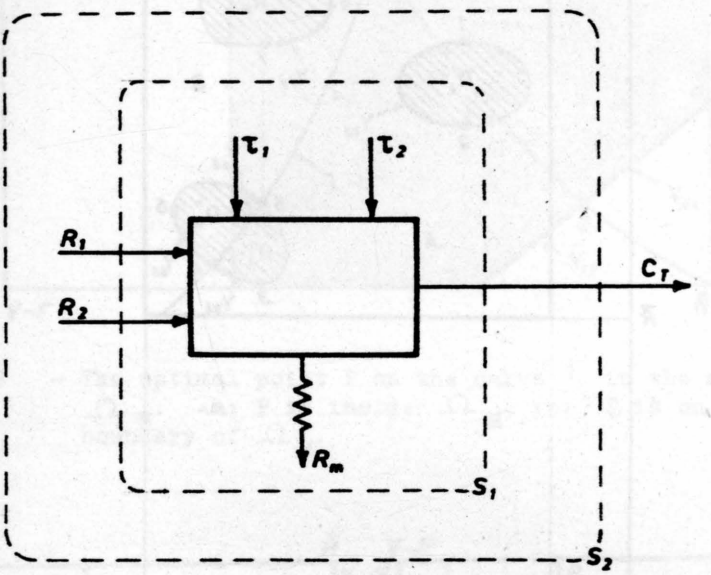

Fig. 3 - Block diagram of the optimization problem.

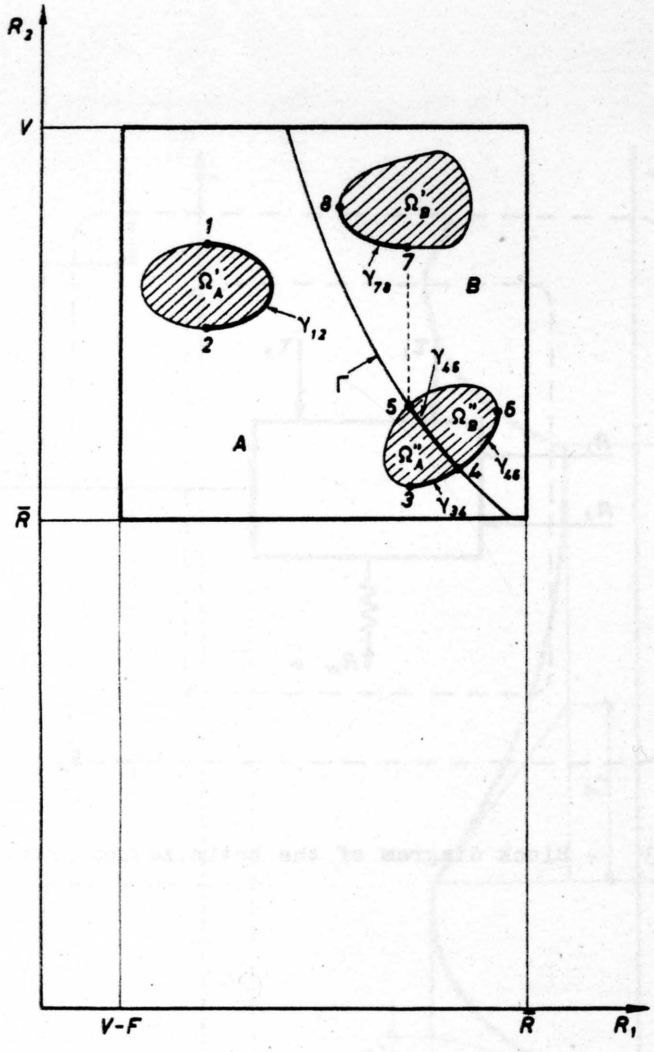

Fig. 4 - The curve Γ and the regions A and B in Ω_M;
Region $\Omega = \Omega_A \cup \Omega_B$ with $\Omega_A = \Omega'_A \cup \Omega''_A$
$\Omega_B = \Omega'_B \cup \Omega''_B$
Set $\phi = \phi^r_A \cup \phi^i_B$ with $\phi^r_A = \gamma_{12} \cup \gamma_{34} \cup \gamma_{45}$, $\phi_B =$
$= \gamma_{45} \cup \gamma_{46} \cup \gamma_{78}$
Line $\phi_\Gamma = \phi \cap \Gamma = \gamma_{45}$.

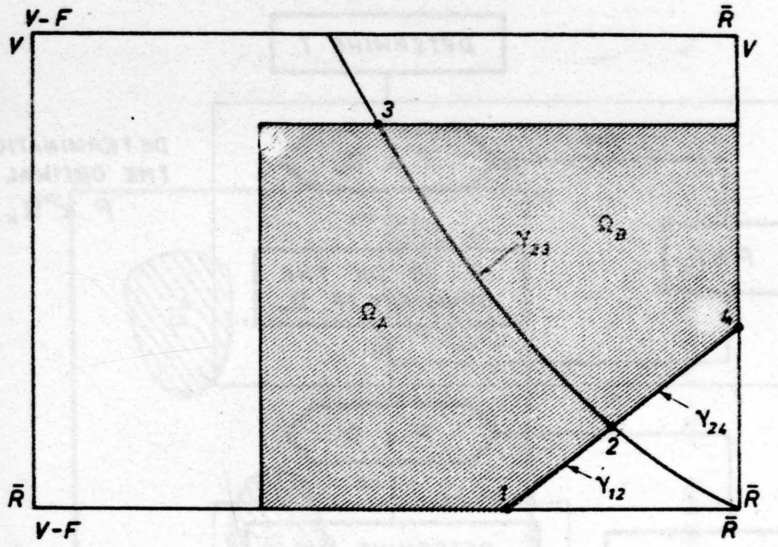

Fig. 5 - The optimal point P on the curve Γ in the region Ω_M. <a> P is inside Ω_M, <b> P is on the boundary of Ω_M.

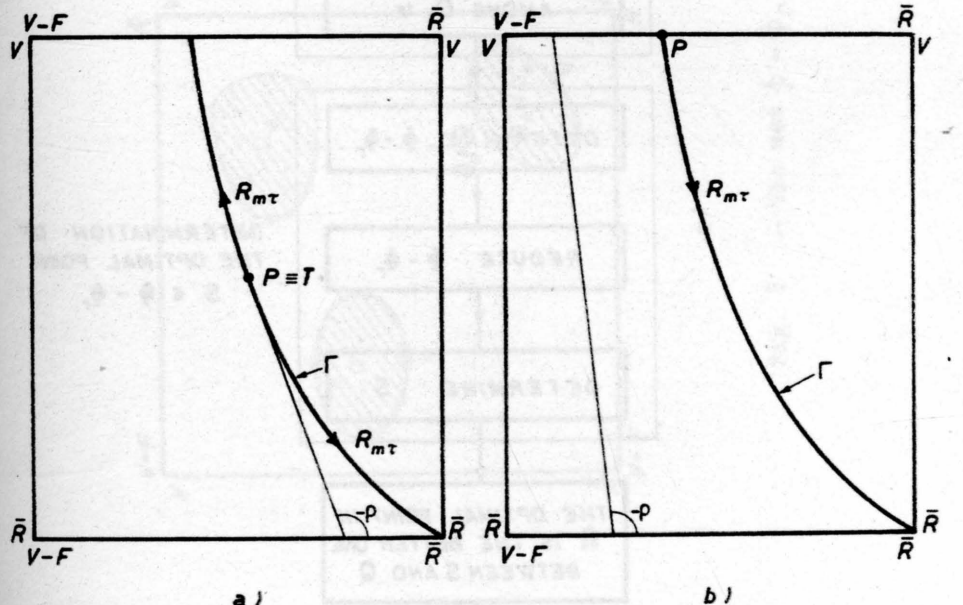

Fig. 6 - Example of possible reduction of $\tilde{\Phi} - \tilde{\Phi}_\Gamma$.

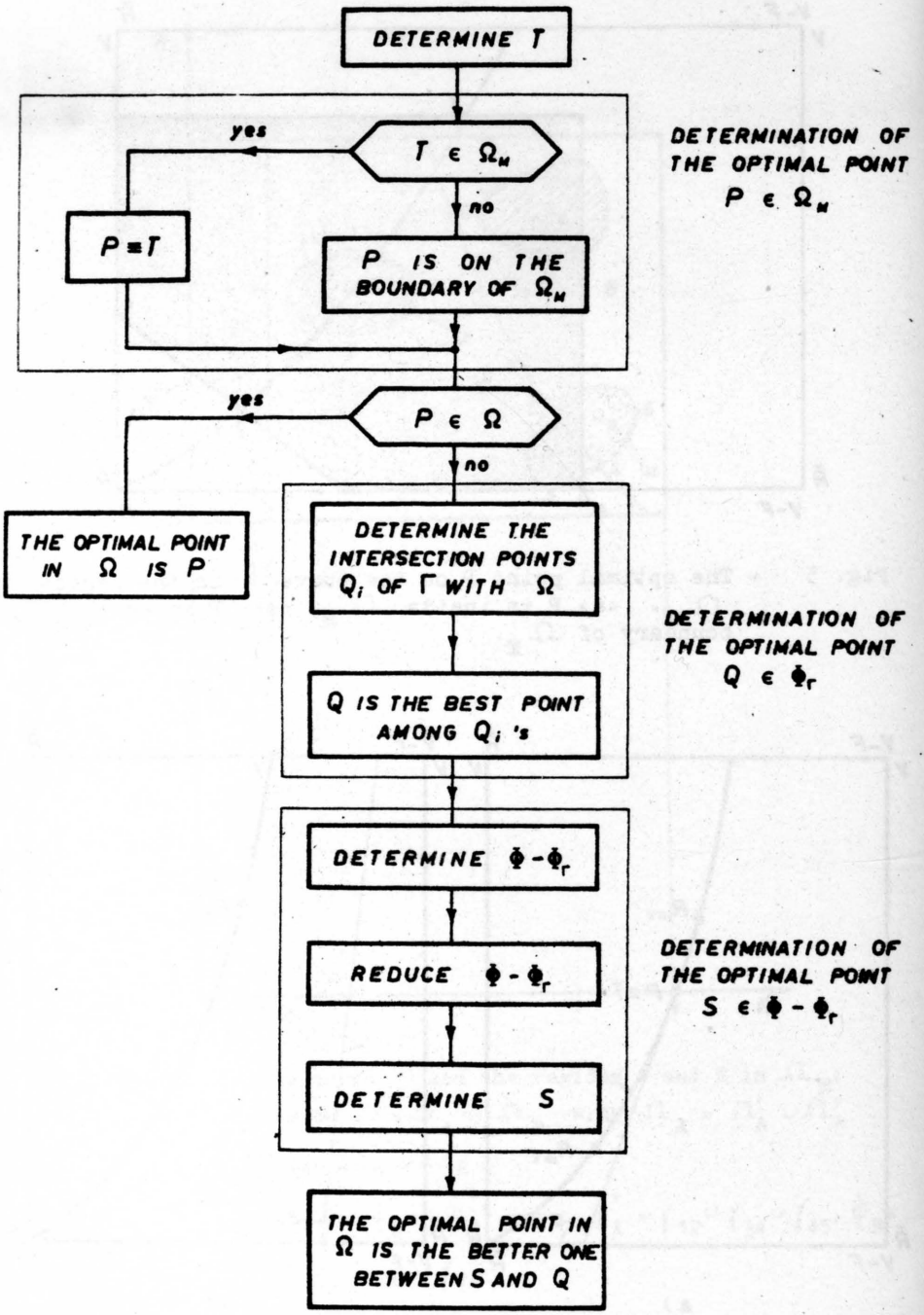

Fig. 7 – Symbolic flow chart of the optimization procedure.

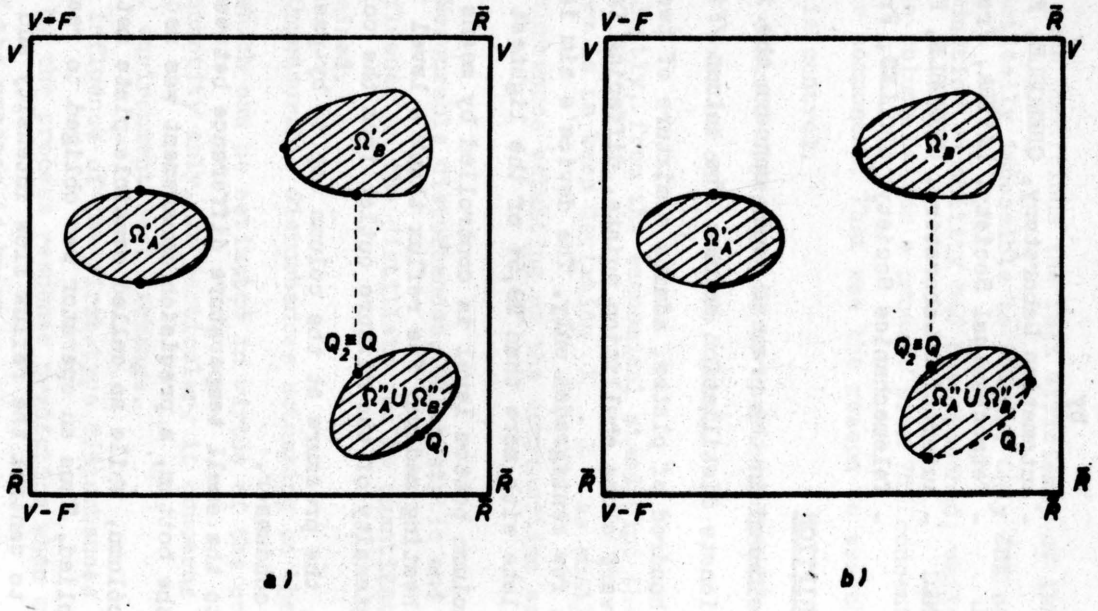

Fig. 8 - The set $\Phi - \Phi_\Gamma$. <a> Determination, <b> reduction.

CLOSED-LOOP PREDICTIVE DIGITAL CONTROL OF THE INDUSTRIAL DISTILLATION COLUMN

by

G. BORNARD - Automation Laboratory, GRENOBLE, France,

G. DUCHATEL - Petrochemical Society, LAVERA, France

J.L. MELENNEC - Automation Laboratory, GRENOBLE, France

B. SEMPE - Telemechanics Society, CROLLES, France

I - PROCESS DESCRIPTION

Studies considered in the present paper concern the industrial superfractionate distillation column. The column /Fig.I/ consisting of a hundred of plates, admits a mixture of two hydrocarbons with very close ebullition points, differing from one another in a few centigrades only. The device's aim is to furnish a distillate with more than 99,5% of the lightest hydrocarbon. The column bottom level is controlled by means of the recuperator heating medium. The reflux thank's level is controlled by intensity of the mixture outlet from the column bottom. Finally, the pressure at the column top is by-pass controlled by a condensor.

According to the small temperature difference between the column top and the bottom, a precision management was necessary to operate the column, while so called sensible-plate method could not be applied. Thus an operator was obliged to read over a chromatograph to control the reflux flow intensity and the mixture outlet from the column bottom, keeping in this way the distillate composition in acceptable bounderies.

Dosage of these control quantities was difficult to appreciate by the operator. Besides, the column dynamics re-

sults in the transient processes' duration time lasting of few hours, hence every change of the operation regime was difficult, too.

In such conditions the full efficiency of the installation was practically impossible to obtain. Only 95% of the nominal production capability had been reached, while obtaining from the column bottom a product with 75% concentration of a volatile component. That was the reason to search for a fully automatic control.

The control objective is to keep the distillate composition X_D over or on $X_{Do} = 0,995$ level.

Evidently, from the economical standpoint the control objective is to keep deviation $X_D - X_{Do}$ as small as possible.

Disturbances actuating on the componsition are of a double type.

a/ Measurable disturbances, which static and dynamic influence on the distillate can be quantitatively determined.

b/ Unmeasurable disturbances actuating on the distillate which can be estimated in virtue of the controlled quantity only. In particular, it concerns to the column - environment heat exchange.

The influence of the first-type disturbances can be eliminated by the process response prediction when mathematical model of the process is known.

In contrary, the second-type disturbances can be compensated by the closed-loop control only. Thus, already in the first phase we are obliged to consider static as well as dyna-

mic mathematical models.

In the second phase the closed-loop control has been developed.

II. STATIC MATHEMATICAL MODELS

A static model is described in form of the relationship between dependent variables /here the composition X_D of the distillate/ and independent ones.

Independent, measurebles variables are of double type.

The disturbances - in the considered problem they are: the pressure P, the composition X_F and intensity of the input product flow F.

The control variables are: intensity of the reflux flow L_R and intensity of the mixture outlet from the bottom W.

Studies of the static model have been carried out in few stages. In the first one the thermodynamic balance at one plate was considered. It enabled to determine the vapor composition Y and the plate temperature T depend upon the liquid composition X and the pressure P.

Afterwards, the Lewis-Sorel method provided facilities for global studying of the column, plate by plate. For the n-th plate it yields in the following relations

$$X_n = A Y_{n-I} + B \quad ; \quad Y_n = Y_{n-I} + E\left(Y^* - Y_{n-I}\right)$$

In the above relation X_n denotes a primary fraction composing the most volatile part of the liquid, Y denotes a primary fraction composing the most volatile part of the vapor at the n-th plate. A and B denote coefficients determined from a mass-balance for the section considered. For the concentration section it yields

$$A = \frac{L_R + D}{L_R} \quad ; \quad B = \frac{D \cdot X_D}{L_R}$$

For the exhaust section we have

$$A=\frac{L_R+F\cdot(I-\zeta)-W}{L_R+F(I-\zeta)} \quad ; \quad B=\frac{W\cdot X_W}{L_R+F(I-\zeta)}$$

where D denotes the distillate outlet intensity and ζ denotes the evaporation coefficient of the feed.

The method utilized is interesting on account of the Murphree efficiency E existing in the previous method. It was determined from data gathered in experimental measurements, as a function of the input product composition and flow-intensity, as well as of the reflux pressure and flow-intensity /Fig.2/.

At last stage of the model development the characteristics $\frac{W}{F}=f\left(\frac{L_R}{F}\right)$ were obtained for a whole set of admissible values of the parameters P and X_F. One of the characteristics, using point by point linear interpolation was fed into computor storage as a reference curve. Statistic point corresponding to optimal disturbance level can be calculated by homography /Fig.3/ Accuracy of the obtained model is of the 2% order when comparing with exprimental data.

Importance of the model discussed consists in simultaneous taking into account of the experimental data indirectly resulting from the efficiency and of the theoretical data resulting from plate by plate calculation. Purely experimental determination of the such model could virtualy be possible, but tough to practical realization because of necessity for extremely long experiments unacceptable in industrial practice.

Instead, the purely theorectical determination could not assure desired accuracy.

Principal role of the static model yields in guidance for automatic operation. Given feed intensity, the model

enables to establish desired values for the regulators of the mixture outlet intensity from the bottom and of the reflux intensity, when the input product's pressure and composition are determined.

Existing degree of freedom can be useful for static optimization purpose. Accepted economical criterion is a minimum of the production unit cost.

In our problem, for production imposed, the cost is given by $$C = \frac{F \cdot P_F + V \cdot P_V + R \cdot P_R - W \cdot P_W}{D}$$ where V and R denote flow intensity of the heating and refrigerating media, respectively. Coefficients P denote unit costs for each of the products considered.

The optimization resuts in extremum seeking of the function of two variables $\frac{L_R}{F}$ and $\frac{W}{F}$, with following constraints:

$$X_D \geqslant 0{,}995$$

$$F \leqslant F_{max} \quad \text{(maximum feed)}$$

$$L_R \leqslant L_M \quad \text{(maximum reflux intensity corresponding to the one in use)}$$

III. CLOSED-LOOP CONTROL

If the system under investigation was purely static and if all disturbances were known, then ideal control could be achived when using the results of the previous paragraph only.

In reality however, to assure precision control of the distillate composition, it proved necessary to apply closed-loop control.

It turned out then, to be convinient to utilize the in-

tensity of the mixture outlet W as a control variable associated by a feedback with X_D . In reference to the control loop, the predictive controls F and L_R represent disturbances to be compensated.

For the compensation purpose as well as for the control loop realization, the appropriate system transmittances should be known.

These transmittances were experimentaly determined for three couples of variables: $X_D - F$; $X_D - L_R$; $X_D - W$. They hold for small variations around the system' s operating regime.

The experiments were carried out for a certain number of the operating points chosen inside the whole domain of the possible variables' variations. It was achived by applying steps of the main desired quantities F, L_R and W.

One can obtain convenient approximations of the transmitances in the form:

$$Hi\ (p) = \frac{K_i \cdot e^{-\tau_i \cdot p}}{I + T_i \cdot p}$$

The coefficients τ_i and T_i are practically unsensible in the operating regime at which the system dynamics has been determined. The values obtained are given in the following table.

τ_f = 20 min. T_f = I30 min.

τ_r = I0 min. T_r = 50 min.

τ_W = 40 min T_W = 200 min.

In contrary, gains K_i depend closely on the cosidered regime. The gains result from graphic representations of the static model /Fig.4/, when using following relations applied to the considered static regime:

$$K_f = \frac{\partial X_D}{\partial F}$$

$$K_W = \frac{\partial X_D}{\partial W}$$

$$K_R = \frac{\partial X_D}{\partial L_R}$$

First, let' s consider the feedback loop. Direct-loop transmittance is of the from:

$$K_W(p) = K_W \frac{e^{-\tau_W \cdot p}}{1 + T_W \cdot p}$$

To assure the closed-loop stability, we shall apply a corrector $C(p)$, such that sufficient stability margin and zero steady-error at the operating regime were guarantied. One may consider the system as equivalent to a cascade of a closed loop containing pure integration $\left(\frac{1}{T_I \cdot p}\right)$ and of a direct loop, equaled to pure delay /Fig.5/.

The corrector $C(p)$ is determined by the relation:

$$\frac{e^{-\tau_W \cdot p}}{1 + T_I \cdot p} = \frac{C(p) \cdot H_W(p)}{1 + C(p) \cdot H_W(p)}$$

This yields in:

$$C(p) = \frac{1}{K_W} = \frac{1 + T_W \cdot p}{1 + T_I \cdot p - e^{-\tau_W \cdot p}}$$

One should notice, that the total transmittance is of the low-frequency filter type. Thus, it is particulary adapted for compensation of the low-frequency disturbances; in particular it regards to variations of the variables. In the control loop under investigation the compensation of the predictive controls F and L_R is accomplished by adding to the control W of a compesating control, such that:

$$W_F \cdot H_W(p) + F \cdot H_F(p) = 0$$

and

$$W_R \cdot H_W(p) + L_R \cdot H_R(p) = 0$$

It results in the following compensation transmittances:

$$P_F(p) = \frac{-H_F(p)}{H_W(p)} = \frac{-K_F}{K_W} e^{-(\tau_F - \tau_W)\cdot p} \cdot \frac{I + T_W \cdot p}{I + T_F \cdot p}$$

$$P_R(p) = \frac{-H_R(p)}{H_W(p)} = \frac{-K_R}{K_W} e^{-(\tau_R - \tau_W)\cdot p} \cdot \frac{I + T_W \cdot p}{I + T_F \cdot p}$$

Notice a considerable advantage of the such compensation yielding in application to whole spectrum of the considered signals. Fig.6 shows the total system diagram.

Practical applications of the described control mode demand for the computer programming of the correctors $P_i(p)$ and $C(p)$ as well as for proper choice of the corresponding variables. For example, the corrector $C(p)$ establishes a functional relation between error variable $\varepsilon(t)$ and the control one $W_A(t)$.

This relation is of form:

$$K_W \left\{ \int \left[W_A(t) - W_A(t - \tau) \right] dt + T_I \cdot W_A(t) \right\} = T_W \cdot \varepsilon(t) + \int \varepsilon(t) \cdot dt$$

To discretize the relation for programming purposes a numerical integration method should be utilized; in particular,

the trapezoid method was chosen.

For the closed-loop control, to comply with initial conditions of the integrators, a stable initial state of the system has been assumed, i.e. an error equaled to zero.

Note, that quantities occuring in the control algorithms are obtained from data processing and recording systems. In particular, at certain control modes the interier reflux is considered as a disturbance. It can not be directly measured but one can calculate it from the reflux temperature and from the vapor temperature at the column top.

The destillate composition was simply appreciated on the ground of a corresponding peak height furnished by a chromatograph. The output product composition at the column bottom can be appreciated by evaluation of the peaks' area corresponding to each of the both product components.

IV - SYSTEM ACTIVATING - RESULTS

All the operations discussed above were effectively realized by using of a digital computer.

The operation-diagram presented in Fig.7 shows different possible program routines. The programs can be brought into effect only when switched on by operator at the computer' s monitor.

Global measurements cycle lasts ten minutes plus, according to time-demands for the chromatographical analysis. It covers data acquization, measurement corrections, calculation of of the control and predictive variables, printing of the twenty system quantities and analyzing of some alarm signals. The computer MAT 01 / Mors-Télémecanique / equipped with 4096

word store enabled for the program execution.

The described control mode, according to permanent process computer control, resulted in a great stability of the process.

Furthermore, one can easily change process operating point, resulting only in slight perturbations of the product composition at the column top.

For example, the composition variations in response to step variations of the mixture outlet intensity at the column bottom are illustrated in Fig. 8 .

From exploitation standpoint the results have prooved to be excellent. The production capability of the column could be progressed for I5% while the volatile product concentration equaled to 40% only.

The improvements were obtained due to the fact, that disposing of the all quantities in use at every time instant and knowing the proccess operation regularities, the computer can permanently evaluate desired values for the process' regulators.

These operations, as demanding pretty large computation capabilities as well as continous attention of the operators, are impossible for manual controlling.

It is worth while to say that researches prior to the automation stage were progress-stimulating themselves because firstly, they permitted for a better quantitative understanding of the process and secondaly, they motivated for the process' instrumentation improvement.

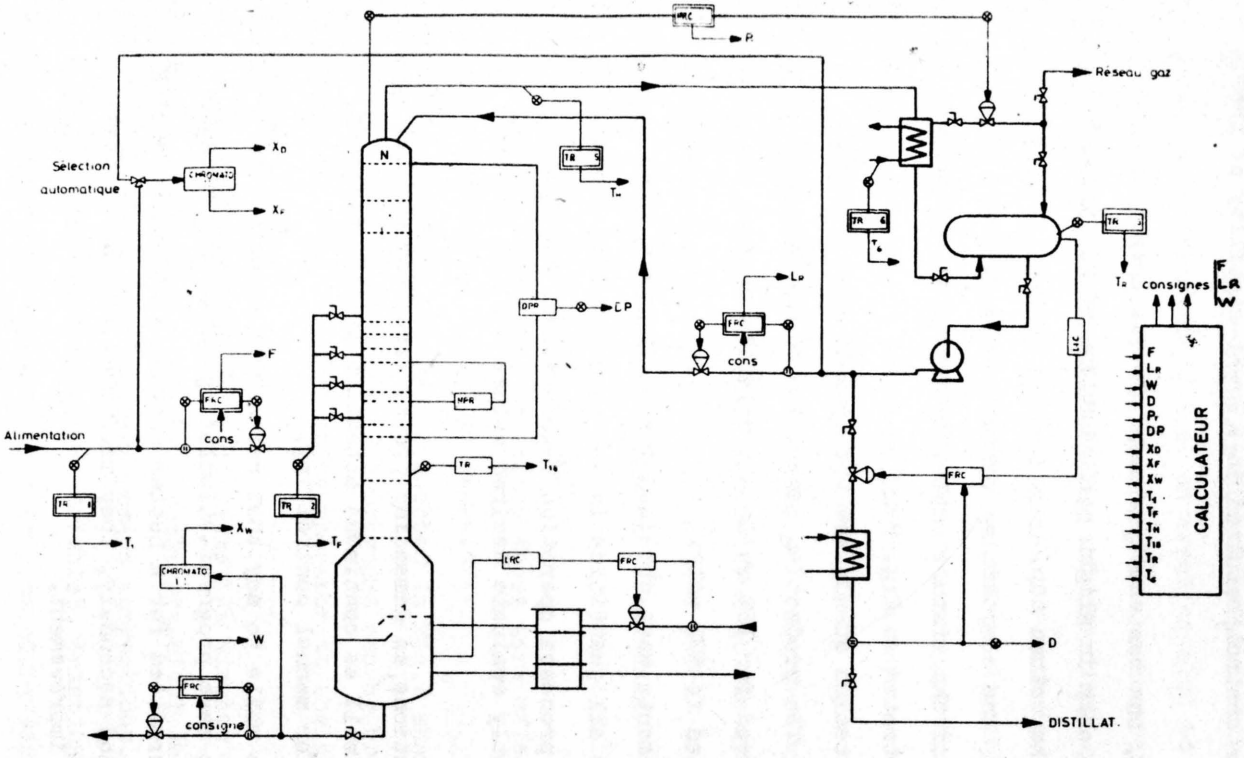

Fig. 1 Installation diagram

DP - pression differential
T_I - feed temperature before dilating
T_F - feed temperature after dilating
T_H - vapor temperature at the column top
T_{18} - column temperature under feed's inlet
T_R - temperature of the exterior reflux
T - refrigerant temperature before the condenser

F - feed intensity
L_R - reflux intensity
W - mixture outlet intensity at the column bottom
D - mixture outlet intensity at the column top
X_F - composition of the input product
X_D - distillate composition at the column top
X_W - distillate composition at the column bottom
P - pression at the column top

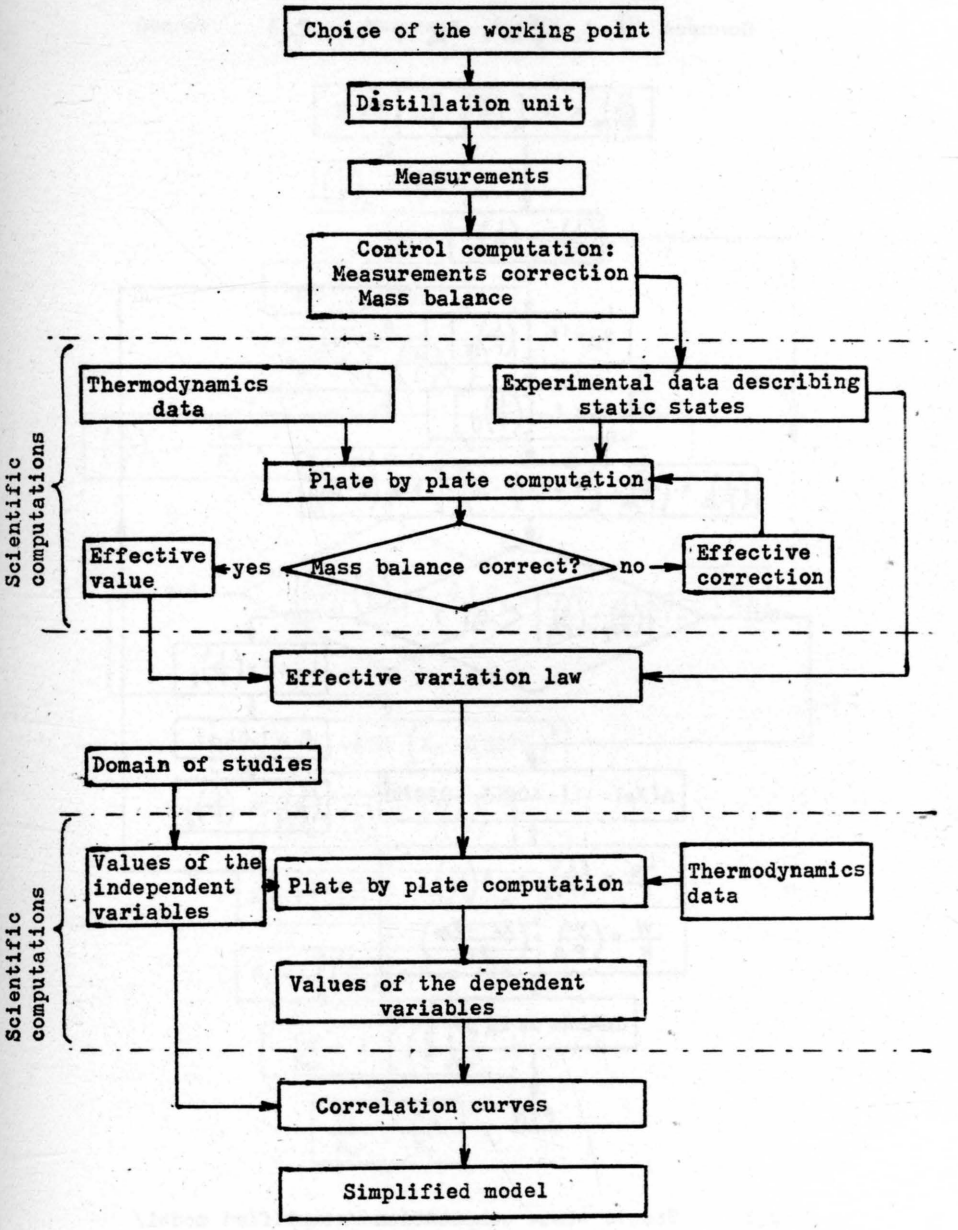

Figure 2. Elaboration of the static model.

CALCUL D'UN ETAT STATIQUE (modèle simplifié)

Données : F , $(\frac{W}{F})_i$, X_{Do} , X_F , P.

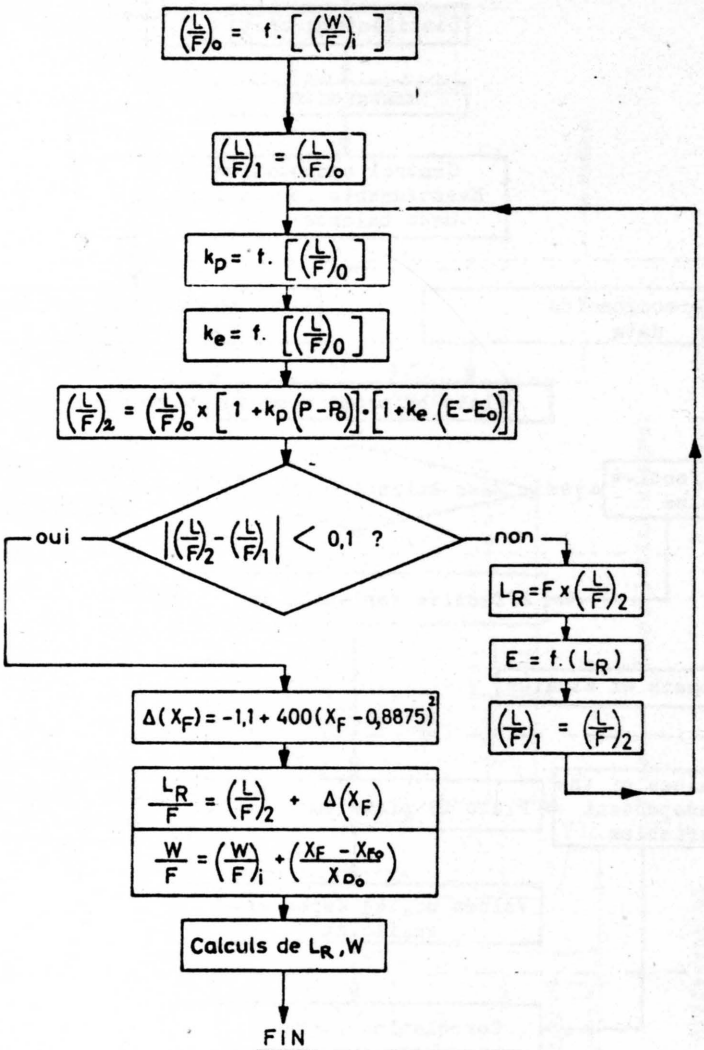

Fig.3 Static state computation /simplified model/

Variables given: $F, \left(\frac{W}{F}\right)_i$, X_{Do} , X_F, P

CALCUL DES COEFFICIENTS DES CORRECTEURS

Donnée : X_{Do} ; Mesures : X_F , F, L_R, P.

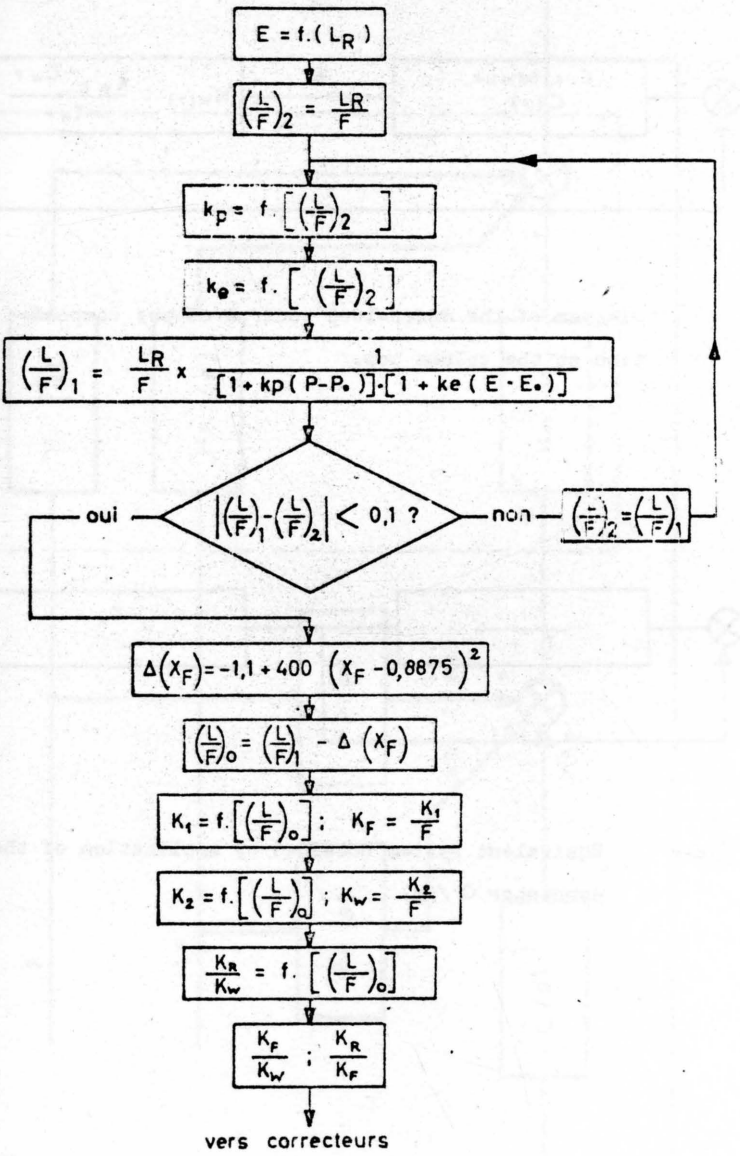

Fig.4 Computation of the correction coefficients

Variables given: X_{Do} ; Measurement: X_F, F, L_R, P

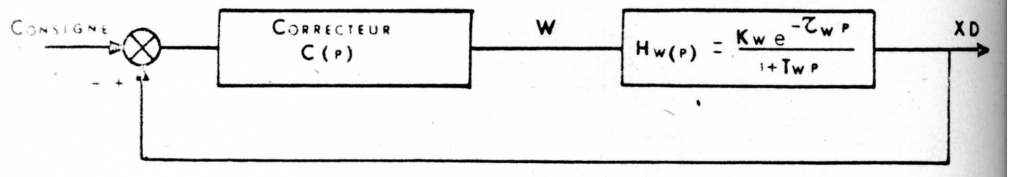

Diagram of the dosed-loop control of the composition at the column top.

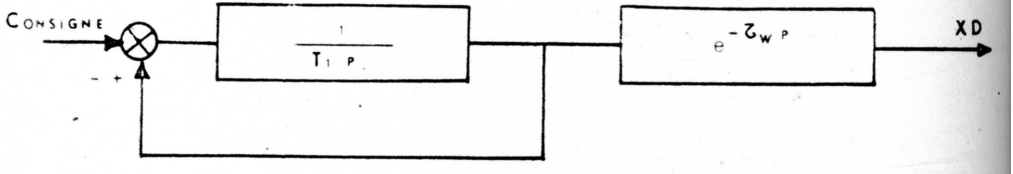

Fig.5 Equivalent system obtained by application of the corrector C /p/.

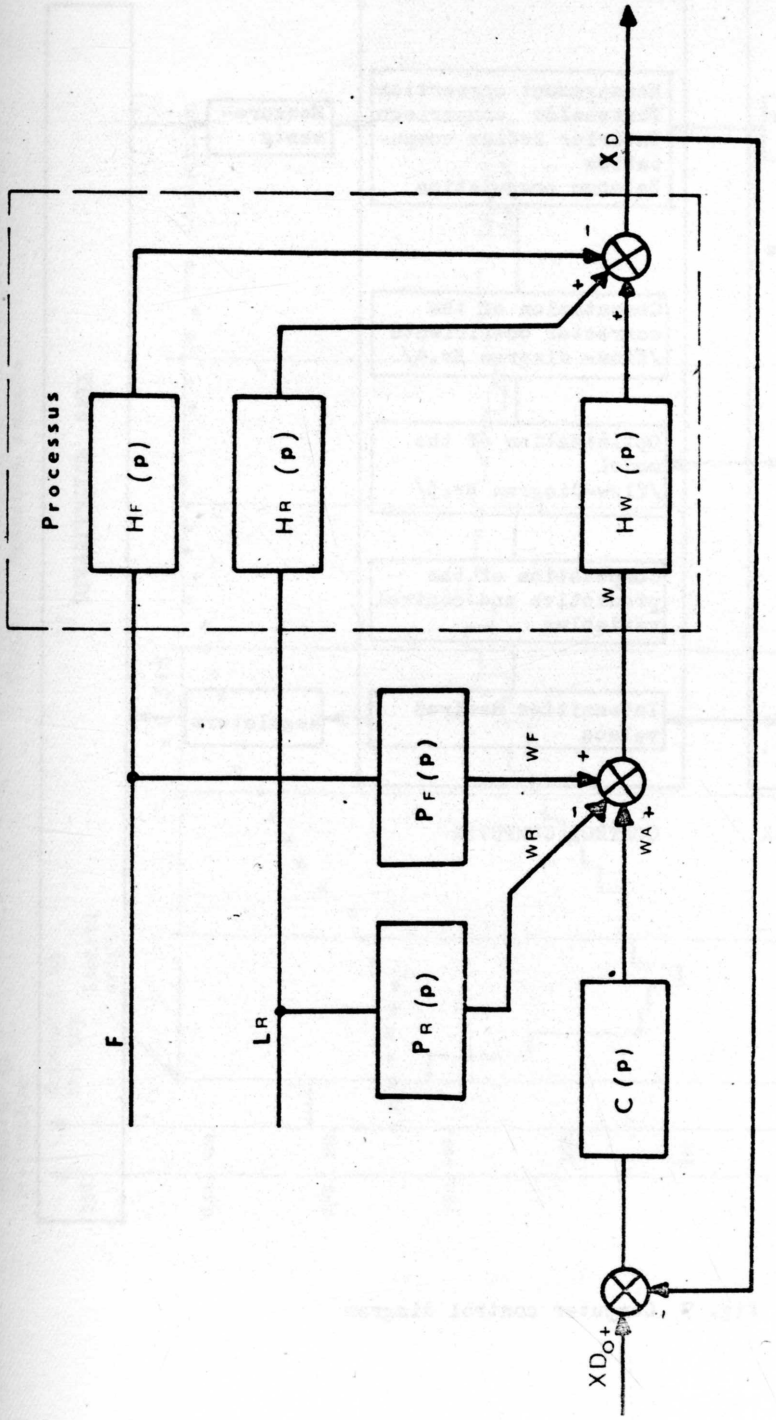

Fig.6 Total control system diagram.

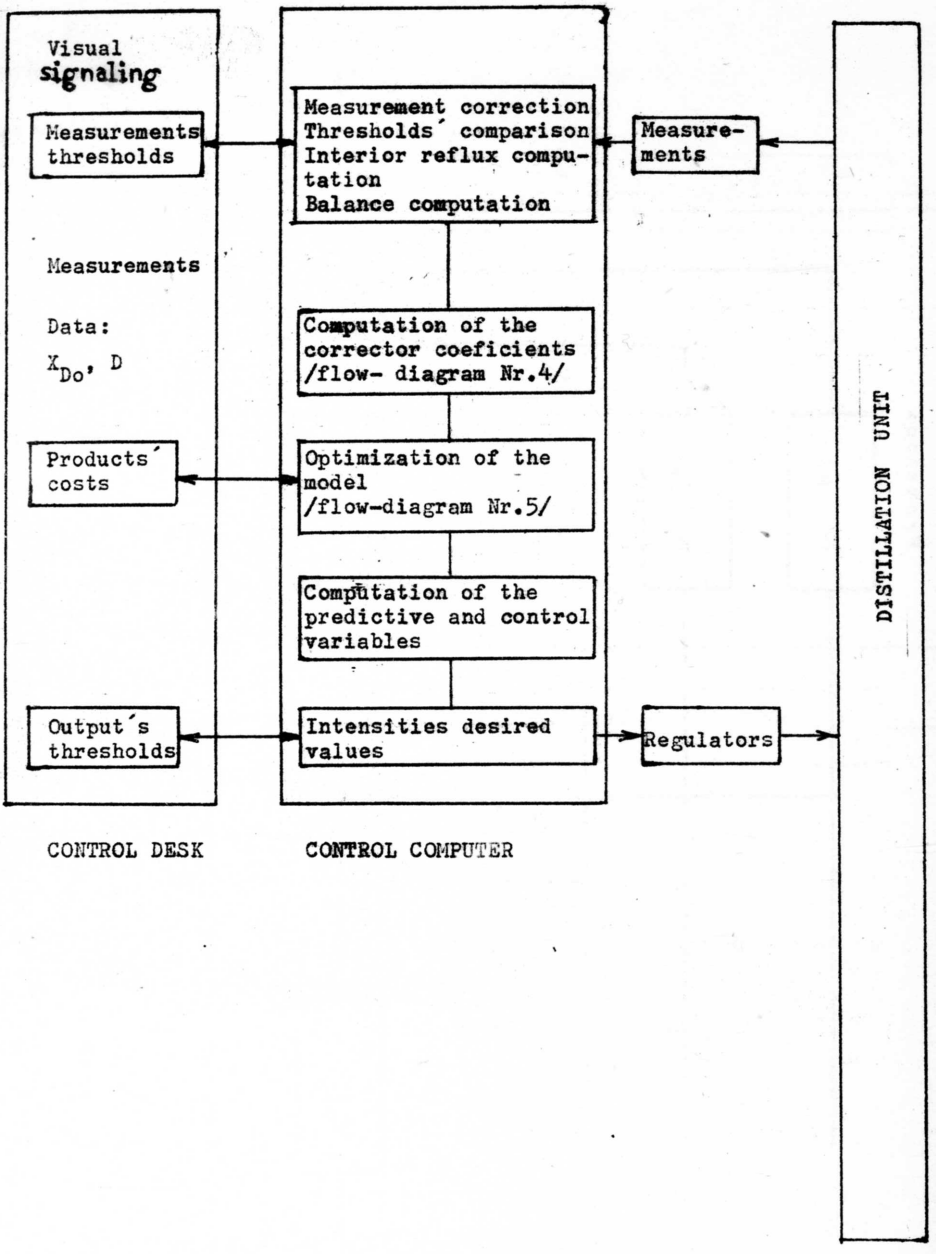

Fig. 7 Computer control diagram

Fig.8 Operation example

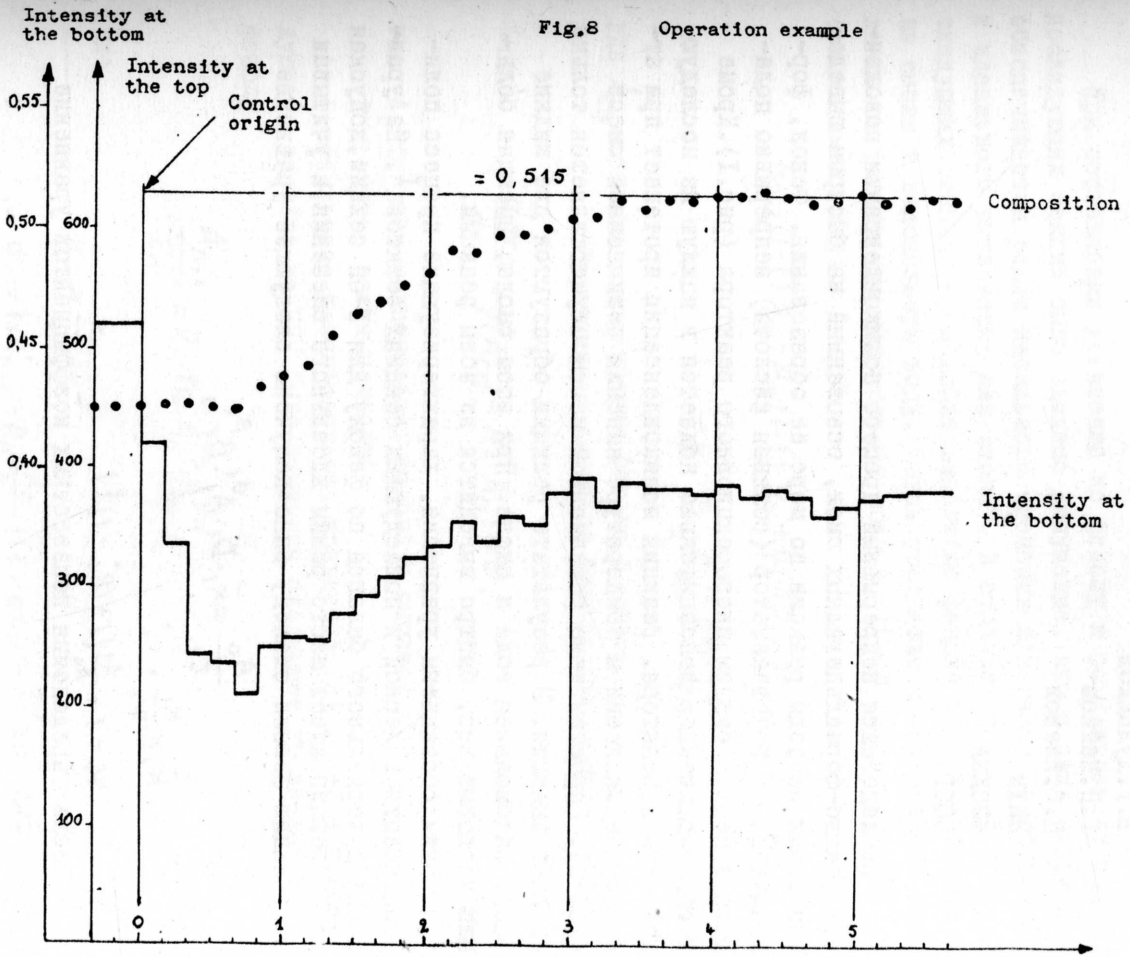

МАТЕМАТИЧЕСКАЯ МОДЕЛЬ И ОПТИМИЗАЦИЯ ПРОЦЕССА ПОЛИКОНДЕНСАЦИИ ФЕНОЛО-ФОРМАЛЬДЕГИДНЫХ СМОЛ.

Е.Г.Дудников
Г.П.Майков
П.С.Иванов
МИХМ
МОСКВА
СССР

Исследовался непрерывный процесс поликонденсации новолачных феноло-формальдегидных смол, основанный на быстром выведении смолы из зоны реакции по мере ее образования. Фенол, формальдегид и катализатор (солянан кислота) непрерывно подаются в первую секцию многосекционного реактора (рис.I).Кроме того, катализатор дополнительно подается в каждую из последующих секций реактора. Реакция поликонденсации протекает при атмосферном давлении и температуре кипения реакционной смеси (100°C). Перемешивание реакционной массы осуществляется только за счёт кипения. В результате реакции образуются две жидкие фазы: надсмольная вода и смола. При этом смола, имеющая бо́льший удельный вес, быстро выводится из зоны реакции.

Были составлены уравнения, характеризующие процесс поликонденсации в первой и последующих секциях реактора[I]. Из уравнения материального баланса по фенолу для I-ой секции,допуская что в секции имеет место режим идеального смешения,и учитывая экстракцию фенола смолой, было получено следующее уравнение

$$\frac{A_0}{\tau_1} = \bar{K}_1 \cdot D_1 \cdot A_1^{\alpha_1} \cdot B_1^{\beta_1},$$

где

$$\bar{K}_1 = \frac{K_1}{\Psi_1},$$

$$\Psi_1 = 1 - \frac{A_1}{A_0}\left[1 + (R_1^* - 1)\right]$$

После определения неизвестных коэффициентов уравнение примет вид

$$\frac{A_0}{Z_1} = 41{,}7 \cdot A_1^{0{,}7} \cdot B_1^{0{,}57}, \qquad (I)$$

где

$$Z_1 = \tau_1 \cdot D_1.$$

Аналогичное уравнение для формальдегида записывается

$$\frac{B_0}{Z_1} = 5{,}8 \cdot A_1^{0{,}42} \cdot B_1^{1{,}12} \qquad (2)$$

При составлении уравнений по фенолу и формальдегиду для последующих секций было сделано допущение, что в этих секциях обеспечивается режим идеального смешения для надсмольной воды и идеального вытеснения для смолы[2]. В отличие от первой в последующих секциях происходит выделение фенола и формальдегида из смолы в надсмольную воду. Тогда уравнение материального баланса по фенолу для надсмольной воды в n-ой (кроме первой) секции имеет вид:

$$A_{n-1}(1-\xi)\cdot q_0 - A_n(1-\xi)\cdot q_0 + \eta(\bar{A}_{cn} - R_n \cdot A_n)\cdot V_n =$$

$$= K_n \cdot D_n \cdot A_n^{\alpha_n} \cdot B_n^{\beta_n} \cdot V_n , \qquad (3)$$

где $\bar{A}_{cn}$-средняя концентрация фенола в смоле.

Уравнение баланса по фенолу для смолы

$$\xi \frac{dA_{cn}}{ds} + \eta(A_{cn} - R_n \cdot A_n) = 0, \qquad (4)$$

где A_c-текущая концентрация фенола в смоле,

s -текущее время контакта.

В результате преобразования уравнений (3) и (4) и последующего расчёта на ЦВМ было получено следующее уравнение по фенолу

$$\frac{A_{n-1}}{\tau_n} = \bar{K}_n \cdot D_n A_n^{\alpha_n} \cdot B_n^{\beta_n}, \qquad (5)$$

где

$$\bar{K}_n = \frac{K_n}{\psi_n},$$

$$\psi_n = \xi\left(R^*_{n-1} - R_n \frac{A_n}{A_{n-1}}\right)\left[1 - \exp\left(-\frac{\eta \cdot \tau_n}{\xi}\right)\right],$$

$$\tau_n = \frac{V_n}{q_0}.$$

При подстановке найденных коэффициентов уравнение (5) записывается

$$\frac{A_{n-1}}{Z_n} = 1,14 \cdot A_n^{1,16} \cdot B^{0,8}, \qquad (6)$$

где $Z_n = \tau_n \cdot D_n$.

Аналогичное уравнение для формальдегида имеет вид

$$\frac{B_{n-1}}{Z_n} = 1,69 \cdot A_n^{0,4} \cdot B_n^{1,36}. \qquad (7)$$

Важным параметром, характеризующим качество новолачной смолы, является степень поликонденсации, которую косвенно можно оценивать по вязкости смолы. Была найдена следующая зависимость

$$m_n = 3,02 + 1,18 \cdot Z_n - 0,256 \cdot A_n + 0,3 B_n, \qquad (8)$$

где m_n -вязкость смолы в n -ой секции (вязкость 20% раствора высушенной смолы в спирте), [сп].

Вязкость новолачной смолы задается в пределах 4-5 [сп], поэтому используя уравнение (8) можно записать

$$0,98 \leqslant 1,18 \cdot Z_n - 0,256 \cdot A_n + 0,3 \cdot B_n \leqslant 1,98 \qquad (9)$$

Адекватность уравнений (I,2,6-8) экспериментальным данным проверялась по критерию Фишера.

Полученные уравнения (I,2,6,7) и неравенство (9) позволяют оптимизировать процесс получения новолачных смол.

В качестве критерия оптимальности принималась сумма концентраций фенола и формальдегида в надсмольной воде на выходе из последней секции реактора $G = A_N + B_N$. Задача оптимизации заключалась в минимизации этого критерия.

Для трехсекционного реактора была решена следующая задача. На основе уравнений связи (I,2,6,7) с учетом ограничения (9) на вязкость смолы найти распределение среднего времени пребывания и концентрации катализатора по секциям, минимизирующих при заданных начальных концентрациях фенола и формальдегида сумму их концентраций на выходе из реактора при заданном количестве смолы.

Особенностью этой задачи является то, что сначала определяется оптимальное распределение величины Z (произведение

среднего времени пребывания на концентрацию катализатора), а затем выбираются оптимальные τ и D . При этом τ можно принимать постоянным для всех секций, т.к. экономически более выгодно делать реакторы одинакового объема, добиваясь того же самого значения критерия оптимальности соответствующей подачей катализатора.

Поставленная задача была решена методом динамического программирования[3,4]. Применение дискретного принципа максимума в этом случае затруднено требованием к качеству смолы, выраженному неравенством (9).

Приведем уравнения связи (I,2,6,7) к виду, необходимому при решении задачи методом динамического программирования

$$A_1 = 0{,}003 \cdot \frac{A_0^{2{,}06}}{Z_1^{1{,}01} \cdot B_0^{1{,}05}}, \qquad (10)$$

$$B_1 = 1{,}84 \frac{B_0^{1{,}29}}{Z_1^{0{,}52} \cdot A_0^{0{,}77}}, \qquad (11)$$

$$A_n = 1{,}19 \frac{A_{n-1}^{1{,}08}}{Z_n^{0{,}34} \cdot B_{n-1}^{0{,}64}}, \qquad (12)$$

$$B_n = 0{,}64 \frac{B_{n-1}^{0{,}92}}{Z_n^{0{,}6} \cdot A_{n-1}^{0{,}32}}. \qquad (13)$$

На основании этих уравнений, описывающих переход системы из одного состояния в другое (от одной секции к другой),можно записать основные рекуррентные соотношения для 3-х секционного реактора.

Для последней секции реактора

$$f_1(A_2, B_2) = \min_{Z_3} G(A_3, B_3) = \qquad (14)$$

$$= \min_{Z_3} \left(1{,}19 \cdot \frac{A_2^{1{,}08}}{Z_3^{0{,}34} \cdot B_2^{0{,}64}} + 0{,}64 \frac{B_2^{0{,}92}}{Z_3^{0{,}6} \cdot A_2^{0{,}32}}\right).$$

Для второй секции реактора

$$f_2(A_1, B_1) = \min_{Z_2} f_1(A_2, B_2) =$$

$$= \min_{Z_2} f_1\left(1{,}19\,\frac{A_1^{1{,}08}}{Z_2^{0{,}34}\cdot B_1^{0{,}64}},\ 0{,}64\,\frac{B_1^{0{,}92}}{Z_2^{0{,}6}\cdot A_1^{0{,}32}}\right). \qquad (15)$$

Наконец, для первой секции реактора

$$f_3(A_0, B_0) = \min_{Z_1} f_2(A_1, B_1) =$$

$$= \min_{Z_1} f_2\left(0{,}003\,\frac{A_0^{2{,}06}}{Z_1^{1{,}01}\cdot B_0^{1{,}05}},\ 1{,}84\,\frac{B_0^{1{,}29}}{Z_1^{0{,}52}\cdot A_0^{0{,}77}}\right). \qquad (16)$$

На основе соотношений (14–16) решаем поставленную задачу, начиная с третьей секции. Строим сетку на плоскости переменных A_2 – B_2. Для каждого узла этой сетки задаем различные Z_3 и находим значения критерия оптимальности, при этом минимальное значение $\min G$ и значение Z_3 запоминаем. При таком способе решения легко выполняются условия ограничения на вязкость. Если для какого-либо узла сетки наложенные ограничения не выполняются, то этот узел не рассматривается. При переходе ко второй секции процедура решения аналогична, только в этом случае для каждого узла сетки на плоскости A_I – B_I находим минимальное значение критерия оптимальности уже для двух последних секций, значения $\min G$, Z_2 и Z_3 запоминаем. Рассчитав аналогично первую секцию, мы получили сетку начальных концентраций A_0 – B_0, для каждого узла которой найдены минимальные значения критерия оптимальности $\min G$ и соответственно оптимальная последовательность величин Z_1, Z_2 и Z_3.

Расчет проводился на ЦВМ "Урал-2". Значения начальных концентраций фенола и формальдегида лежали в пределах A_0=45–65 [вес %], B_0= 8 – 15 [вес.%]. В таблице I приведены значения $\min G$ и Z для A_0= 55 [вес.%].

УСЛОВНЫЕ ОБОЗНАЧЕНИЯ

A_0, B_0 – соответственно концентрация фенола и формальдегида в исходной смеси, [вес.%],

A, B – концентрация фенола и формальдегида в надсмольной воде, [вес.%],

D – концентрация катализатора в надсмольной воде, [вес.%],

q_0 – общая весовая скорость смеси, [кг./час],

ξ – коэффициент, характеризующий долю расхода жидкой смолы в общем расходе,

V – количество реакционной смеси в секции, [кг],

τ – среднее время пребывания, [час]

k – удельная константа скорости химической реакции,

$$\left[\frac{I}{\text{час}\ (\text{вес.}\%)^{\alpha+\beta}}\right]$$

α, β – показатель степени при концентрации фенола и формальдегида,

η – эффективная константа скорости диффузии фенола из смолы в надсмольную воду, $\left[\frac{\text{вес.}\%}{\text{час}}\right]$

R – равновесный коэффициент распределения фенола,

R^* – рабочий коэффициент распределения фенола,

Индекс n при соответствующем условном обозначении означает номер секции.

Таблица I.

A_0	B_0	min G	Z_1	Z_2	Z_3
55	8,0	I,I5	I,4	I,4	I,6
"	I0,0	I,29	I,2	I,2	I,5
"	II	I,84	I,2	I,2	I,2
"	I2	2,00	I,0	I,I	I,2
"	I3	2,II	I,0	I,I	I,I
"	I5	2,58	0,8	0,8	I,I

На рис. 2 показано оптимальное распределение катализатора по секциям при среднем времени пребывания τ =0,5 [час] для секции при A_0= 55 [вес.%].

ЛИТЕРАТУРА

[I] Г.П. Майков, П.С.Иванов,Н.И.Кабыкина,"Исследование процесса поликонденсации фенола и формальдегида в многосекционном реакторе непрерывного действия", Теоретические основы химической технологии №2, I968г.

[2] И.И.Иоффе, Л.М.Письмен, Инженерная химия гетерогенного катализа, изд. Химия, I965г.

[3] Р.Беллман, Процессы регулирования с адаптацией. Из-во "Наука", I964г.

[4] С.Робертс, Динамическое программирование в процессах химической технологии и методы управления. Из-во"Мир", I965г.

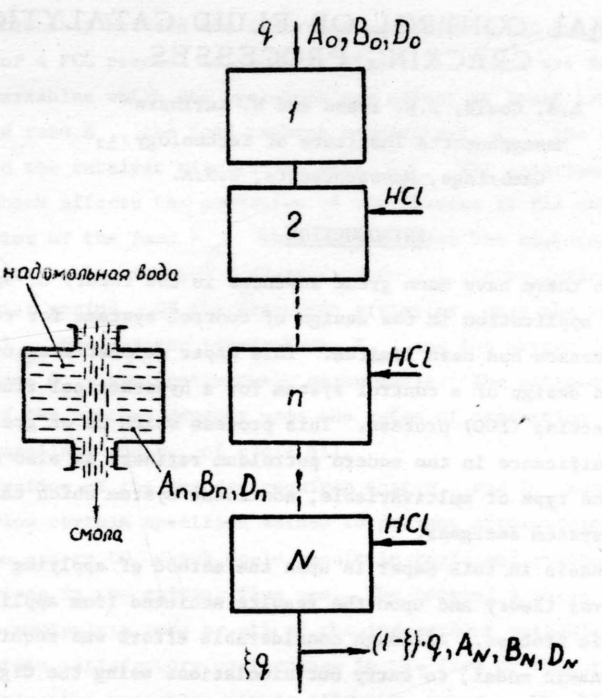
q
A_0, B_0, D_0
1
2
HCl
надиминальная вода
n
HCl
A_n, B_n, D_n
смола
N
HCl
$(1-\xi)\cdot q, A_N, B_N, D_N$
ξq

Рис.1

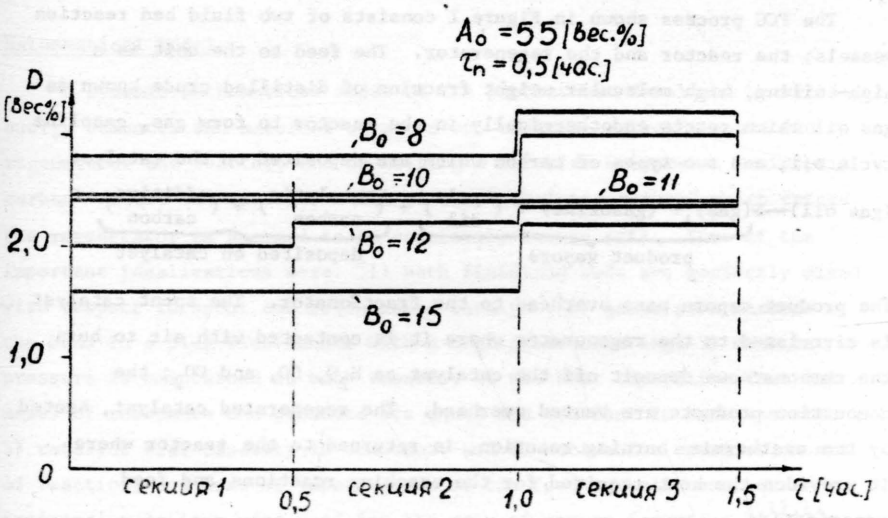
$A_0 = 55$ [вес.%]
$\tau_n = 0,5$ [час.]
D
[вес%]
$B_0 = 8$
$B_0 = 10$
$B_0 = 11$
$B_0 = 12$
$B_0 = 15$
2,0
1,0
0
секция 1
0,5
секция 2
1,0
секция 3
1,5
τ [час]

Рис.2

OPTIMAL CONTROL OF FLUID CATALYTIC CRACKING PROCESSES

L.A. Gould, L.B. Evans and H. Kurihara*
Massachusetts Institute of Technology
Cambridge, Massachusetts, U.S.A.

INTRODUCTION

Although there have been great advances in the theory of optimal control, its application in the design of control systems for realistic chemical processes has been limited. This paper demonstrates use of the theory in design of a control system for a hypothetical fluid catalytic cracking (FCC) process. This process which is of great economic significance in the modern petroleum refinery is also a typical example of the type of multivariable, nonlinear system which challenges the control system designer.

The emphasis in this paper is upon the method of applying the optimal control theory and upon the results achieved from application to a realistic process. Although considerable effort was required to develop a dynamic model, to carry out simulations using the digital computer, and to compute numerical solutions to the optimal control problem, space does not permit describing these aspects of the work here. The details are available elsewhere.[10]

Description of the Process

The FCC process shown in Figure 1 consists of two fluid bed reaction vessels; the reactor and the regenerator. The feed to the unit is a high-boiling, high molecular weight fraction of distilled crude known as gas oil which reacts endothermically in the reactor to form gas, gasoline cycle oil, and two types of carbon which are deposited on the catalyst.

$$\text{(gas oil)} \longrightarrow \underbrace{\text{(gas)} + \text{(gasoline)} + \left(\begin{matrix}\text{cycle}\\ \text{oil}\end{matrix}\right)}_{\text{product vapors}} + \underbrace{\left(\begin{matrix}\text{catalytic}\\ \text{carbon}\end{matrix}\right) + \left(\begin{matrix}\text{additive}\\ \text{carbon}\end{matrix}\right)}_{\text{deposited on catalyst}}$$

The product vapors pass overhead to the fractionator. The spent catalyst is circulated to the regenerator where it is contacted with air to burn the carbonaceous deposit off the catalyst as H_2O, CO, and CO_2; the combustion products are vented overhead. The regenerated catalyst, heated by the exothermic burning reaction, is returned to the reactor where it provides the heat required for the cracking reactions and feed vaporization.

* Now with Toa Nenryo Kogyo K.K., Tokyo, Japan

The relationship between the important variables which describe the behavior of a FCC process is shown in Figure 2. There are four independent variables which the operators may adjust at least indirectly: the total feed rate, R_{tf}, the feed preheat temperature, T_{fp}, the air rate, R_{ai}, and the catalyst circulation rate, R_{rc}. The principal disturbance which affects the operation of the process is the carbon formation factor of the feed F_{cf}. This results from the unavoidable necessity of processing several different crude-oil stocks during a relatively brief period. Of the dependent variables, only the regenerator temperature, T_{rg}, the reactor temperature, T_{ra}, and the oxygen content of the flue gas, O_{fg}, are continuously measureable. The ultimate performance of the process depends upon the rates of production R_{gs} of gas, R_{gl} of gasoline, and R_{co} of cycle oil.

Safe operation of the process requires that O_{fg} and T_{rg} must be maintained below certain specified values to prevent afterburning of CO in the flue gas to CO_2 which would result in rapid and excessive temperature rises in the exiting flue gas. The control problem is, therefore, to manipulate some or all of the independent variables in order to maintain satisfactory performance in the face of disturbances, while restricting the variables within allowable ranges. The highly interactive nature of the process demands great skill on the part of the operators with present methods of control.[5]

DYNAMIC SIMULATION

Mathematical Model

A dynamic mathematical model of the process was developed by writing energy balances and material balances on "additive carbon" around the regenerator and reactor, and by writing a material balance on "catalytic carbon" around the reactor. (All of the "catalytic carbon" which enters the regenerator is assumed to be completely burned off). Some of the important idealizations were: 1) both fluidized beds are perfectly mixed with respect to spent and regenerated catalyst; 2) gases pass through the beds in a plug-flow manner with a negligible time lag; 3) constant pressure is maintained in both vessels; 4) the heat capacities (per unit mass) of reactants and products are equal and constant in each vessel; 5) catalyst heat capacity is constant; and 6) activation energies, heats of reaction, and heat of vaporization of the feed are all constant. Empirical relations were used for the rate of carbon formation,[1,11,17] the rate of carbon burning,[12] the rate of cracking,[3,11] and for the yields of gas, gasoline, and cycle oil. The details of the derivation

have been presented by Kurihara.[10] The resulting mathematical model is a system of nonlinear ordinary differential equations that define five state variables coupled with a system of nonlinear albegraic equations that define four additional output variables. The equations are of the following form.

State variables:

$$\dot{T}_{rg} = f_1(T_{rg}, C_{rc}, T_{ra}, R_{ai}, R_{rc}) \tag{1}$$

$$\dot{C}_{rc} = f_2(T_{rg}, C_{rc}, C_{sc}, R_{ai}, R_{rc}) \tag{2}$$

$$\dot{T}_{ra} = f_3(T_{rg}, C_{rc}, T_{ra}, C_{cat}, R_{rc}, T_{fp}, R_{tf}) \tag{3}$$

$$\dot{C}_{sc} = f_4(C_{rc}, T_{ra}, C_{sc}, C_{cat}, F_{cf}) \tag{4}$$

$$\dot{C}_{cat} = f_5(C_{rc}, T_{ra}, C_{cat}, R_{rc}) \tag{5}$$

Output variables:

$$O_{fg} = g_1(T_{rg}, C_{rc}, R_{ai}) \tag{6}$$

$$R_{gs} = g_2(T_{ra}, C_{rc}, C_{cat}, R_{tf}) \tag{7}$$

$$R_{gl} = g_3(T_{ta}, C_{rc}, C_{cat}, R_{tf}) \tag{8}$$

$$R_{co} = g_4(T_{ra}, C_{rc}, C_{cat}, R_{tf}) \tag{9}$$

A typical method of controlling the process that is frequently described in the literature[4,13] and is referred to herein as the "conventional control scheme" is indicated in Figure 2. In the conventional scheme, reactor temperature is controlled by catalyst circulation rate and oxygen level is controlled by air rate using ordinary feedback controllers with proportional plus integral modes. The equations describing the action of the controllers are

$$R_{rc} = R^s_{rc} + K_{PT}(T_{ra} - T^s_{ra}) + K_{IT} \int_0^t (T_{ra} - T^s_{ra})dt \tag{10}$$

$$R_{ai} = R^s_{ai} + K_{PO}(O_{fg} - O^s_{fg}) + K_{IO} \int_0^t (O_{fg} - O^s_{fg})dt \tag{11}$$

where K_{PT}, K_{IT}, K_{PO}, and K_{IO} are controller parameters; the superscript s denotes a steady-state value.

Simulation of the Conventional Control Scheme

The dynamic behavior of this FCC process with the conventional control scheme was illustrated by simulating the process and its control system on the digital computer using DYNAMO[15] (a general purpose simulation program). DYNAMO effectively integrated Equations 1 through

ll by Euler's method. Initial steady state operating conditions were chosen that satisfy equations 1 through 9 with the time derivatives set equal to zero. These values are shown in parentheses in the section on NOTATION.

Figure 3 shows the response of the system to an initial perturbation in carbon level slightly above its steady-state level. The performance with the best controller parameter tunings (selected by trial-and-error adjustment) is shown by the solid lines. The performance for other controller tunings is also shown by broken lines. Figure 4 shows the response of the system disturbed from an initial steady state condition by a step increase in the carbon formation factor of the feed (resulting in a 2.5% increase in the rate of carbon production). This dynamic behavior is explained by the following step-by-step analysis:

1. The increased carbon production results in an increased carbon content.
2. The increased carbon content tends to increase the conversion of oxygen. Then, because of the decreased oxygen level, the oxygen controller raises the air rate.
3. The increased air rate, together with the increased carbon level, results in higher regenerator and reactor temperatures.
4. Because of the increased reactor temperature, the temperature controller reduces the catalyst rate, and hence accelerates the regenerator temperature increase.
5. The increased air rate, together with the high regenerator temperature, tends to decrease the carbon level which, in turn, tends to increase the oxygen level.
6. The increased oxygen level reduces the air rate and so on.

The disadvantages of this conventional control scheme are summarized as follows:

1. This control scheme cannot eliminate the relatively large variation in the regenerator temperature and the oxygen level. These phenomena are extremely undesirable when the regenerator is operated at an allowable maximum temperature.
2. This control scheme has a relatively small damping ratio or small degree of stability and the tunings of controllers are not trivial but require great care.
3. The period of oscillation is relatively long; in other words, the control system is very sluggish, and a quick recovery from an upset condition cannot be achieved.

Thus far the general background and conventional means of control of catalytic crackers has been described. Next the results of the optimal control study will be discussed.

The theory of optimal control[2,9,14,16] assumes a plant described by a set of ordinary differential equations:

$$\dot{\underline{x}} = \underline{f}(\underline{x},\underline{u}) \tag{12}$$

where $\underline{x}$ represents a vector of state variables and $\underline{u}$ represents a vector of control variables. An objective functional J is defined as

$$J(\underline{u}) = \int_0^{t_1} L(\underline{x},\underline{u})dt \tag{13}$$

where L may be any arbitrary function of $\underline{x}$ and $\underline{u}$. The objective functional is a measure of the performance of the plant during the period of operation from t = 0 to t = t_1 and may be based on profit, cost, or some artificial measure of performance. Optimal control theory asks how should $\underline{u}(t)$ be chosen for $0 \leq t \leq t_1$ to make J a maximum (or minimum)? Once the problem is posed, the necessary conditions which must be satisfied by u(t) can be derived by mathematical techniques, such as the calculus of variation,[8] or its extension, the maximum principle of Pontryagin.[14] In general, for plants described by nonlinear differential equations and for all but a few specialized types of the function L, analytical solution for $\underline{u}(t)$ is not possible. Techniques have been developed, however, for calculating $\underline{u}(t)$ by numerical iterative procedures and, although the computations are nontrivial, the techniques have been successful in a number of applications.[6,9,16]

For many chemical processes there is a unique optimal steady-state operating point which maximizes the value of L with a set of constant (steady-state) values of $\underline{u} = \underline{u}^s$ and $\underline{x} = \underline{x}^s$. If the time t_1 of operation is effectively infinite, then the optimal control policy will show how $\underline{u}(t)$ should be selected to bring the plant from any arbitrary initial state $\underline{x}(0)$ to the steady-state optimal state $\underline{x}^s$ and the control policy will have the property that $\lim_{t\to\infty} \underline{u}(t) = \underline{u}^s$. As a practical matter it has been found that t_1 need not be infinite; if it is significantly larger than the settling time for the process, then the optimal control policy $\underline{u}(t)$ over the interval of time during which the process is brought to its optimal steady-state condition is effectively independent of t_1.

The $\underline{u}(t)$ determined from optimal control theory is an open loop control policy, since it gives $\underline{u}$ as an explicit function of t. In principle, if a process is disturbed away from an optimal steady-state operating condition, the explicit optimal control law could be used to

restore the process to its steady-state operating point in the optimal manner. This control policy will depend only on the initial condition $\underline{x}(0)$.

The optimal control policy can be expressed in an alternate form by using the principle of optimality, namely--Whatever the previous state and previous decision, the remaining decisions must constitute an optimal policy with respect to the state resulting from the previous decision. This principle states that the explicit optimal control law which determines $\underline{u}(t)$ and the resulting $\underline{x}(t)$ along the trajectory as the process is brought from $\underline{x}(0)$ to $\underline{x}^s$ also determines a unique implicit relationship between $\underline{u}$ and $\underline{x}$ which can be expressed[2,7] as

$$\underline{u} = h(\underline{x}) \tag{14}$$

This relation, if it exists, is called a closed-loop structure of the optimal control system, and may be considered an implicit solution (or optimal control law).

This closed-loop structure essentially has the following advantages over the open-loop structure:

1. A closed-loop structure does not require extensive on-line computations to implement it in a real-time operation. According to Equations 12 and 14, the plant should obey the differential equations:

$$\dot{\underline{x}} = \underline{f}\ \{\underline{x}, h(\underline{x})\} \tag{15}$$

and the resulting behavior corresponds to optimal operation. An open-loop structure requires an optimizing computation for an operation with a different initial condition.

2. Generally, real plant performance will be affected less by disturbances and by errors in the mathematical model when a closed-loop structure is implemented than when an open-loop structure is implemented.

The application of the approach outlined above to the problem of designing a control system for the catalytic cracking process will now be discussed.

OPTIMAL CONTROL OF THE FCC PROCESS

An outline of the optimal control study for this hypothetical fluid catalytic cracking unit is shown diagrammatically in Figure 5. First, the original mathematical model (Model No. 1) will be reduced to a simpler one (Model No. 2) involving only two differential equations, in

order to reduce the computing time required to solve the dynamic optimization problem. The optimal air rate and catalyst rate will be determined as two functions of time for a given initial condition to give the optimal open-loop control policy. Numerical solutions will be obtained by the method of steepest ascent of the Hamiltonian (or gradient method in function space) which has been used successfully by a number of workers.[6,9,16] Second, the optimal open-loop control structure will be converted into a closed-loop structure. Finally, an alternative control scheme will be designed by simplifying the optimal feedback control laws. The performance of this control scheme will be tested by using the original mathematical Model No. 1 with disturbances.

The simpler mathematical Model No. 2 was derived by assuming that, since the catalyst holdup in the reactor is considerably smaller than in the regenerator, the unsteady parts of the differential equations (Equations 3-5) for the reactor can be set equal to zero and the resulting algebraic equations solved for T_{ra}, C_{sc}, and C_{cat} as functions of the two remaining state variables T_{rg} and C_{rc} and the control variables R_{rc} and R_{ai}. All of the other independent variables are assumed specified at the steady-state operating point.

The integrand L of the performance functional is defined as

$$L = P_{ig} - P_{e1} - P_{e2} \tag{16}$$

the instantaneous gross profit rate minus two penalty functions which impose an artificial penalty for exceeding the allowable regenerator temperature or oxygen content in the flue gas. The instantaneous gross profit rate is defined as

$$P_{ig} = (P_{gs} R_{gs} + P_{gl} R_{gl} + P_{co} R_{co} - P_{tf} R_{tf})/24 \tag{17}$$

where P_{gs}, P_{gl}, and P_{co} are the economic values assigned to gas, gasoline, and unconverted gas oil respectively leaving the process and P_{tf} is the cost of feed to the process.

The penalty functions to constrain the regenerator temperature and oxygen in the flue gas were defined as follows:

$$P_{e1}(T_{rg}) = \begin{cases} G_1 \{T_{rg} - (T_{rg})_{max}\}^{m_1} & \text{if } T_{rg} > (T_{rg})_{max} \\ 0 & \text{if } T_{rg} \leq (T_{rg})_{max} \end{cases} \tag{18}$$

$$P_{e2}(O_{fg}) = \begin{cases} G_2 \{O_{fg}-(O_{fg})_{max}\}^{m_2} & \text{if } O_{fg} > (O_{fg})_{max} \\ 0 & \text{if } O_{fg} \leq (O_{fg})_{max} \end{cases} \quad (19)$$

where G_1 and G_2 are large positive constants and m_1 and m_2 are integers which must be selected carefuly.

The optimal steady-state operating point for this particular FCC unit which was investigated corresponded to $T^s_{rg} = 1160^oF$ and $C^s_{rc} = 0.60$, $R_{ai} = 400$ M lb/hr, $R_{rc} = 40$ ton/min, $T_{ra} = 930^oF$ and $O_{fg} = 0.20$ mol percent. The optimal control policy was determined for the case in which the regenerator temperature was at its steady-state value, but the carbon content C_{rc} was slightly above its steady-state value at t=0. The resulting solutions for R_{ai} and R_{rc} as functions of time are shown in Figure 6 together with the corresponding values of T_{ra} and O_{fg}. If one compares these solutions with the results of dynamic simulation of the conventional control scheme, as shown in Figure 3 (considering the difference in time scale), then one can see that the dynamic optimization results in considerably improved performance, since C_{rc} returns to the optimal steady-state condition very quickly without causing an excessively high T_{rg}.

This optimal control solution with initial condition No. 1 can be plotted in the phase plane O_{fg} vs. T_{rg}, as shown in Figure 7 by trajectories denoted by circles with the numeral 1 inside. Point S in the figure represents the optimal steady state. The output variable O_{fg} is plotted in the phase plane instead of the state variable C_{rc}, since it is very difficult to measure C_{rc} directly. Dynamic optimizations with different initial conditions were solved in the same way and the solutions are plotted in Figure 7 by trajectories denoted by circles with the numerals 2,4,5,6 and 7 inside. Starting from several initial conditions, the trajectories move to an optimal steady state in an optimal manner (maximizing the objective function). A trajectory starting from any initial condition never crosses a trajectory starting from any other initial condition. In other words, an optimal trajectory is unique and depends only on the initial condition. This fact is known as the principle of optimality, as discussed before.

Now for points along any trajectory on this phase plane, it is possible to plot an optimal solution for R_{ai} as a function of O_{fg} and T_{rg}. For example, from Figure 6 this functional relation at t = 0.1 is $R_{ai} \doteq 1{,}165$ and $O_{fg} \doteq 0.14$. Thus, one data point (shown by a square) can be plotted in Figure 8. By plotting similar values at

other times, one can obtain a sufficiently clear picutre of R_{ai} as a function of T_{rg} and O_{fg}, as shown by contour lines in the figure. In a plot of T_{rg} vs. O_{fg}, a mountain is apparently located in the southwest, and a sea is the northeast. A similar functional relation for R_{rc} is shown in Figure 9. For a plot of T_{rg} vs. O_{fg}, a mountain is apparently located in the northeast and a sea in the southwest. These functional relations between control variables and state variables are called optimal feedback (or closed-loop) control laws.

Now we can design an alternative control scheme for this fluid catalytic cracker. We know the optimal feedback control laws, at least approximately. All that we have to do is to utilize the result of this optimal control study. First, we linearize the optimal control laws around the optimal steady state. This is done directly by measuring slopes around an optimal steady-state point of Figures 8 and 9, to give

$$R_{ai} - R^s_{ai} = -1.0(T_{rg}-T^s_{rg}) - 100(O_{fg}-O^s_{fg}) \tag{20}$$

$$R_{rc} - R^s_{rc} = 0.5(T_{rg}-T^s_{rg}) + 50(O_{fg}-O^s_{fg}) \tag{21}$$

where a superscript s represents optimal steady state. Secondly, we investigate the contribution of each term in Equations 20 and 21 to the overall performance of the optimal system by comparing the performances with and without each term. By neglecting the second term on the right side of Equation 20 and the first term on the right side of Equation 21, a new control scheme referred to as the "alternative control scheme" was developed.

A dynamic simulation (with Model No. 1) of this alternative control scheme, where the initial carbon level is slightly higher than the steady-state level, is shown in Figure 10. If this performance is compared with that of the conventional control scheme shown in Figure 3, considering the difference in time scale, then one can see that the alternative control scheme results in a considerably better performance, since C_{rc} reaches an optimal steady-state condition very quickly without causing any excessively high T_{rg}. If this is compared with the optimal control solution shown in Figure 6 then it can be seen that they are very similar.

Figure 11 shows the case where the carbon production is suddenly increased by a certain mechanism, which is due to feed composition variation. The resulting dynamic behavior will be explained by the following step-by-step analysis.

1. The increased carbon production causes the carbon level to increase.
2. The increased carbon level causes the regenerator temperature to increase and simultaneously decreases the oxygen level.
3. The decreased oxygen level causes the catalyst rate to decrease by action of the oxygen controller, and simultaneously the increased regenerator temperature decreases the air rate by action of the temperature controller.
4. The decreased catalyst rate compensates for the increased carbon production.

As shown in the figure, this scheme is practically insensitive to this disturbance in carbon production. If this is compared with Figure 4, the superiority of this scheme over the conventional one will be reconfirmed.

CONCLUSIONS

A method of applying optimal control theory was demonstrated for the design of a control system for a hypothetical fluid catalytic cracking unit and resulted in an entirely different control scheme from the one that is typically used in refinery operation. The performance of the new control scheme was demonstrated by dynamic simulation to be significantly better than the conventional system.

The new design approach was found to have significant advantages over conventional trial-and-error methods, because it is systematic, and because it provides information to evaluate the desirability of each design step, since the ultimate performance of the system is known from the optimal control theory.

ACKNOWLEDGEMENT

This research was supported by the National Science Foundation under NSF Grant GK-563.

The computations were performed at the M.I.T. Computation Center.

NOTATION

C_{cat} = Catalytic carbon on spent catalyst (0.9) wt. %

C_{rc} = Carbon on regenerated catalyst (0.6) wt. %

C_{sc} = Carbon (total) on spent catalyst (1.5) wt. %

F_{cf} = Carbon formation factor of the feed (0.0) (M lb. carbon/hr.)/(M bbl./day)

G_1 = Constant (5×10^{-4})

G_2 = Constant (1.0)

K_{IO} = Integral gain for oxygen controller (-10) (Mlb. air/hr.)/ mol % oxygen,hr.

K_{IT} = Integral gain for temperature controller(ton cat./min.)/ (-0.1) ^{o}F, hr.

K_{PO} = Proportional gain for oxygen controller (M lb. air/hr.)/ (-40) mol % oxygen

K_{PT} = Proportional gain for temperature controller (ton cat./min)/F (-0.2)

m_1 = Integer (2)

m_2 = Integer (1)

O_{fg} = Oxygen in flue gas (0.2) mol %

$(O_{fg})_{max}$ = Allowable maximum oxygen in flue gas (0.2) mol %

P_{co} = Price of cycle oil (3.42) $/bbl.

P_{el} = Penalty function for regenerator temperature M$/hr.

P_{e2} = Penalty function for oxygen in flue gas M$/hr.

$P_{g\ell}$ = Price of gasoline (4.59) $/bbl.

P_{gs} = Price of gas (0.0112) $/lb.

P_{ig} = Instantaneous gross profit rate M$/hr.

P_{tf} = Price of total feed (3.15) $/bbl.

R_{ai} = Air rate (400) M lb./hr.

R_{co} = Cycle oil production rate bbl/day

$R_{g\ell}$ = Gasoline production rate bbl/day

R_{gs} = Gas production rate lb/day

R_{rc} = Catalyst circulation rate (40) ton/min

R_{tf} = Total feed rate (100) M bbl./day

t = time hr

T_{fp} = Feed preheater temperature (700) ^{o}F

T_{ra} = Reactor temperature (930) ^{o}F

T_{rg} = Regenerator temperature (1,160) ^{o}F

$(T_{fg})_{max}$ = Allowable maximum regenerator temperature (1,160) ^{o}F

$\underline{u}$ = Vector of control variables

$\underline{x}$ = Vector of state variables

Superscript

s = Steady-state

REFERENCES

1. Andrews, J.M., Ind. Eng. Chem., 51, 4, p. 507 (April, 1959)
2. Athans, M. et al., Optimal Control,McGraw-Hill, (1966)
3. Blanding, F.H., Ind. Eng. Chem., 45, p. 1186 (June, 1953)
4. Gandsey, L.J., Chem. Eng. Prog., 61, 10, p. 93 (Oct., 1965)
5. Hicks, R.C., et al., Oil Gas J., pp. 97-105 (Jan. 24, 1966)
6. Horn, F., Chem. Ing. Tech., 32, pp. 382-393 (1960)
7. Kalman, R.E., Bol. Soc. Mat. Mex., 5, pp. 102-109 (1960)
8. Kipiniak, W., Dynamic Optimization and Control, M.I.T. Press, (1961)
9. Kurihara, H., Technical Report, ESL-R-267, M.I.T. (May, 1966)
10. Kurihara, H., Optimal Control of Fluid Catalytic Cracking Processes, Sc.D. Thesis, M.I.T. Cambridge, Mass. (June, 1967) also distributed as Technical Report ESL-R-309, Electronic Systems Laboratory,M.I.T.
11. Oden, E.G., et al., Ind. Eng. Chem., 44, p. 896 (1952)
12. Pansing, W.F., A.I.Ch.E.J., 2, 1, pp. 71-74 (March, 1956)
13. Pohlenz, J.B., Oil Gas J., p. 124 (April 1, 1963)
14. Pontryagin, L.S., et al., The Mathematical Theory of Optimal Processes, Interscience Publishers, (1962)
15. Pugh, A.L., DYNAMO Users Manual, M.I.T. Press, (1961)
16. Rosenbrock, H.H., et al., Computational Techniques for Chemical Engineers, Pergamon Press (1966)
17. Voorhies, A., Ind. Eng. Chem.,37, p. 318 (1945)

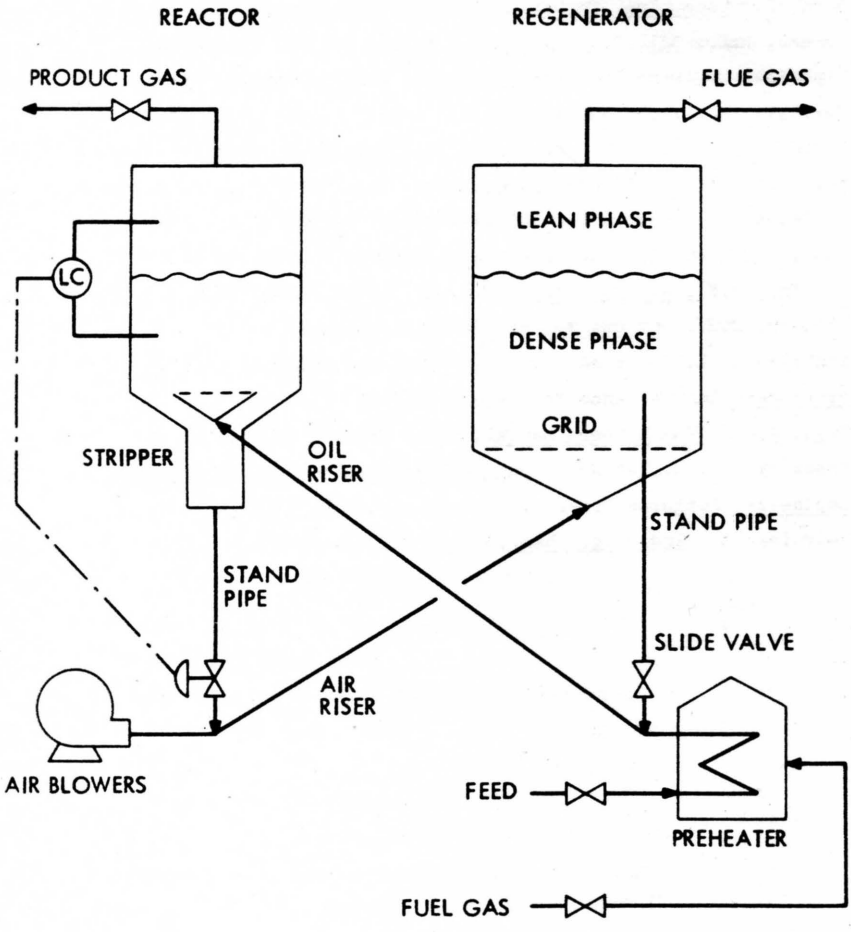

Figure 1. A Typical Fluid Catalytic Cracking Unit

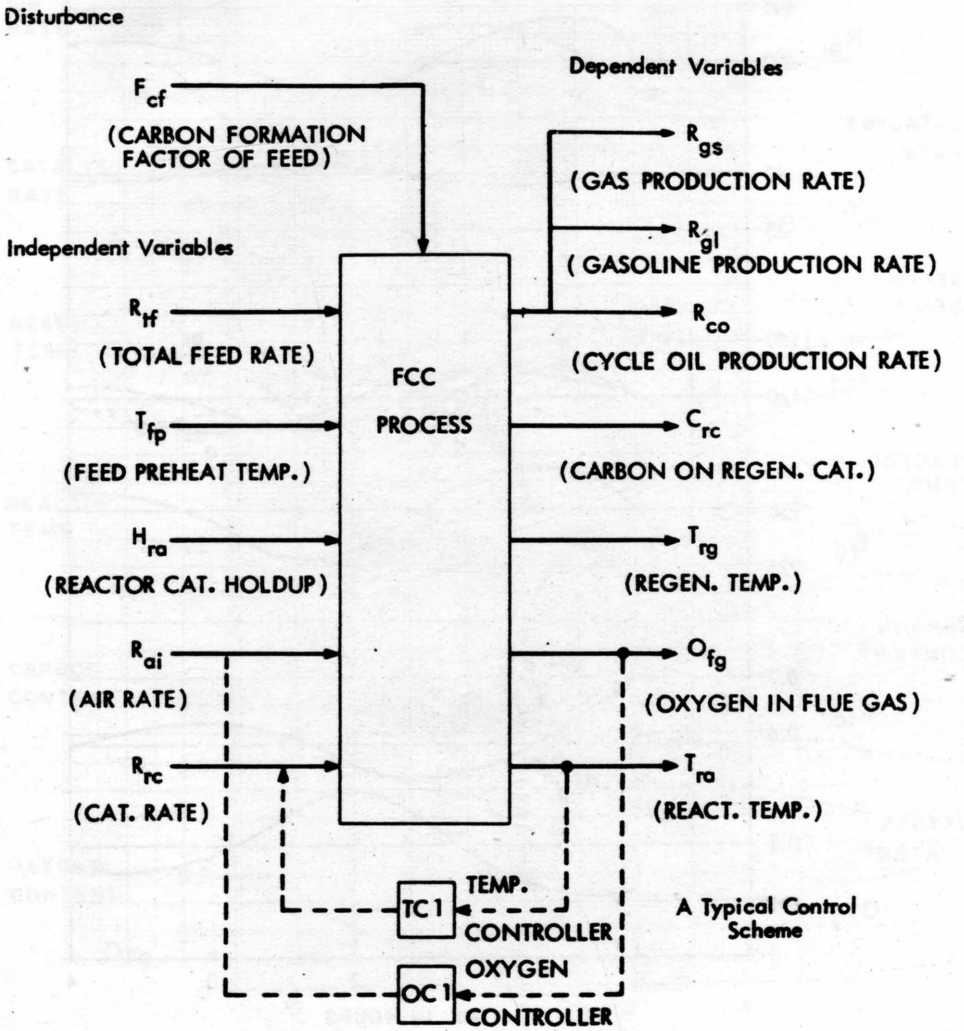

Figure 2. Control Aspect of a FCC Mathematical Model

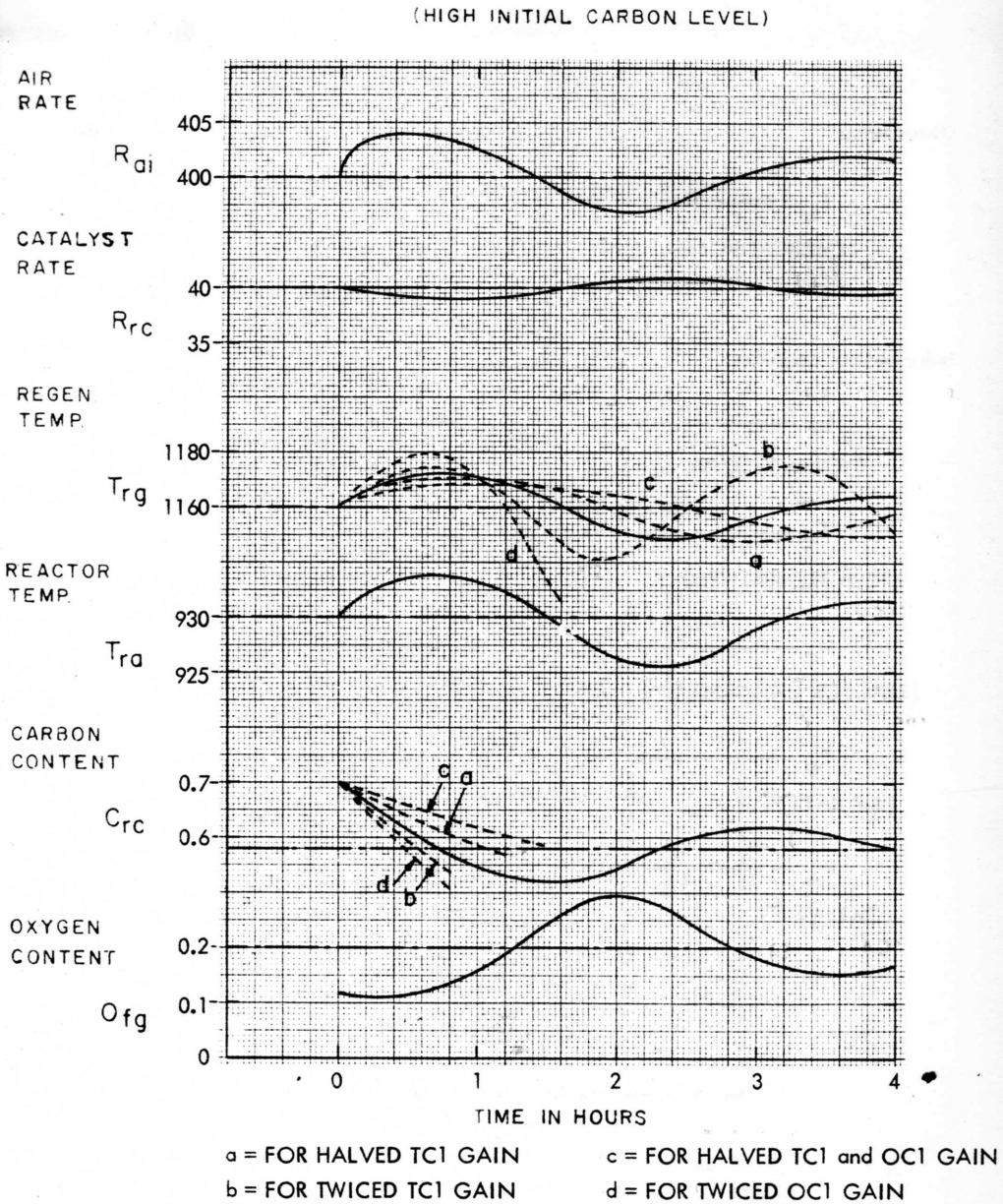

Figure 3. Conventional Control Scheme for Perturbation in Initial Carbon Content

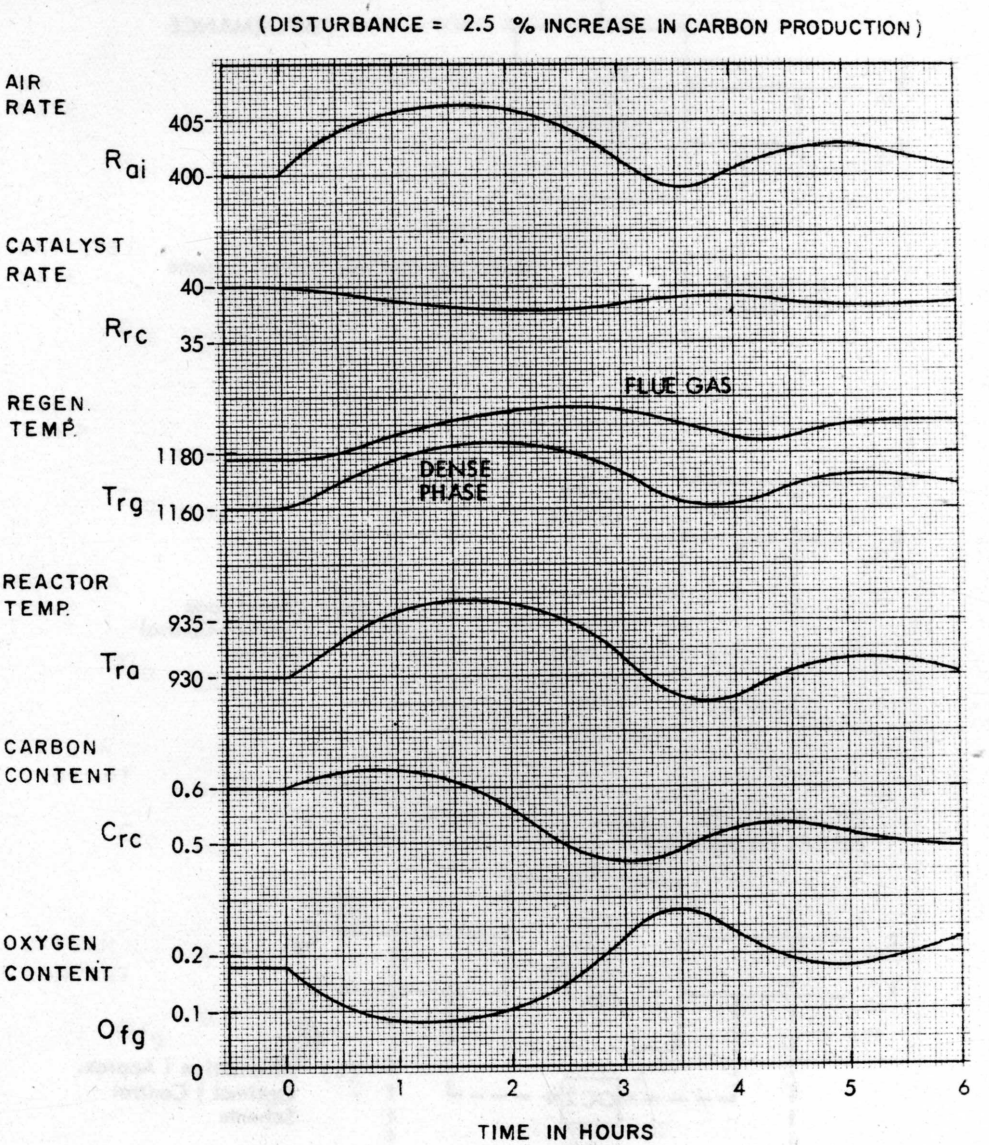

Figure 4. Performances of Conventional Control Scheme for Step Increase in Rate of Carbon Production

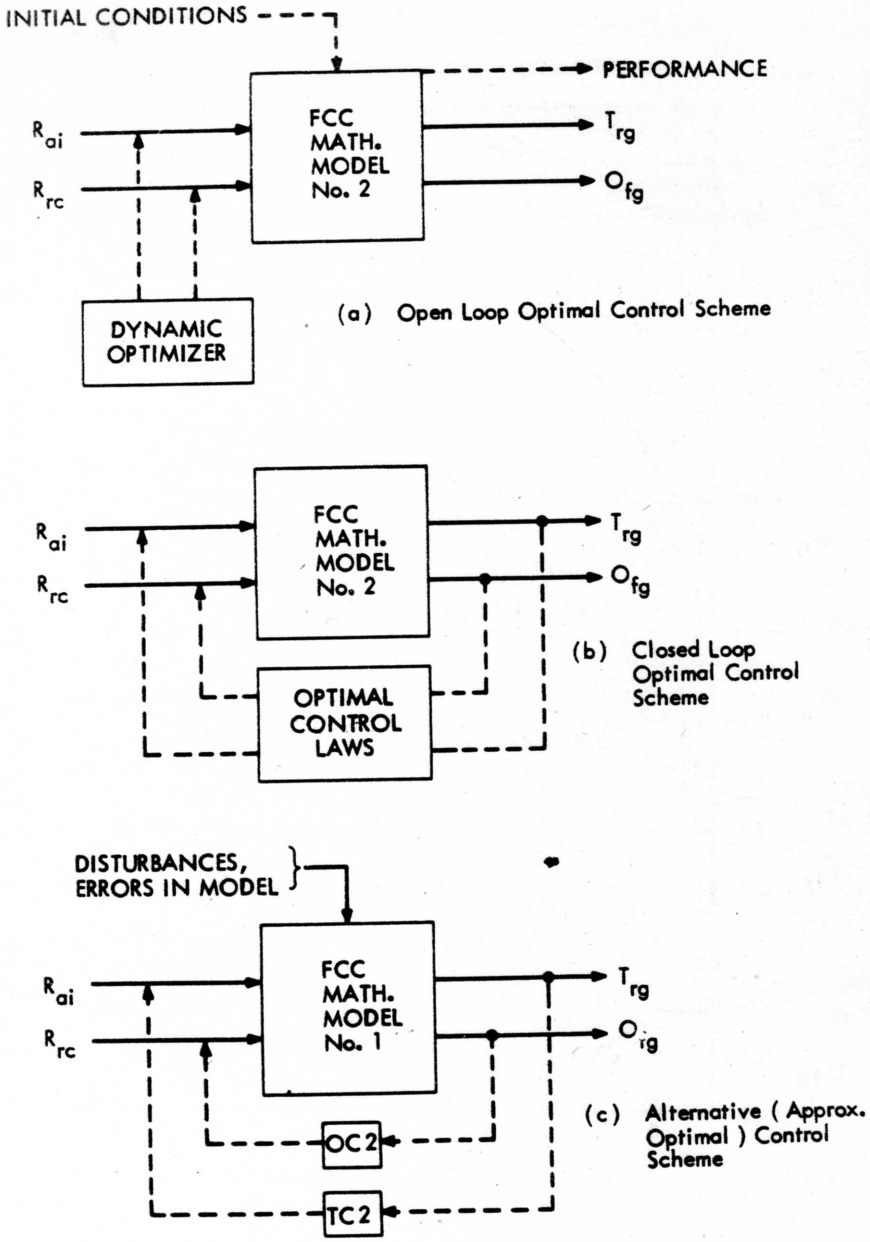

Figure 5. An Approach for Control System Design

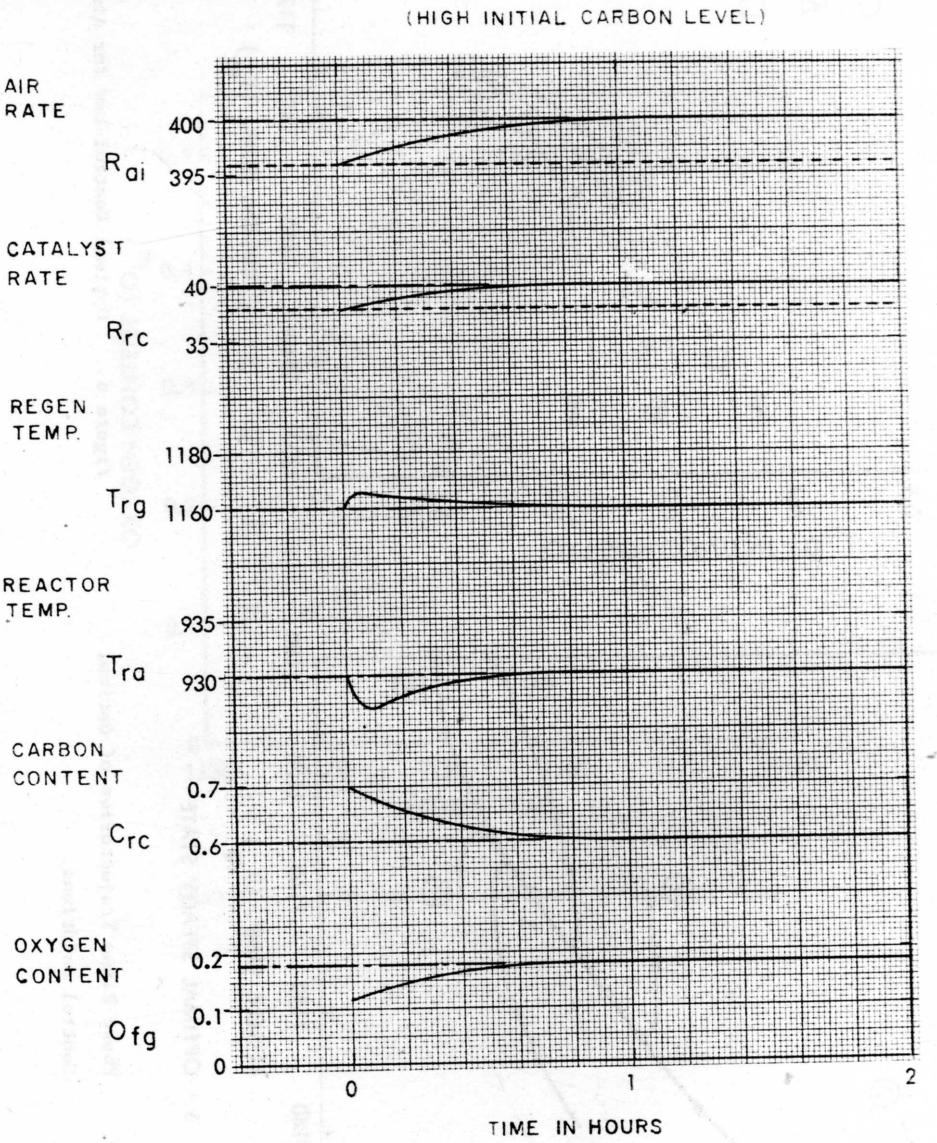

Figure 6. Optimal Control Solution for Perturbation in Initial Carbon Content

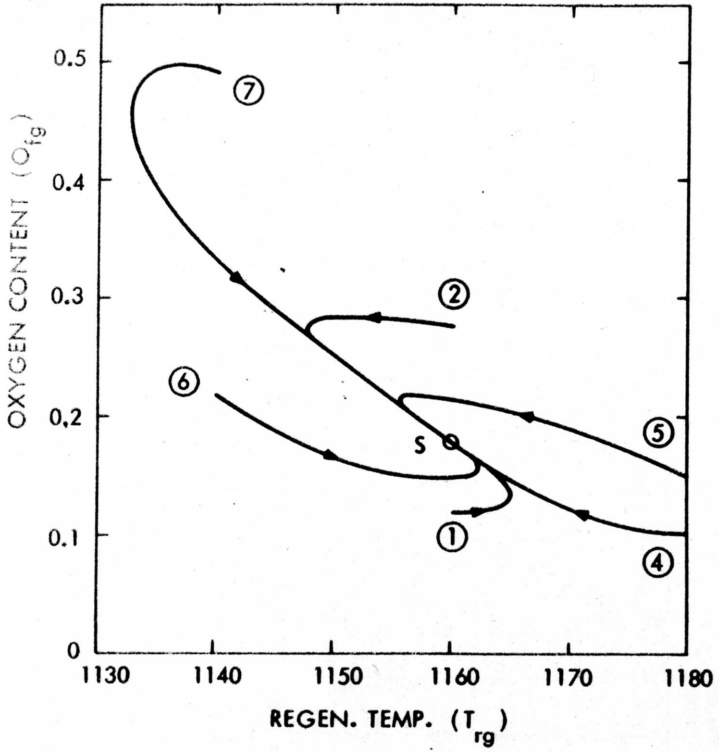

Figure 7. Phase Plane Trajectories of Optimal Control Solutions

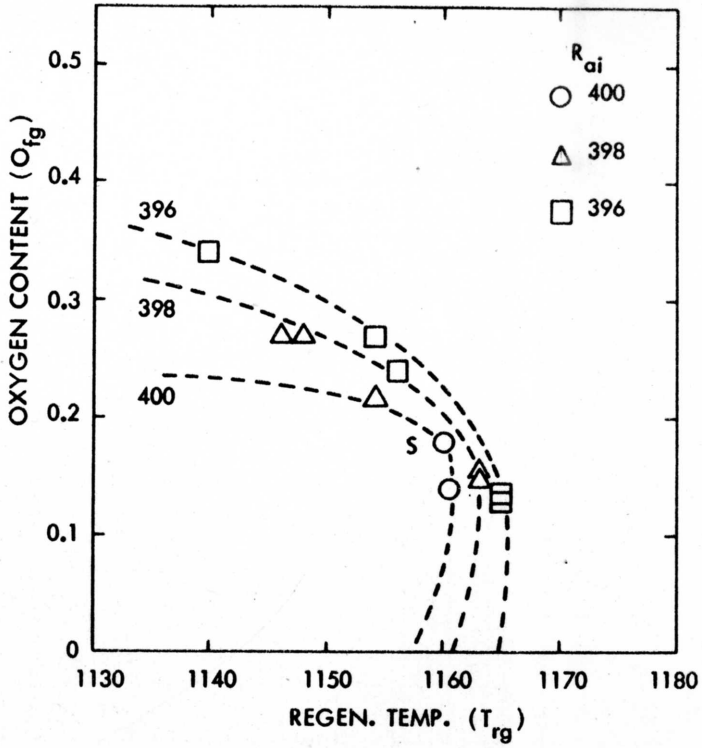

Figure 8. Optimal Control Law for Air Rate

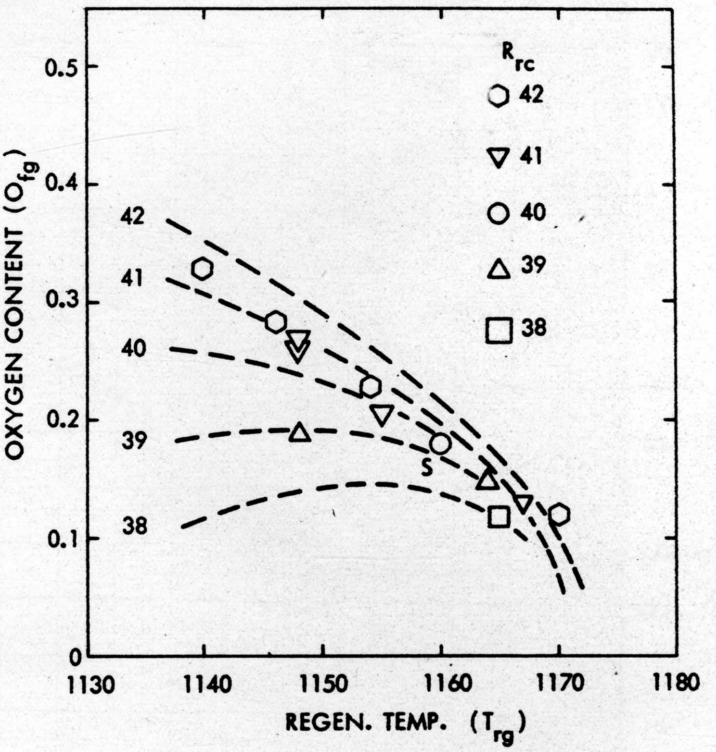

Figure 9. Optimal Control Law for Catalyst Rate

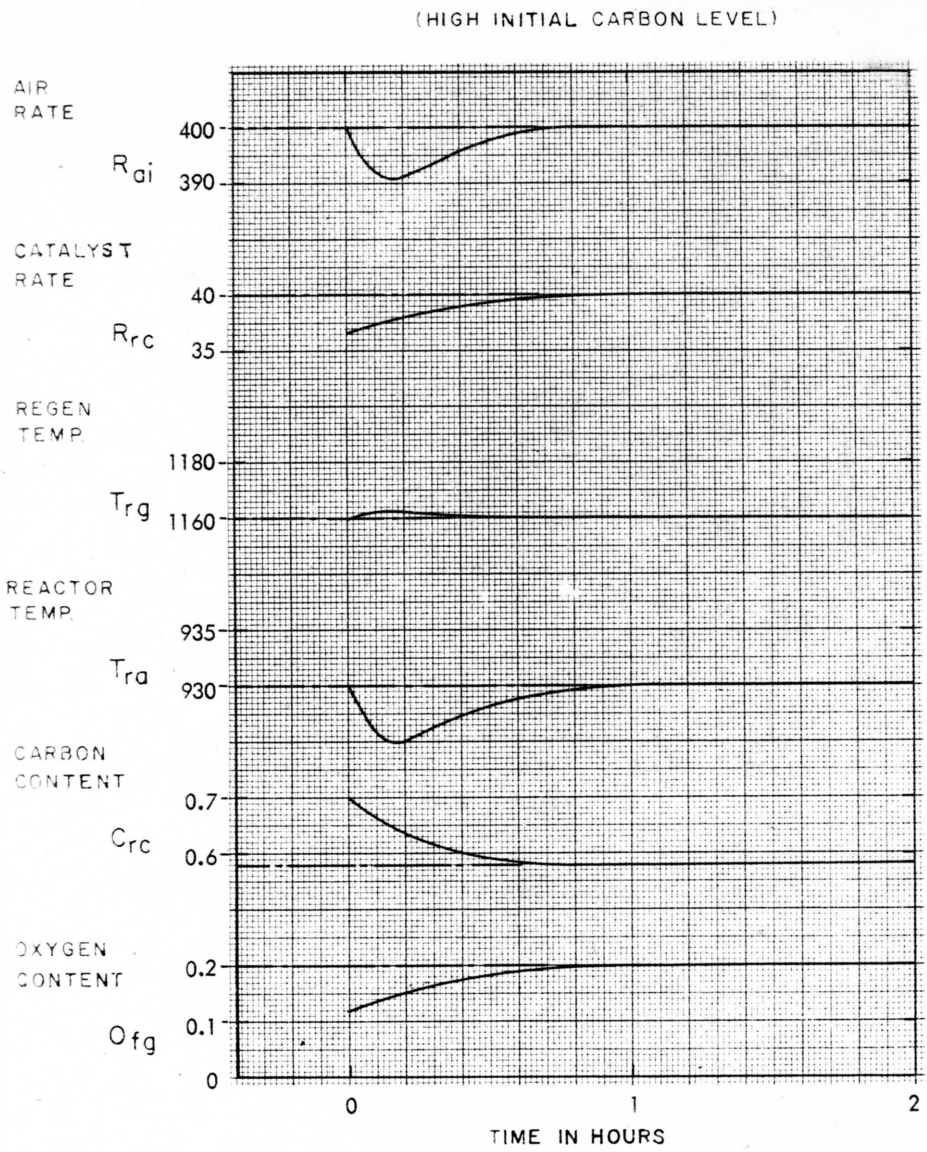

Figure 10. Alternative Control Scheme for Perturbation in Initial Carbon Content

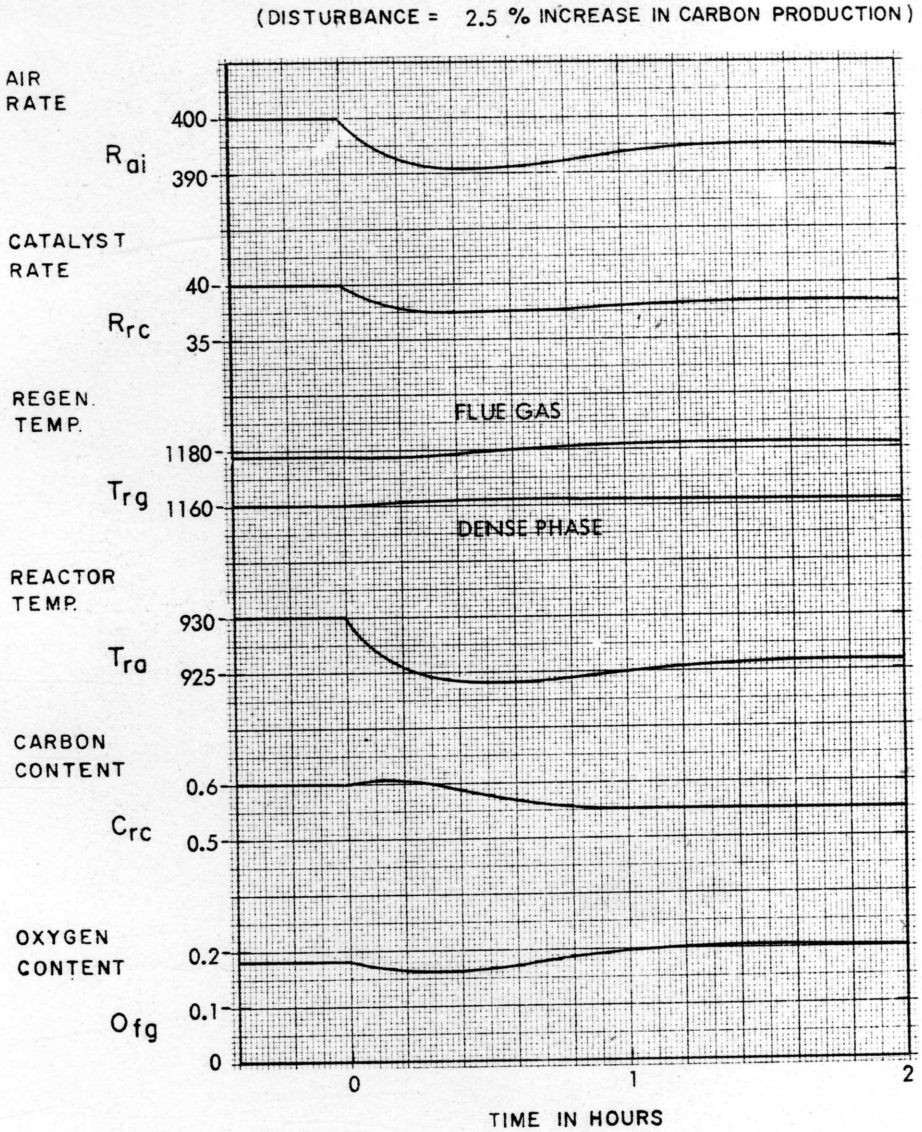

Figure 11. Performances of Alternative Control Scheme for Step Increase in Rate of Carbon Production